THE
PHYSICAL REVIEW
A Journal of Experimental and Theoretical Physics Established by E. L. Nichols in 1893
VOL. 60, NO. 7 OCTOBER 1, 1941 SECOND SERIES

Transmutation of Mercury by Fast Neutrons

R. SHERR AND K. T. BAINBRIDGE, *Research Laboratory of Physics, Harvard University, Cambridge, Massachusetts*
AND
H. H. ANDERSON, *Mallinckrodt Laboratory, Department of Chemistry, Harvard University, Cambridge, Massachusetts*
(Received August 13, 1941)

The products of the transmutation of mercury by fast (Li+D) neutrons were investigated. Three radioactive gold isotopes were found to be formed by the $n-p$ reactions: 65-hour Au^{198}, 78-hour Au^{199}, and a new unassigned electron emitter with a period of 48 min. Three radioactive platinum isotopes were observed and attributed to $n-\alpha$ reactions in mercury: 29-min. Pt^{199}, 19-hour Pt^{197}, and a new activity with an 80-min. half-life. The latter period was also observed in deuteron and fast neutron bombardment of platinum, but was not found in slow neutron irradiation of platinum. Radioactive mercury isotopes with 43-min., 25-hour, and 50-day periods were observed in the fast neutron irradiation of mercury. The 43-min. and 25-hour activities were also formed by bombarding platinum with α-particles. Difficulties in the assignment of the 80-min. Pt and the 43-min. and 25-hour Hg activities are discussed.

INTRODUCTION

THE bombardment of nuclei by fast neutrons may result in radioactive nuclei following simple neutron capture or transmutations involving the emission of neutrons, protons and α-particles. The emission of neutrons has been observed for practically every element. Radioactivity following the emission of heavy charged particles has been observed for the light and medium weight nuclei, but the number of such observations falls rapidly with the increasing atomic number of the elements bombarded.[1] This trend can be attributed largely to the effect of the increasing potential barrier on emission of protons and alpha-particles. The energy requirement for an $n-p$ reaction is

$$E_n = E_{max} - 0.8 \text{ Mev}$$

where E_n and E_{max} represent the neutron threshold energy and the energy of the radioactive transition, respectively, and 0.8 Mev is the energy equivalent of the difference in mass between the neutron and proton. The $n-p$ reaction will ordinarily be slightly endoergic. The $n-\alpha$ reactions will in general be exoergic because of the high internal binding energy of the α-particle. Despite the fact that the energy considerations favor the $n-\alpha$ and $n-p$ reactions over the $n-2n$ reaction, the effective cross sections for the former are greatly reduced by the high potential barriers.

As a consequence of the rapid decrease of cross section with increasing atomic number, the $n-p$ and $n-\alpha$ reactions require very high neutron energies and large quantities of target material to produce sufficient activity for experimental study. The most energetic neutrons available are those produced in the bombardment of lithium

[1] G. T. Seaborg, Chem. Rev. **27**, 199 (1940).

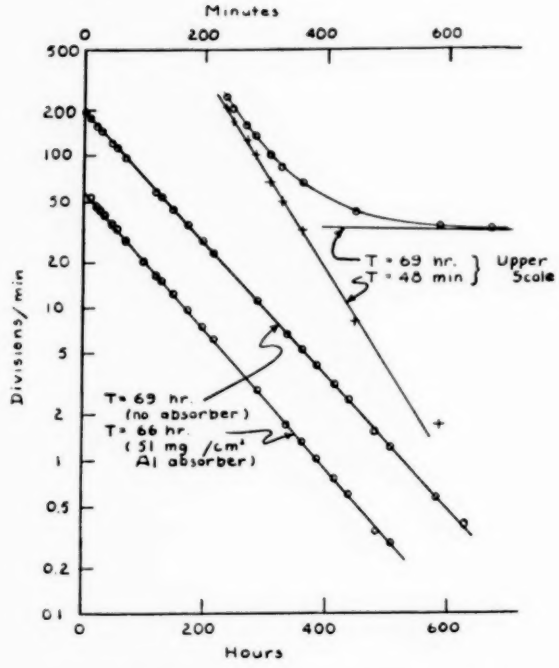

FIG. 1. Radioactive gold from Hg+Li neutrons.

by deuterons. However, even for these, the cross sections are very small and large quantities of material must be used. This, in general, complicates the chemical treatment required to identify the resulting radioactive nuclei. In this respect mercury is an ideal element, since it has been shown that microscopic quantities of gold and platinum can be easily separated from mercury by distilling the mercury in vacuum.[2]

METHOD

Three to four hundred grams of mercury were bombarded with fast neutrons from the Li+D reaction. The deuterons used were produced by the Harvard cyclotron with an energy of 11 Mev and currents of 5–15μa. After irradiation, the mercury was placed in a vacuum distilling flask with the addition of 50 mg of gold. The latter readily formed an amalgam with the mercury and served as a carrier for the radioactive gold and platinum. The residue of the distillation was then treated chemically to separate the gold and platinum activities.

The mercury had been subjected to a number of distillations before use and gave results in complete quantitative agreement with samples of C.P. analyzed mercury, indicating a high state of purity. Furthermore, the same mercury was used repeatedly with concordant results, indicating that the distilling process carried out at the rate of approximately 50 cc per hour was indeed removing at least 99 percent of the added gold. Control tests made by bombarding Pt and Au simultaneously with the mercury showed that the amounts of Pt and Au which would have to be present in the mercury as impurities were of the order of 10 mg of Au and 250 mg of Pt. Impurities of this magnitude are impossible, as shown by the fact that a second distillation yielded an activity of less than 0.1 div./min., while the first distillation gave 30 div./min. for the gold fraction and 6 div./min. for the platinum fractions.

The activities were observed with a Lauritsen electroscope of the conventional type. The radioactive samples were placed on aluminum holders and covered with Cellophane tape. The aluminum holders could be inserted into a series of shelves directly below the 1-mil Al electroscope window. The samples were as thin as possible to prevent self-absorption, but, in general, the radiations had to penetrate a thickness of 15 mg/cm^2 (window+tape). The sign of the emitted electrons was determined by deflecting them by means of a magnetic field into a Geiger counter.

It should be noted that any radioactivity with half-life values less than 15 min. would have been difficult to observe, since the distillation and the chemical separation required about two hours.

TABLE I. *Stable isotopes of platinum, gold, and mercury.**

Z	ELEMENT	A	% ABUNDANCE	Z	ELEMENT	A	% ABUNDANCE
78	Pt[a]	192	0.8	80	Hg[c]	196	0.15
		194	30.2			198	10.1
		195	35.3			199	17.0
		196	26.6			200	23.3
		198	7.2			201	13.2
						202	29.6
						204	6.7
79	Au[b]	197	100				

[2] A. Miethe, Naturwiss. **12**, 597 (1924); **13**, 635 (1925); M. W. Garrett, Proc. Roy. Soc. **A112**, 391 (1926).

* [a] M. B. Sampson and W. Bleakney, Phys. Rev. **50**, 732 (1936); [b] A. J. Dempster, Nature **136**, 65 (1935); [c] A. O. Nier, Phys. Rev. **52**, 933 (1937).

Chemical Procedure[3]

The residue (gold) of the mercury distillation was dissolved in aqua regia and platinum carrier added. The solution was adjusted to 1.2 N in hydrochloric acid after complete removal of nitric acid. Gold was precipitated with hydroquinone and removed by filtration. Platinum was reduced by hydrazine.

For a more critical study of the platinum activities, the following methods were used. After removal of the gold by hydroquinone, the latter was destroyed by nitric acid. Platinum and iridium carriers were separated by the use of sodium bicarbonate with bromphenol blue indicator.[3] Iridium hydroxide precipitated out at this point. (Other metals of the platinum group, except platinum, would also be precipitated.) Platinum was then recovered from the solution by the use of hydrazine. This method was also used to prepare "spectroscopically pure" platinum. An alternative method was the addition of potassium chloride solution to precipitate potassium chlorplatinate and potassium chloriridate in the presence of other metallic carriers (iron, calcium, sodium, mercuric and gold chlorides.) The potassium chlorplatinate and chloriridate were reduced to the metals by hydrazine. After a sodium peroxide fusion, the resulting hydroxides were dissolved in hydrochloric acid. Platinum and iridium were then separated by the sodium bicarbonate method (above).

Results

(a) Gold

A glance at the isotope chart (Table I) for this region of the periodic table indicates that at least six radioactive gold isotopes may result by $n-p$ reactions in mercury: 198, 199, 200, 201, 202, and 204 (the abundance of Hg^{196} is so small that it could scarcely yield an observable activity under the fast neutron bombardment conditions of this experiment). Au^{198} is the well-known activity of half-life, 2.7 days.[1] Au^{199} has a half-life of 3.3 days and has been observed by McMillan, Kamen and Ruben,[4] as the product of the decay of the 31-min. Pt^{199}. Cork and Halpern[5] have reported a gold period of 164 days which they assigned to Au^{199}. The gold isotopes of higher mass number have not been observed.

The gold fraction in the present experiment gave the decay curve shown in Fig. 1. Two activities are apparent, one of 48±2-min. half-life and one with a 69-hour half-life. However, when the longer period activity was observed through a 50-mg/cm² aluminum absorber, a value of 66 hours was obtained. This indicated

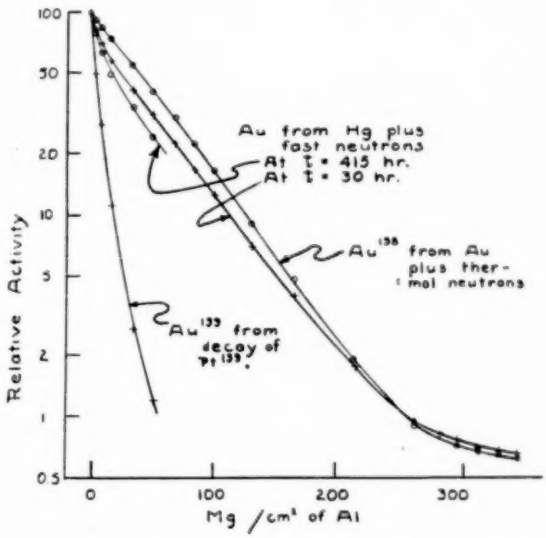

Fig. 2. Absorption in aluminum of 69-hour gold from Hg+Li neutrons, 65-hour Au^{198} and 78-hour Au^{199}.

that the 69-hour activity was actually complex, despite the fact that the decay was linear within the limits of accuracy over a factor of 500 in intensity. This complexity was also indicated by the absorption data in Fig. 2, which show that the radiation was softer at $t=415$ hours after irradiation than at $t=30$ hours. Absorption curves for the 65-hour Au^{198} and 78-hour Au^{199} were obtained by bombarding gold with slow neutrons, and platinum with slow neutrons. In the latter case, the gold was separated after allowing the platinum to decay for a number of hours. These absorption curves are also shown in Fig. 2. It was found that both the 69-hour decay curve (Fig. 1) and the absorption curve at 30 hours (Fig. 2) of the gold obtained from the mercury could be fitted by a mixture of 75 percent Au^{198} (65 hours) and 25 percent Au^{199} (78

[3] See Beamish, Russell, *et al.* Ind. Eng. Chem. (1936–37).
[4] McMillan, Kamen, and Ruben, Phys. Rev. **52**, 375 (1937).
[5] J. M. Cork and J. Halpern, Phys. Rev. **58**, 201A (1940).

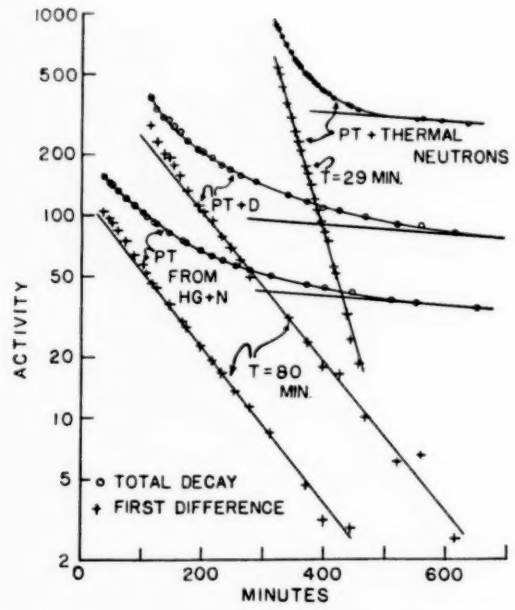

FIG. 3. Short period platinum activities produced by Hg+Li neutrons, Pt+D and Pt+slow neutrons. In each "total decay" curve, the background is due to the 19-hour +longer periods. The departure of points from the 80-min. lines is due to the 29-min. activity.

hours). Actually, the intensities of the 65-hour and 78-hour activities would be roughly equal if one corrected for the absorption in the material covering the samples (15 mg/cm²). Both isotopes emit negative electrons. The 65-hour electrons have a maximum energy of 0.8 Mev, while the 78-hour electrons have an energy of several hundred kilovolts.

The 48-min. activity emits negative electrons with a maximum energy of about 2.5 Mev. Its absorption curve is shown in Fig. 6. It is observed to be much more energetic than the 43-min. Hg activity and, therefore, could not be confused with the latter. This gold activity must be assigned to a gold isotope of mass number >199. On reducing the observed activities to the activities for infinite bombardment time, one finds that all three periods are formed with approximately the same intensity. No evidence for a 164-day period was found, although it would have been observable if its formation had a comparable cross section. The energy ascribed to this activity is 0.45 Mev[5] and the emitted particles would not have been absorbed to an appreciable extent by the electroscope window and Cellophane tape.

(b) Platinum

The platinum fraction from the mercury bombardment gave a decay curve with four observable periods. A long period (>2 days) of weak intensity was observed but its relative intensity was erratic, indicating that it might be due, at least in part, to a slight gold contamination. The other periods observed were 19 ± 1 hours, 80 ± 5 min. and 27 ± 5 min., with approximately equal intensities (estimated for infinite bombardment time). All three emit negative electrons.

The isotope chart shows that the following mass numbers in Pt can result from an $n-\alpha$ reaction in mercury: 195, 196, 197, 198, 199, 201. McMillan, Kamen, and Ruben[4] found and assigned a 31-min. period to Pt^{199} and an 18-hour period to Pt^{197}, by neutrom bombardment of Pt. The same periods are found in platinum activated by deuterons.[6] A deuteron bombardment was made in the present work and an absorption curve for the observed 19 ± 1-hour period was obtained. By comparison with the absorption curve of the 19-hour Pt resulting from the Hg+n reaction, it was established that they were the same. The reaction is ascribed to Hg^{200}. A satisfactory identification of the 27 ± 5-min. activity by absorption measurements was not possible, since its intensity was too small by the time the activity could be measured (about 2 hours after bombardment). However, it seems probable that it is the 31-min. Pt^{199}, formed by an $n-\alpha$ reaction from Hg^{202}.

No 80-min. period in Pt has previously been reported. In the course of this work it was found that this activity could be produced by bombarding Pt with deuterons (Fig. 3) and with fast neutrons. It is surprising that slow neutron

TABLE II. *Relative intensities of three platinum activities as produced by different reactions.*

REACTION	SUPERFICIAL DENSITY OF SAMPLE	29 ± 1 MIN.	80 ± 3 MIN.	19 ± 1 HR.
Hg+Li neutrons	15 mg/cm²	1	0.8	0.9
Pt +D	20 mg/cm²	1	1.4	3.7
Pt +Li neutrons	150 mg/cm²	1	3.5	6.0
Pt +slow neutrons	150 mg/cm²	1	not observed (<0.1)	0.3

[6] J. M. Cork and E. O. Lawrence, Phys. Rev. **49**, 788 (1936).

bombardment failed to produce the 80-min. activity (Fig. 3). A number of chemical tests (above) were made before and after irradiation in order to establish the chemical identity of this period. The results indicated that the 80-min. activity was due to a Pt isotope.

The relative intensities for infinite time of irradiation (but not corrected for absorption) are shown in Table II, for the various reactions studied. The results for fast and slow neutrons are consistent with the assignment of the 29-min. period to Pt^{199} and the 19-hr. period to Pt^{197}, since the latter can be formed by an $n-2n$ reaction from Pt^{198}, whereas the former can be formed only by neutron capture. The assignment of the 80-min. period is difficult. If the failure to observe it with slow neutrons is taken to indicate that it cannot be formed by simple capture, then it must be assigned to Pt^{198*} and would have to be formed by deuterons by a reaction $Pt^{198}(D, ?)$ Pt^{198*}; that is, by some form of excitation. In order to check this possibility, a stack of 6 Pt foils (1 mil) was irradiated with deuterons and the activity of each foil analyzed. Since a number of long period gold activities are formed (the 37-min. positron emitter reported by Cork and Halpern[5] in Au was not found), only the 29-min. and the 80-min. periods were compared (Table III). The first three foils gave the same ratio of

TABLE III. *Stacked foil bombardment of platinum. The energy values are the mean energy of the deuterons. The "energy thickness" of each foil is about* 1.7 *Mev.*

FOIL	1	2	3	4	5	6
Mean energy within foil	10 Mev	8.3	6.5	3.9	1.5	0
29-min. activity*	3.5×10^4	1.3×10^4	1.0×10^3	~ 7	~3.6	3.6
80-min. activity	4.6×10^4	1.4×10^4	1.3×10^3	~14	~7.2	7.2

* The activities listed here correspond to a time of 120 min. after irradiation. These data were obtained with an ionization chamber and cannot be directly compared with the data of Table II which were observed with the electroscope, because of differences in the sensitivity of the two instruments.

the 80-min. to 29-min. period within 25 percent, while the relative activity of the foils decreased by a factor of 30. The low activity of the fourth foil shows that the yield drops very rapidly below 6 Mev. The fourth foil had an activity about twice that of the fifth and sixth foils, which show the neutron background activity. This, incidentally, shows that fast neutrons, which are always present during deuteron bombardment, can be responsible for only a fraction

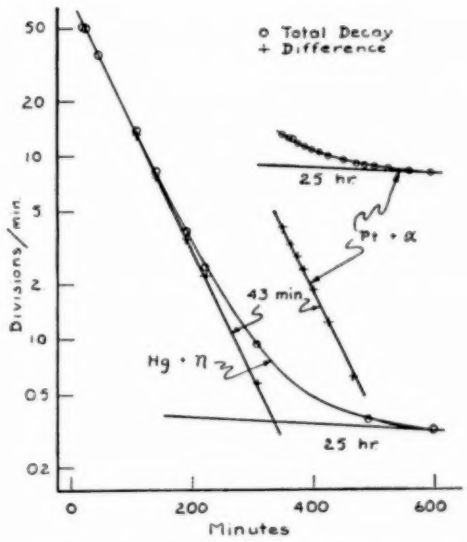

FIG. 4. 43-min. Hg activity as produced by mercury+lithium neutrons and platinum+α-particles.

of a percent of the observed 80-min. activity. This experiment indicates that the 80-min. and the 29-min. activities are formed by similar reactions, although it is, perhaps, possible that the cross section for some type of excitation process might have the same energy dependence as that for a (D, P) reaction. The high yield at relatively low deuteron energies makes it improbable that the 80-min. period is being formed by a (D, H^3) or $(D, 2n, p)$ reaction.

It is possible that the cross section for the production of the 80-min. period by slow neutron capture is finite but small. If its cross section were only a few percent of that for the formation of the 29-min. period it could easily escape observation, because of masking by the 29-min. and 19-hour activities. Attempts to find the 80-min. period by bombarding osmium with α-particles and iridium with deuterons were unsuccessful. These results suggest that the 80-min. period may be assigned to Pt^{196*} or Pt^{197}.

Absorption data show that the maximum electron energies of the 19-hour and 29-min. activities are 0.65 Mev, and 1.8 Mev, respectively. The absorption curve for the 80-min. period as produced by deuterons is concave in shape and indicates that it is probably composed of a line or lines, with an energy of several hundred kilovolts.

McMillan *et al.*[4] observed a 3.3-day Pt period of equal intensity with the 19-hour Pt^{197}, when platinum was irradiated with slow neutrons. We have observed a long period of small intensity, but it is possible that the electroscope window and Cellophane tape absorbed most of the 3.3-day electrons.

(c) Mercury

McMillan, Kamen and Ruben[1] reported 43-min. and 25-hour activities induced by fast neutrons on mercury. In the present work an additional weak period of about 50 days was observed but not studied. Krishnan[7] found by deuteron bombardment of mercury strong activities of 5 min. and 48 min., and weaker activities of 36 hours and 60 days. In addition, he found that deuteron bombardment of gold yielded a mercury activity of 36 hours. In a more recent publication,[8] he reports the mercury activity from deuteron bombardment of gold as having a period of 32 ± 2 hours, which he ascribes to Hg^{198*}, on the basis of selective absorption measurements on the γ-radiations, formed by $Au^{197}(D, n)$.

Since the present work gave a value of 25 ± 1 hours for the neutron-induced mercury activity, a deuteron bombardment of gold was made to see whether our 25-hour and Krishnan's 32-hour activities actually were different. The decay curve of the chemically separated mercury gave a period of 25 ± 1 hours and a longer weak period of 60–70 hours which was ascribed to a slight contamination of 65-hour Au^{198}.

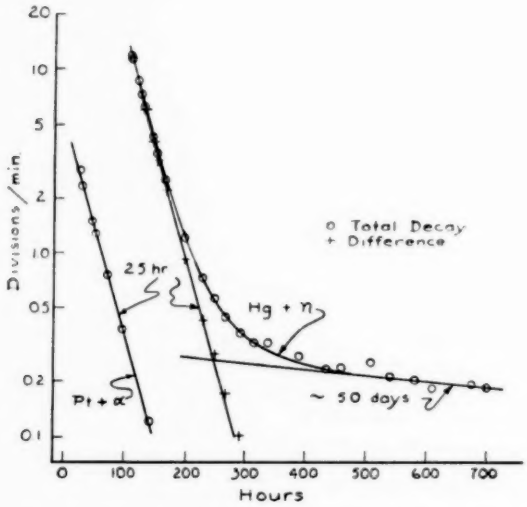

FIG. 5. 25-hour activity as produced by Hg+Li neutrons and Pt+α. A decay curve identical with the Pt+α curve was obtained with Au+D except for the presence of a very weak activity of longer life.

If the assignment of the 25-hour period to Hg^{198*} were correct, one might expect it to be formed by the decay of the 65-hour Au^{198}. A slow neutron bombardment gave a very intense 65-hour activity and, after several days, a small amount of mercury was added to the gold in solution and then precipitated. The mercury showed no detectable activity above the background indicating that the transition $Au^{198} \rightarrow Hg^{198*}$ occurred to less than 1 part in 14,000. This was surprising, since the gold has sufficient energy (0.8 Mev above the ground state of Hg^{198}) to decay to a 25-hour isomer, which has a much lower energy (0.2 Mev).

Bombardment of platinum with α-particles gave two periods of 43 min. (Fig. 4) and 25 hours (Fig. 5) (without chemical separation), with a corrected intensity ratio of 1 : 50. The absorption data for the 25-hour activity (Fig. 6) produced by Hg+n, Au+D, and Pt+α are in excellent agreement, and indicate an energy of approximately 200 kev (the Au+D data are not shown in Fig. 6).

Valley[9] examined the 25-hour activity produced in the Au+D reaction by means of a β-ray spectrometer and found that it was composed of a number of conversion lines whose energies agree very well with the x-ray level separations in gold rather than in mercury. These results indicate that the 25-hour activity is to be assigned to Hg^{197} formed by $Au^{197}(D, 2n)$, which decays by K capture to Au^{197}. Valley also found an activity of 62 hours in the mercury precipitate, consisting of very soft electrons. This period was not observed in the present work because of the thickness of the electroscope window. It is possible that Krishnan's value of 32 hours was the 25-hour period affected by the presence of the 62-hour activity.

The assignment of the 25-hour period to Hg^{197} is consistent with the present investigations

[7] R. S. Krishnan, Proc. Camb. Phil. Soc. **36**, 490 (1940).
[8] R. S. Krishnan, Proc. Camb. Phil. Soc. **37**, 186 (1941).
[9] G. E. Valley, private communication.

since this activity can be formed by the reactions

$$Hg^{198}(n, 2n)\ Hg^{197}, \quad Pt^{194}(\alpha, n)\ Hg^{197},$$

and explains the failure to observe the growth of the 25-hour activity from the decay of Au^{198}.

The 43-min. Hg activity has been assigned to Hg^{197}.[1,7] However, we did not observe it with bombardment of gold by deuterons. One would expect it to show up fairly strongly as a $(D, 2n)$ product if it were isomeric with the 25-hour period, and even more strongly if its correct assignment were Hg^{198*}, formed by a (D, n) reaction. Failure to observe this result from the bombardment of gold by deuterons would indicate a higher mass number than 198; the only numbers consistent with its production by $Pt+\alpha$ are 199 and 201, which can be formed from $Pt^{196 \text{ or } 198}$. This reasoning would, therefore, assign the 43 min. to an excited state of stable $Hg^{199,201}$. However, either of these should be formed by neutron capture in $Hg^{198,200}$. This slow neutron reaction has not been reported by other investigators. Observations made in the present work are obscured somewhat by the difficulty of eliminating all fast neutrons. Indications are that the cross section for slow neutrons is small.

Summarizing, the cross section for the formation of the 43-min. activity seems to be "small" for the reaction Hg+slow neutrons, "small" for $Pt+\alpha$ (1/50 of 25-hour activity), "large" for fast neutrons on Hg (25 times the 25-hour activity with Li neutrons), and "large" for its formation by $Hg+D$.[7] These changes cannot be attributed to the relative abundance of the initial nuclei concerned in these reactions.

It would be of interest to know the relative cross sections for the various fast neutron reactions. Unfortunately, the neutrons coming from the thick lithium target have an energy spread of 20–25 Mev. In view of this inhomogeneity, only rough measurements on the relative yields were made, corrected to infinite bombardment time and for absorption. The 29-min., 80-min., and 19-hour activities in platinum have equal intensities, each of which is 10^{-4} as large as the yield of the 43-min. Hg activity. The 48-min., 65-hour, and 78-hour gold activities have equal intensities, each being 10 times stronger than the platinum, and 10^{-3} as strong as the 43-min. mercury. The 25-hour intensity is 4 percent of the 43-min. mercury activity, which was 3000 div./min. per g of mercury for 10μa of deuterons at 11 Mev on Li. With Be neutrons, which have about half the energy, the yield of the 43-min. activity increases slightly, while the intensity of the gold yield drops by a factor of 7.

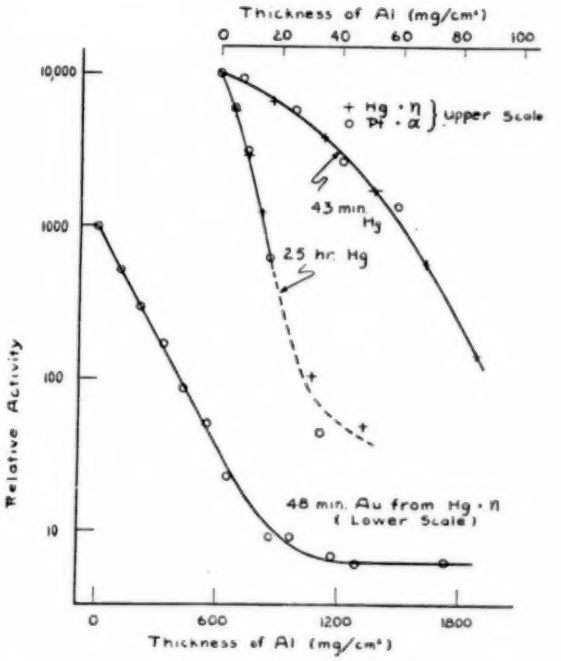

FIG. 6. Absorption in aluminum of 48-min. Au, 43-min. Hg and 25-hour Hg.

It is hoped that a further study of the cross sections for neutrons of various energies will help to clarify the identity of the 43-min. Hg and 80-min. Pt activities.

It is a pleasure to acknowledge the ready cooperation of Drs. B. R. Curtis, E. P. Clancy, and L. Fussell, Jr., and Mr. R. S. Bender and other members of the cyclotron laboratory.

Radioactive Isotopes of Barium from Cesium

J. M. Cork and Gail P. Smith
Department of Physics, University of Michigan, Ann Arbor, Michigan

(Received August 11, 1941)

Radioactive isotopes of barium of half-lives 40.0 hours and 340 hours are made by bombarding cesium with deuterons of 9.5 Mev energy. The former is shown by absorption measurements and by the magnetic beta-spectrometer to consist of a partially converted gamma-ray of energy 276.4 kev. The latter activity is associated with K-electron capture in Ba^{133} and consists solely of a 17-kev gamma-ray and the K x-radiation of cesium of energy about 30 kev. The 40.0-hour activity is probably due also to a highly excited state of Ba^{133}, although the existence of an excited state of the stable Ba^{134} would equally well satisfy the data. The probability of total conversion for the 40.0-hour gamma-ray is about 71 percent, and the ratio of the K and L components is found to be 3.18. From the calculations of Hebb and Nelson this indicates a change in angular momentum of four units.

CESIUM bombarded with deuterons of 9.5-Mev energy, gives rise to strong radioactivity in barium. Since cesium has but a single isotope of mass 133 only three possibilities exist for the masses of the barium atoms formed. The most likely process is the (D, N) reaction resulting in barium (134). The less probable $(D, 2N)$ transformation leads to barium (133) while the least probable (D, γ) interaction would result in barium (135). Since both barium isotopes of mass 134 and 135 exist in nature any radioactivity due to them must be associated with the existence of excited states of the stable element.

Kalbfell and Cooley[1] bombarded barium with neutrons and reported a radioactivity of 30 hours half-life consisting of a characteristic gamma-ray of energy about 250 kev but too weak to be observed in their spectrometer. This activity whose half-life is shown to be 40.0 ± 0.5 hr. is made very strong by the bombardment of cesium with deuterons and a subsequent separation of barium. In addition to absorption measurements by an ionization chamber and string electrometer, it has been studied in a magnetic spectrometer[2] of high resolution. A preliminary report[3] of the observed results has already been given. In addition to the activity of half-life 40.0 hr. another radioactivity of half-life 340 ± 10 hr. is found in the barium precipitate.

The radioactivity of shorter half-life is shown to be due to a gamma-ray of energy 276.4 kev. This gamma-ray on leaving the nucleus has a large probability of ejecting electrons from the outer atomic levels of the same barium atom. There thus appear electrons of discrete energy values together with the unconverted gamma-radiation. This electron distribution as observed in the beta-spectrometer for two slit widths is shown in Fig. 1. The intensities have been normalized to the same ordinate, and in order not to overlap, the zero ordinate for the curve with the 3-mm slit is shifted upward. The small upper figure is an enlarged view of the M component. These observations have been corrected for background, decay of the source, efficiency of the counter, absorption in the window of the counter, and losses due to counting rate. The peaks correspond to conversion of K, L, and M orbital electrons by the gamma-rays from the active nuclei. In terms of energies these values are 239.0, 270.5, and 275.0 kev, respectively.

These data when compared with the known binding energies for electrons from x-ray spectroscopy, enable a choice to be made regarding the atomic number of the element which emits the gamma-ray. Thus if the radioactive barium should emit a charged particle as a positron and immediately a gamma-ray then the conversion and the K–L difference would be characteristic of cesium; whereas if the half-life is attributed to the gamma-emission the conversion and the K–L energy difference would be characteristic of barium. This latter condition is found to be the

[1] D. C. Kalbfell and R. A. Cooley, Phys. Rev. **58**, 91 (1940).
[2] For description see Phys. Rev. **57**, 6 (1940).
[3] H. W. Collar, J. M. Cork, and G. P. Smith, Phys. Rev. **59**, 937A (1941).

case since the observed K–L difference is 31.5 kev and the corresponding differences in K–L binding energies are 30.2 for cesium and 31.4 for barium. Moreover, no general electron or positron radiation of half-life 40.0 hr. was observed. From this evidence the active body could be either Ba^{133} or an excited state of Ba^{134}.

A gamma-radiation can be characterized by such a long half-life only when a large change in spin accompanies the emission. By observing quantitatively the conversion coefficients an estimate can be made of this spin change. An approximate value of the total conversion factor can be obtained by means of an ionization chamber if the relative sensitivity of the chamber to electrons and to photons is known.

To do this it is possible to make use of an absolute calibration[4] already made in the study of the radioactivity of indium. Here the partially converted 4.5-hr. indium activity is in equilibrium with its parent 56-hr. cadium electron activity so that the areas corresponding to the number of electrons could be integrated and the ratio determined. To the same accuracy that the total conversion in the 4.5-hr. indium was found to be 49 ± 10 percent, the total conversion coefficient for the 40.0-hr. barium activity is found to be 71 percent.

The ratio of the conversion coefficients α_K, α_L, and α_M for the various shells can be determined with considerable accuracy by integration of the separate peaks. From the data for a 3-mm slit system the ratio $\alpha_K/(\alpha_L+\alpha_M)$ was found to be 2.76 and for the 1-mm slit system, 2.80. From the shape of the lines obtained with best resolution an estimate can be made of the M conversion alone. Such an estimate is $\alpha_L/\alpha_M=7$, from which it follows that $\alpha_K/\alpha_L=3.18$. Hebb and Nelson[5] have calculated the probability of conversion of a gamma-ray in the L shell and have indicated the dependence of the K, L ratio of conversion upon the charge of the nucleus, the angular momentum and the energy of the gamma-ray. For a gamma-ray of energy 276.4 kev in barium the ratio $\alpha_K/\alpha_L=3.18$, indicates very closely a change in angular momentum of four units.

The 40.0-hr. activity was also made by neutron excitation. It was found that the radioactivity induced by 9.5-Mev deuterons on Be in a sample placed at right angles to the direction of the beam was almost as strong as in the sample placed directly behind the Be target. Samples in paraffin however were not noticeably activated. It thus appears that the threshold excitation is not exceedingly high. If the activity were due to an excited state of Ba^{134} there might exist the possibility of activation by exposing barium to photon radiation of sufficiently high energy. A quantity of barium was given an enormous exposure[6] to 500-kv x-rays. No trace of radioactivity was observed.

From the data obtained it is evident that this activity could be ascribed equally well to either Ba^{133} or Ba^{134}. However it is known[7] that the Rochester group have found this same activity by bombarding cesium with protons. In their bombardment it is possible to produce barium by the (P, N) and (P, γ) reactions. Although the latter process is known to occur, the former is much more probable and favors the assignment to Ba^{133}.

The activity in barium whose half-life is 340 hr. is shown to consist of two low energy gamma-

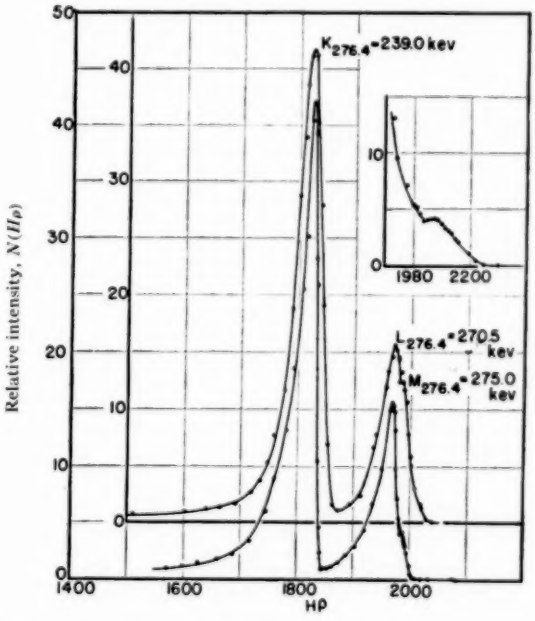

FIG. 1. Distribution of electrons due to internal conversion in 40-hr. barium activity. Upper curve, 3-mm slit; lower curve, 1-mm slit. Intensities are normalized and curves shifted to avoid overlap.

[4] J. L. Lawson and J. M. Cork, Phys. Rev. **57**, 982 (1940).
[5] M. H. Hebb and E. Nelson, Phys. Rev. **58**, 486 (1940).
[6] This exposure was very kindly made by Dr. K. Corrigan with the high voltage x-ray tube of Harper Hospital.
[7] Private communication.

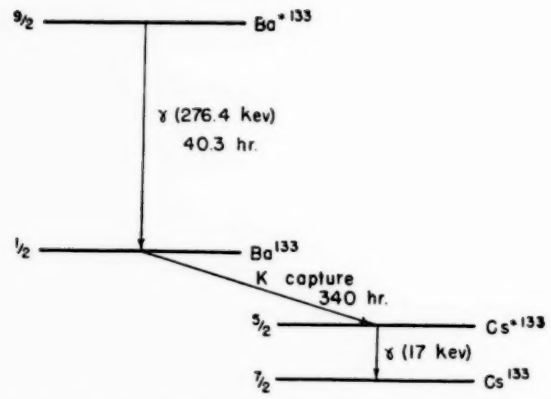

FIG. 2. Energy level scheme to account for observed radioactivities in barium.

rays. By absorption in aluminum the energies of the gamma-radiations appear to be 17 kev and 30 kev. Isotopes of barium could decay to stable cesium only by the emission of positrons, or an equivalent process, namely the capture by the nucleus of the atom of one of its own K electrons. No positron emission appeared to accompany the gamma-radiation, hence the radioactive decay was undoubtedly associated with the K-capture process. This would suggest that the 30-kev radiation is the characteristic K radiation of the atom after the capture of the K electron and hence in this case would be the K radiation of cesium. To establish this fact, absorbing films having about 21 mg/cm² were prepared of the following elements; iodine, antimony, tellurium, and tin. If the x-rays are characteristic of cesium they should be weakly absorbed by iodine and tellurium and strongly absorbed in antimony and tin. If originating in barium the x-rays should be weakly absorbed in iodine and strongly absorbed in tellurium, antimony and tin. The percentage of the incident beam absorbed by the foils is shown in Table I. It is thus quite certain that the radiation is characteristic of cesium following K-electron capture by the barium nucleus. The existence of the 17-kev gamma-ray indicates that the nucleus after K capture is left in an excited state. This probably has a short half-life and is in equilibrium with the component of long life. It thus appears reasonable to construct an energy level scheme as shown in Fig. 2. The values assigned to the spins are not unique but are sufficient to allow transitions leading to the observed results.

In studying the products formed by the fission of thorium and uranium an activity in barium of half-life 300 hr. has been reported.[8] This activity, however, has been identified as linked in a chain reaction with a cesium activity of 33-min. half-life, which in turn is derived from a xenon activity of very short half-life. It has therefore been assigned to an isotope of barium of mass 139 or greater and hence is not the activity observed in this investigation.

TABLE I. *Absorption of x-rays.*

ABSORBERS	PERCENT ABSORBED
Iodine	8±4
Tellurium	7±4
Antimony	26±4
Tin	32±5

The chemical separations have been made by Mr. T. Berlin. For discussions of the theory we are especially indebted to Professor G. E. Uhlenbeck. This investigation was made possible by a grant from the Horace H. Rackham Fund.

[8] Heyn, Aten and Bakker, Nature **143**, 516 (1939); Hahn and Strassmann, Naturwiss. **27**, 529 (1939).

A Microcalorimetric Determination of the Mean Energy of β-Rays from Radium E*

IGNACY ZLOTOWSKI†
Laboratoire de Chimie Nucléaire, Collège de France, Paris

(Received April 7, 1941)

A very precise microcalorimetric method of determining the mean energy of Ra E β-rays is described. The method involves an adiabatic change of temperature of a small calorimeter whose heat capacity is measured by determining the change in temperature produced by several strong sources of polonium. With the aid of Mme. P. Curie's absolute apparatus, the absolute value of the polonium content in these sources as well as in the Ra E samples after the decay of the parent substance could be determined with an accuracy of from 1 to 2 percent. The average value of the β-ray mean energy of Ra E deduced from these experiments is 320,000 ±5000 ev. The measurements made in air gave a mean energy of 323.6±3.5 kev, or slightly higher than those carried out in nitrogen (317.6±2.5 kev). It has been pointed out that the most probable value is nearer the lower limit. The results have been compared with those derived from other calorimetric determinations as well as with the values calculated from β-ray spectra of Ra E established by different authors.

I. INTRODUCTION

THE total or mean energy of β-rays from radioactive bodies may be determined by integration of the continuous spectrum of emitted electrons or by calorimetric measurements. The chief advantage of the first is that the mean energy may be calculated independent of both the amount of radioactive substance present and the number of electrons emitted by each disintegrating atom. Its accuracy is, however, limited by the correctness of the energy distribution curve for electrons escaping from the parent nuclei. In the calorimetric method, the total energy evolved in the form of heat by the emitted radiation is measured independently of secondary processes and with the same precision for slow and fast particles. If β-rays alone are emitted, the results depend only on calorimetric measurements, which now may be made with an error of about 2 percent.[1] Ra E is suitable for calorimetric study, as its β-activity is not accompanied by any other radiation of appreciable intensity,[2] its initial quantity can always be determined with very great accuracy by measuring the polonium accumulated in the source and finally it appears[3] certain that each Ra E atom emits one electron per disintegration.

Early determinations of the mean energy of disintegration of Ra E by the calorimetric method yielded values from 3.44 to 3.37×10^5 ev with errors of 10 to 15 percent.[4,5] More precise measurements with improved technique and stronger Ra E sources seemed desirable.[6]

II. EXPERIMENTAL PROCEDURE

Preparation of Ra E sources

The Ra E was prepared from radio-lead from Joachimstahl pitchblende by Foucauld's extraction method.[7] The Ra E is practically free of radioactive impurities other than polonium, and can be further purified by spontaneous deposition on nickel or by electrolysis with Pt electrodes in

* The above work was carried out jointly with M. Lecoin during the school year 1938–39 [see M. Lecoin and I. Zlotowski, Nature **144**, 440 (1939)]. Because of the exigencies of war, the writer was not able, despite many attempts, to reach M. Lecoin and as a result some details and data of the electrometric measurements, as well as a discussion of the discrepancies between the determinations of the mean energy values for Ra E β-rays and the value obtained in former work by M. Lecoin had, of necessity, to be omitted. It is sincerely hoped that M. Lecoin will be in a position to publish these data in a separate publication at some later date.

† Present address: University of Minnesota, Minneapolis, Minnesota.

[1] See I. Zlotowski, J. de phys. et rad. [7] **6**, 242 (1935).

[2] According to S. Bramson [Zeits. f. Physik **66**, 721 (1930)] there is from 0.25 to 0.5 γ per 100 Ra E atoms and from the recent work of G. v. Droste [Zeits. f. Physik **104**, 335 (1937)] it may be stated that the total γ-ray energy per disintegration ($h\nu > 0.3$ mC²) represents less than 0.004 percent of the mean energy of β-rays.

[3] N. Riehl, Zeits. f. Physik **46**, 478 (1928).

[4] C. D. Ellis and W. A. Wooster, Proc. Roy. Soc. **A117**, 109 (1927).

[5] L. Meitner and W. Orthmann, Zeits. f. Physik **60**, 143 (1930).

[6] A preliminary report has been published by M. Lecoin and I. Zlotowski, Nature **144**, 440 (1939).

[7] P. Foucauld, J. chim. phys. **29**, 479 (1932).

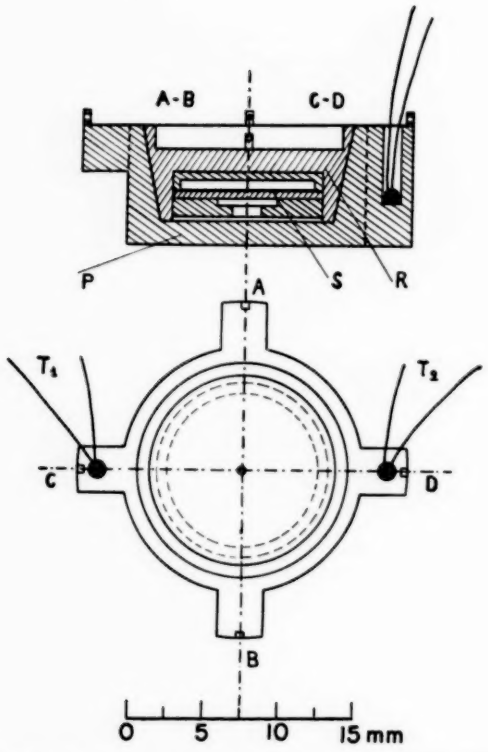

FIG. 1. Calorimeter in which source (S) of Ra E was placed.

the presence of tartaric acid. The removal of Po was then effected by deposition on silver leaves. The final solution thus purified was either evaporated in an atmosphere of argon, or electrolyzed onto one side of a nickel cathode which was later used as the source support in the calorimeter. Two sources were prepared containing about 45 and 80 millicuries of Ra E, respectively. The Po content in both the sources was less than 300 e.s.u.

Calorimetric method

The method, an adaptation of Swietoslawski's adiabatic microcalorimeter,[8] involves the maintenance of the same temperature of the calorimeter and the surrounding water bath. The difference of temperature of bath and calorimeter never exceed 0.001°C. If, then, the heat capacity of the calorimeter is determined and its increase in temperature measured by determining the change of temperature in the sourrounding bath, the amount of heat produced by the radiation can be calculated.

The calorimeter (Fig. 1) was used as an absorbing shield for all rays emitted by the source and consisted of a hollow nickel cylinder P suspended by means of four silk threads inside the calorimetric vessel and of a well-fitted cover R, whose function was to allow introduction of the small disks S of nickel with the radioactive deposits. Although the mass of the calorimeter was small (about 10 g) no rays emitted by the source could escape from the calorimeter without passing through at least 3 mm of nickel, a thickness quite satisfactory for a practically complete stoppage of Po α-rays and Ra E β-rays.[9] The calorimetric cylindrical vessel (about 18 cm in diameter) containing the calorimeter was surrounded by water in a closed tank about 75 cm in diameter.

The adiabatic equilibrium in our experiments was rigorously controlled by means of two copper-constantan thermocouples, the junctions of which were placed in the calorimeter mass and in the walls of the surrounding vessel. The junctions were separated from the source by at least 4 mm of nickel to avoid eventual influence of the thermoelectric circuits by β-rays. A Zernicke type galvanometer with a sensitivity of 1.8×10^{-8} volt per mm at 2 m, which corresponded to 0.0005°C, was used with the thermocouple. An equilibrium between the surrounding bath and the calorimeter was maintained by adding hot water through a pipe with numerous small openings at the bottom of the tank. Saturated air bubbling through the tank stirred the whole mass of water.

The temperature rise of the surrounding water, and therefore of the calorimeter, was determined by two carefully calibrated Beckmann thermometers. The calibration of these was carried out against an "ultra-Beckman" [10] in the same bath and under conditions identical with those

[8] W. Swietoslawski and A. Dorabialska, Comptes rendus **185**, 763 (1927); W. Swietoslawski, Ann. de chim. **16**, 251 (1931); W. Swietoslawski and E. Bartoszewicz, Bull. Acad. Sci. Pol. A 1931, 336; W. Swietoslawski, Bull. Acad. Sci. Pol. A 1934, 80.

[9] The primary γ-rays are practically negligible (if they exist at all) and the secondary γ-rays in nickel, which represent about 2 percent of the energy emitted, are extremely soft. For details see: E. Stahel and J. Guillissen, J. de phys. et rad. [8] **1**, 12 (1940).

[10] According to *PTR* in Berlin, the accuracy of the temperature readings on the "ultra-Beckmann" was 2×10^{-4}°C.

in which the measurements were made. All temperatures are reported to the nearest 0.001°C.

Calorimetric measurements

The calorimetric capacity for each series of measurements was tested and determined by measuring the heat given off by several sources of polonium deposited on a nickel foil, the strength of which was near the amount of Po built up in the used Ra E source after the practically complete decay of the parent substance. The measurements with six sources of Po between 400 and 4000 e.s.u. (1 millicurie Po equals 1340 e.s.u.; solid angle 2π) yielded an increase of temperature of 0.0166°C per hr. for each 1000 e.s.u. of Po with no determination varying more than 0.0001° from the mean. It is obvious that the precision depends directly upon the accuracy of the electrometric evaluation of the Po source. By using the Mme. Curie absolute apparatus,[11] with its precision of 1 to 2 percent, it appears reasonable to assume that all calorimetric capacity values were correct to within 2 percent.

With precautions to obtain thermal equilibrium before readings were taken, Ra E sources of 40 to 80 millicuries were used and the temperature rise (0.2° to 0.4°C) over four-hour periods noted. Such sets of readings were made daily over a period of about 30 days until the parent Ra E had practically disappeared. The regularity of the curves when decrease in thermal effect is plotted against the time (Fig. 2) best indicates the accuracy of all the measurements. However, in each set of experiments the values found in the first 36 hours were systematically high. Since the first set was carried out in air, it was supposed that supplementary effects had been produced by some chemical reactions with oxygen. Hence, a second series of measurements was carried out in an atmosphere of nitrogen, but despite this precaution the effect was not suppressed. The actual explanation of this phenomenon is given later.

Method of calculation

In calculating the mean energy for Ra E β-rays, the Po content at the beginning, and the contribution of the Po formed later, must be taken into account. If X denotes the number of millicuries of Ra E, Y the number of millicuries of Po present in the Ra E deposit at the moment of its final purification, and C the heat capacity of the calorimeter, the mean energy of disintegration of a Ra E atom ($E_{\text{Ra E}}$ in kev) may readily be calculated for each calorimetric measurement by means of the following equation:

$$\begin{aligned} Q = C\cdot\Delta T_t = {} & k_1\cdot X\cdot\exp(-\lambda_{\text{Ra E}}\cdot\theta)\cdot E_{\text{Ra E}} \\ & + k_2\cdot Y\cdot\exp(-\lambda_{\text{Po}}\cdot\theta)\cdot E_{\text{Po}} \\ & + k_3\cdot X\left[\frac{1-\exp(-\lambda_{\text{Po}}\cdot t)}{\text{Po}}\cdot\exp(-\lambda_{\text{Po}}\theta)\right. \\ & \left. - \frac{1-\exp(-\lambda_{\text{Ra E}}\cdot t)}{\text{Ra E}}\cdot\exp(-\lambda_{\text{Ra E}}\cdot\theta)\right]\cdot E_{\text{Po}}, \end{aligned}$$

where ΔT_t is the temperature rise during time t, θ the age of the source (i.e., the time elapsed between its preparation and the starting moment of the measurement), E_{Po} the disintegration energy of Po (per atom), and k_1, k_2 and k_3 numerical constants depending upon the units of measurement used. The value of E_{Po} is taken as 5.4×10^6 ev.[12]

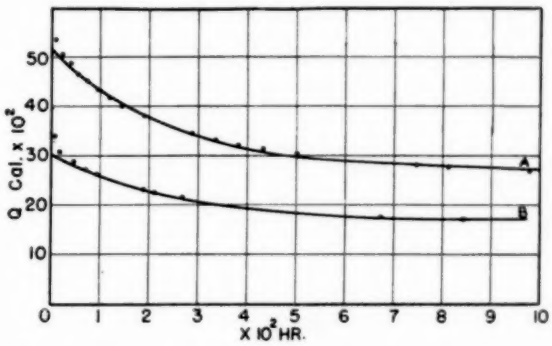

FIG. 2. Diagram of the heat evolution from Ra E sources. Curve A, Ra E source of 80 mC. Curve B, Ra E source of 45.5 mC.

The quantity Y of Po present at any moment in the Ra E source can also be determined by Mme. Curie's absolute apparatus after all the β-rays are deflected by a sufficiently strong magnetic field. Careful consideration of the errors in the determination of Y, which never exceeded

[11] Mme. P. Curie, J. chim. phys. **22**, 142 (1925).

[12] G. H. Briggs, Proc. Roy. Soc. **A143**, 604 (1934); G. Mano, Ann. de physique **1**, 504 (1934).

300 e.s.u., and of the absorption of α-rays in the active deposit itself showed that in the experiments carried out with strong Ra E sources, both suggested sources of error do not affect the accuracy of our measurements.

Determination of Ra E

The electrometric measurements of Ra E based on β-ray ionization measurements carried out with the so-called P chamber (for penetrating radiation) suggested by Mme. Curie,[13] yielded results with a probable error of about 5 percent. Nevertheless, taking into account the difficulties of calibration of this chamber, it is reasonable to expect that the actual systematic error in all the evaluation may be much greater. The calorimetric determination is believed to be much more accurate.

If Y, the initial amount of polonium in the radioactive deposit is known, the calorimetric measurement of the amount of Po at the end of the experiments permits the evaluation of the quantity X of Ra E, present at the beginning of the experiment to within 1 or 2 percent. Therefore, calculations have been effected in each case with several values of Y, all within the limits fixed by the accuracy of the electrometric determinations of Po, as well as by the eventual absorption of α-rays by the radioactive Ra E deposit.

Thus, for source No. 1, where no trace of Po was found at the beginning, calculations carried out, with $Y=0$, 55 and 110 e.s.u., gave the following values for X: 81.5, 80.0 and 78.9 millicuries, figures not very far off from those obtained by electrometric determination (78.5 mC). Taking into account the precision of the calorimetric measurements, we finally adopted 80 mC as the most probable value.

With source No. 2, where 233 e.s.u. of Po were found to be present at the beginning of the experiment by direct electrometric measurement, similar calculations, with the following values for Y: 233, 270, and 300 e.s.u. gave 46.2, 45.5, and 44.9 millicuries, respectively, for the value of X. For reasons discussed above, the following values were adopted: 45.5 mC for X and 270 e.s.u. (0.202 mC) for Y.

TABLE I. *Temperature of surrounding water bath.*

Source No. 1 Experiment on April 2, 1939 Temperature			Source No. 2 Experiment on June 23, 1939 Temperature		
Time P.M.	Thermometer I	Thermometer II	Time P.M.	Thermometer I	Thermometer II
4:00	2.736°C		7:30	2.814°C	
4:10		2.743°C	7:45		2.817°C
4:30	2.776		8:00	2.832	
4:45		2.784	8:15		2.835
5:00	2.817		8:30	2.850	
5:15		2.824	8:45		2.854
5:30	2.859		9:00	2.868	
5:45		2.865	9:15		2.872
6:00	2.899		9:30	2.887	
6:15		2.907	9:45		2.891
6:30	2.940		10:00	2.905	
6:45		2.947	10:15		2.910
7:00	2.982		10:30	2.925	
7:15		2.988	10:45		2.928
7:30	3.022		11:00	2.943	
7:45		3.029	11:15		2.947
8:00	3.062		11:30	2.961	
8:15		3.069	11:45		2.965
ΔT (4 hr.)	0.326	0.326	ΔT (4 hr.)	0.147	0.148
		0.326°C			0.147₅°C

[13] I. Curie, J. chim. phys. **22**, 471 (1925).

Determination of the Ra D content in the Ra E sources

Because of the carefully controlled purification of the Ra E sources, it was almost certain that they would be practically free from any trace of Ra D. Nevertheless, a series of calculations were carried out, based on data from our electrometric and calorimetric measurements, in order to confirm these expectations, as well as to establish in what proportion very small amounts of Ra D could affect the final results of our determinations. Calculations show that all measurements made during the first 30 days are quite independent of the presence of less than 1 percent Ra D. The fact that the results of our measurements conform, within an experimental error of about 3 percent, with those obtained in longer experiments (50 and 80 days) is evidence for assuming that the Ra D content in our Ra E sources was always below 1 percent.

III. Experimental Results

Typical data are shown in Table I. These indicate the consistency of our measurements. The measurements made during the first 24 to 36 hours after the last purification of the source give values for $E_{Ra\ E}$ which are systematically too high. The measurements made in air (mean value: 323.6±3.5 kev) are also slightly higher than those made in nitrogen (mean value: 317.6±2.5 kev) and less coherent. It appears at first that the observed discrepancies are due to

TABLE II. *Experimental data. Source No. 1 (X = 80 mC of* Ra E; *Y = 55 e.s.u. of* Po. *Last elimination of* Po *on March 27, 4* P.M.). *For the significance of all symbols see section, Method of calculation.*

No.	Thermo-couple	Date of the Experiment	θ Hours	ΔT_4 $\times 10^3$	Q Cal. $\times 10^2$	B Cal. $\times 10^2$	C Cal. $\times 10^2$	A Cal. $\times 10^3$	$E_{\text{Ra E}}$ kev
1	I	Mar. 28, 0.00	8.0	435	53.43	0.461	1.790	51.18	336.5
2	I	Mar. 28, 3.30 P.M.	23.5	411	50.50	0.460	4.288	45.75	329.2
3	I	Mar. 29, 9.30 A.M.	41.5	397	48.80	0.459	6.903	41.44	330.7
4	II	Mar. 29, 10.00 P.M.	54.0	380	46.66	0.457	8.582	37.62	322.9
5	II	Mar. 30, 4.00 P.M.	72.0	369	45.31	0.455	10.75	34.01	323.9
6	II	Mar. 31, 3.00 P.M.	95.0	354	43.47	0.453	13.20	29.82	324.1
7	II	Apr. 1, 4.30 P.M.	120.5	339	41.63	0.452	15.56	25.62	322.7
8	II	Apr. 2, 4.00 P.M.	144.0	326	40.03	0.449	17.42	22.16	319.8
9	I	Apr. 4, 3.00 P.M.	191.0	310	38.07	0.444	20.41	17.22	326.1
10	I	Apr. 8, 3.30 P.M.	287.5	282	34.62	0.435	24.29	9.89	326.5
11	I	Apr. 10, 4.00 P.M.	336.0	272	33.41	0.431	25.48	7.30	323.8
12	II	Apr. 12, 2.30 P.M.	382.5	263	32.30	0.427	26.26	5.61	321.0
13	II	Apr. 14, 4.00 P.M.	432.0	256	31.47	0.423	26.82	4.23	322.0
14	II	Apr. 17, 2.00 P.M.	502.0	248	30.53	0.417	27.27	2.84	323.5
15	I	Apr. 27, 9.00 P.M.	749.0	230	28.24	0.396	27.16	0.69	323.5
16	I	Apr. 30, 1.00 P.M.	813.0	226	27.75	0.391	26.93	0.47	326.5
17	I	May 7, 10.30 A.M.	979.5	218	26.77	0.378	26.21	0.18	324.3
								Mean value	323.6±5.0 kev

some secondary chemical phenomenon taking place either in the material of the source support or in the radioactive deposit under the action of the oxygen in the air, or to traces of some oxidizing agents not eliminated from the source by the preparatory treatment. This assumption seems to find confirmation in the fact that, after a comparatively short period of time, all measurements carried out during many subsequent days lead to $E_{\text{Ra E}}$ values lying within experimental error.

Table II gives a summarized comparison of the results obtained in one set of measurements; the values A, B, and C contain the heat due respectively to Ra E, Po from initial contamination and Po built up by Ra E disintegration. Besides the first three measurements, the spread between the extreme values of $E_{\text{Ra E}}$ is not greater than 2.2 percent. It is interesting to note that the accuracy of our determination seems to be practically independent of the amount of Ra E present in the source. As a matter of fact, the calculated $E_{\text{Ra E}}$ values are pretty constant, although at the end of experiments the total heat effect due to Ra E represented only 0.5 percent of the initial heat evolution.

The fair agreement observed in our experiments shows that the Po accumulated in the Ra E sources does not give any additional heat effect of the type observed by Sanielevici in the case of very strong pure Po deposits.[14] Since the Po content in a Ra E source rises with the decay of the parent substance, a direct consequence of such an effect would be a systematic increase in the calculated mean values of the Ra E disintegration energy. Moreover, we have also verified with exactness that our Po sources, used for check calibration of the calorimeter, did not reveal any abnormal heat evolution.

[14] A. S. Sanielevici, J. chim. phys. **33**, 759 (1936).

IV. Discussion and Interpretation of Results

The mean value of the energy of disintegration of Ra E, deduced from our measurements, is 320,000±5000 ev. If the amount of Ra E is expressed in millicuries, the heat effect due to the emitted β-rays is equal to 1.61±0.03 cal./mC of Ra E hr. As the measurements made in air and in the first 36 hours are always slightly higher, it would seem reasonable to suppose that the most probable value is nearer the lower limit of our final result. It is interesting to compare these results with other values obtained from calorimetric experiments carried out by other authors, as well as with the values calculated from the β-ray spectra established by various authors.

Ellis and Wooster[4] obtained by calorimetric methods values somewhat higher (350,000 ±40,000 ev) than ours. An analysis of their data and methods leads one to expect a value too high.

The various sources of error mentioned in the work of Meitner and Orthmann,[5] as well as the

strength of their Ra E deposits (1.7 and 4.0 mC), make it seem likely that the error of their measurements was substantially larger than 6 percent. The determination of Ra E, based on the ionization carried out in the presence of Po, could not be very precise. The evaluation of Po itself was not any more accurate than that of Ellis and Wooster. Moreover, in the same sets of measurements, the $E_{\text{Ra E}}$ values varied from 325,000 ev to 355,000 ev, depending on the method used for the determination of polonium at the beginning of the experiments. These, with other calibration errors, lead one to expect an error of about 10 percent.

The integration of the continuous spectra of Ra E β-rays, obtained by various workers, leads to an average energy value differing little from 330,000 ev. The most probable value given by Sargent,[15] as a result of an analysis of all experimental papers published between 1915 and 1933, is 340,000 ev. Recently, Neary[16] found a similar figure from a new experimental study of β-ray distribution. However, it should be pointed out that the first precise evaluation made by Magdwick,[17] by means of magnetic focusing and an ionization chamber, gave 395,000 ev for $E_{\text{Ra E}}$, Scott[18] found $E_{\text{Ra E}}=400{,}000$ ev by using a Geiger counter, and Ho and Wang[19] found $E_{\text{Ra E}}$ equal to 401,000 ev from measurements on Wilson cloud-chamber tracks. In both of these studies the high mean energy values are accompanied by an evident over-emphasis of the high velocity limit determinations ($H_{\max}=6600$ and 7500 g cm, respectively).

On the other hand, Alichanow, Alichanian and Dzelepow,[20] using a magnetic focusing arrangement with Geiger-Müller counters, found $E_{\text{Ra E}}$ equal to about 300,000 ev, and more recently Lecoin[21] deduced a value of 250,000 ev from measurements of the magnetic curvature of Wilson tracks, which figure seems to be too low. A comparison of our calorimetric results with those based on the study of the β-ray spectra leads to the conclusion that the number of electrons with energies below the average limit fixed by spectral analysis (20–50 kev) must be very small, and that certainly no more than 1 or 2 percent of the β-ray energies lie below 1 Mev.

It is to be noted that the mean energy of Ra E disintegration calculated by Martin and Townsend[22] in 1939, by careful investigation of the β-ray spectrum, was equal to 321,000 ev, and the very precise energy distribution (down to 5 kev) published by Flammersfeld,[23] after our work was completed, leads to a value of from 315,000 to 320,000 ev, which nearly agrees with our evaluation.

Acknowledgments

I wish to express my sincere appreciation to Professor Irene Joliot-Curie for her elucidating and stimulating discussions and to Professor F. Joliot for his continued interest and encouragement. I also wish gratefully to acknowledge the receipt of a grant from the Carnegie-Curie Foundation which enabled me to carry out this work.

[15] B. W. Sargent, Proc. Roy. Soc. **A139**, 659 (1933).
[16] G. J. Neary, Proc. Roy. Soc. **A175**, 71 (1940).
[17] E. Magdwick, Proc. Camb. Phil. Soc. **23**, 982 (1927).
[18] F. A. Scott, Phys. Rev. **48**, 391 (1935).
[19] P. C. Ho and M. H. Wang, Chinese J. Phys. **2**, 1 (1936).
[20] A. I. Alichanow, Physik. Zeits. Sowjetunion **1**, 78 (1936); A. I. Alichanian, A. I. Alichanow and P. S. Dzelepow, Bull. Acad. Sci. USSR, Ser. Phys. [19] **5**, 375 (1938).
[21] M. Lecoin, J. de phys. et rad. [7] **9**, 81 (1938).
[22] L. H. Martin and A. A. Townsend, Proc. Roy. Soc. **A170**, 190 (1939).
[23] A. Flammersfeld, Zeits. f. Physik **112**, 727 (1939).

Extension of the Radioactive Series, $Z=N\pm1$

D. R. ELLIOTT AND L. D. P. KING
Purdue University, West Lafayette, Indiana

(Received July 29, 1941)

The radioactive positron emitters Si^{27}, S^{31} and A^{35} were produced by 15-Mev alpha-particles while Sc^{41} was obtained by 8-Mev deutrons. The half-lives of these elements have been determined as 4.92 ± 0.1 seconds, 3.18 ± 0.04 seconds, 1.88 ± 0.04 seconds, and 0.87 ± 0.03 seconds, respectively. The upper limit of the energies of the positrons emitted by S^{31}, A^{35}, and Sc^{41} were measured and found to be 3.87 ± 0.15 Mev, 4.41 ± 0.09 Mev, and 4.94 ± 0.07 Mev, respectively. The Coulomb energies of the "extra proton" of the nuclei of the $Z-N=1$ were calculated according to two nuclear models. The variations in the Coulomb energies indicate a nuclear "shell" structure similar to that given by the Hartree model of the nucleus.

RADIOACTIVE nuclei for which $Z-N=\pm1$ are of particular interest in nuclear physics. It is possible to deduce the difference of Coulomb energy of an isobaric pair of nuclei of this type from the measured mass difference and from these measurements the radius of each of these nuclei can be calculated.[1,2] The high degree of symmetry of the nuclei of this type enables one to determine theoretically the difference in Coulomb energy. The calculation depends upon the assumption that the binding energy due to the specific nuclear forces is the same for each member of a pair of these isobaric nuclei.[1,2] Taking into account the conservation of energy it follows that the Coulomb energy associated with the "extra" proton is given by

$$E_c=E_{\max}+1.78 \text{ Mev}, \qquad (1)$$

where $E_{\max}$ is the upper limit of the positron spectrum.

The shortest periods of the series $Z-N=+1$ have been investigated in several laboratories[3-5] by different methods. The measurement of very short periods presents two difficulties not ordinarily encountered. The time lag of the recording instrument should be small compared to the period being measured, and the time intervals used should be equal in length or short compared to the half-life. In this laboratory a Geiger counter scaling circuit was used. The time lag of such a circuit is less than 10^{-4} second, and the sensitivity extends over a wide range, which makes it possible to use equal time intervals for a short period and still make proper corrections for the background. With a scale-of-16 it was possible to obtain accurate counting rates of 50,000 counts per minute. For the shortest periods measured it was necessary to use time intervals of about one-half second. This means that only 400 counts, at most, would appear in each time interval. Since the probable error of so few counts is of the order of five percent it is seen that such data give rather large statistical fluctuations.

In order to improve the statistics of these data the most obvious method is to increase the number of counts occurring in any time interval. Since this cannot be done directly because of the limited speed of the mechanical recorder, a procedure was followed that gives the same effect indirectly.

Each activity curve was measured several times (say n) for equal time intervals and the total number of counts occurring in the n first intervals, the n second intervals, etc., were plotted. Then the resulting "sum" curve is an activity curve in which the effective number of counts per time interval will be increased approximately n times that of any one set of data, and thus the statistical fluctuations will be reduced. This method made it possible to obtain at least 2000 counts for every point used in the determination of the half-lives. The samples do not have to be of the same strength, since no

[1] E. Wigner, Phys. Rev. **56**, 519 (1939).
[2] H. A. Bethe, Phys. Rev. **54**, 436 (1938).
[3] G. Kuerti and S. N. Van Voorhis, Phys. Rev. **56**, 614 (1939).
[4] White, Delsasso, Fox, and Creutz, Phys. Rev. **56**, 512 (1939).
[5] L. D. P. King and D. R. Elliott, Phys. Rev. **58**, 846 (1940).

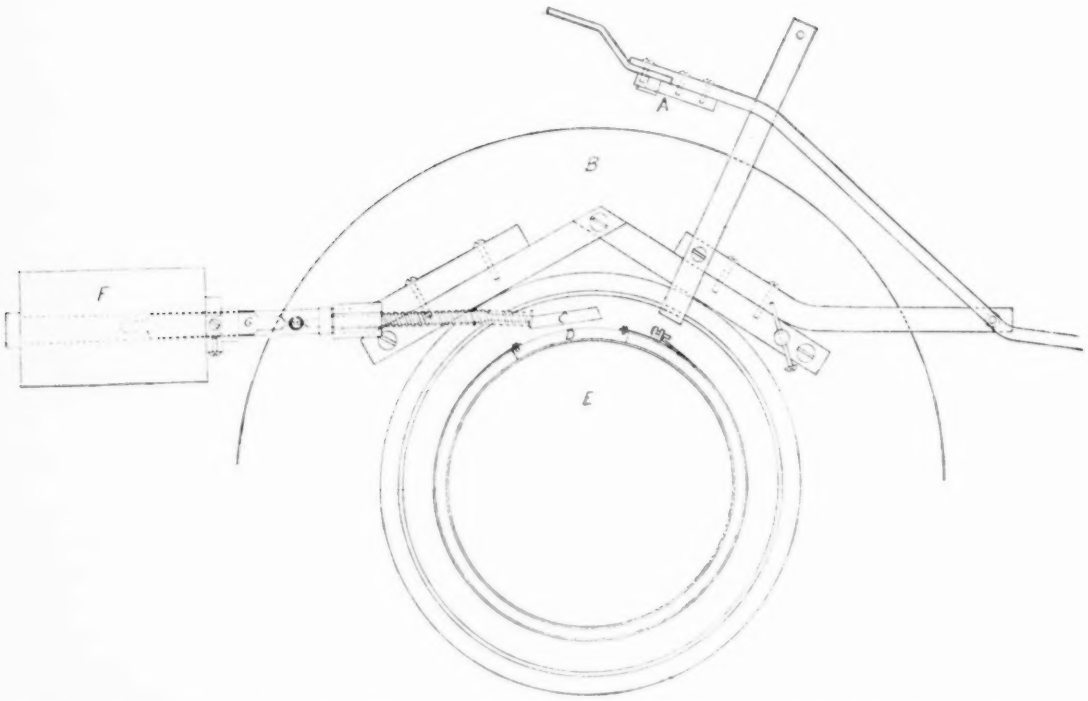

FIG. 1. Target holder of cloud chamber. The target holder *A* moves into place just behind the shutter *C*. *A*—target holder; *B*—coil face; *C*—shutter; *D*—window; *E*—chamber; *F*—solenoid; *G*—core.

error arises due to variations in beam energy, bombardment time, etc., if one is interested only in the rate of decay.

This procedure may be justified in the following way. In the first place, it is certainly equivalent to measuring the activity curves of all n samples simultaneously with n counters and recording only the total number of counts occurring in each time interval. This, again, is equivalent to measuring the activity curves of one sample consisting of the sum of the n samples with a single counter capable of registering the total number of counts.

The dial readings of the mechanical counter and a stop-watch were photographed by an electrically driven camera using a shutter speed of 1/100 second. Accurate timing was obtained by a motor-driven cam switch, the variations in speed of which varied less than 0.1 percent. The stop-watch readings served only as a check. After the short-lived activity had disappeared, the background reading was taken so that proper corrections for any long period components of the activity curve could be made.

The short half-lives of these elements made it necessary to bombard the samples outside of the cyclotron. The beam was brought into the air through a 0.006-inch aluminum window. The time required to transfer the samples from the beam to the recorder was less than 2 seconds. In order to eliminate any background due to air recoil nuclei, the samples were bathed in a hydrogen atmosphere during bombardment. In both the period and energy measurements several samples were used in rotation in order to reduce the influence of any longer periods. The cyclotron was "on" only during actual bombardments which varied from $\frac{1}{2}$ to 5 seconds depending on the sample used. Beam intensities of $\frac{1}{20}$ microampere were used in both the alpha- and deuteron bombardments.

Energy measurements were made by means of a cloud chamber. Figure 1 shows the arrangement of the source relative to the chamber. The positrons emitted from the source pass through a copper window $1\frac{1}{2}''$ long by $\frac{1}{2}''$ high, and 0.001" thick located in the wall of the chamber. Since tracks entering the chamber before expansion may appear diffuse, a shutter made of $\frac{1}{4}''$ brass was placed between the window and source. The

shutter was drawn back immediately after the chamber expanded. By placing the source about two inches in front of the window, a partial collimation was obtained. With this arrangement a very high percentage of the tracks traversed the full width of the chamber, thus making their measurement both easy and accurate. Moreover, it is seen that with proper magnetic field adjustment one-third of the chamber is accessible only to the highest energy rays. Thus it was possible to use a strong source and favor a high energy end of the spectrum, thereby reducing to a minimum the number of exposures needed to determine the upper spectrum limit. An average of four to five measurable tracks was obtained in each exposure. Because of the high energies of the positrons measured, an air-filled chamber was satisfactory. Only one photograph was made for each bombardment and four bombardments were made per minute. The radii of the tracks were measured by reprojecting them onto a screen by the same optical system used in taking the pictures. The curvatures of the tracks were then measured by comparing them with arcs of circles of known radii ruled on a thin celluloid sheet.

$_{14}Si^{27}$

The Rochester group,[3] and more recently the Princeton group,[4] have obtained this radioactive isotope by using high energy protons on aluminum. In this laboratory[5] Si^{27} was produced by alpha-bombardment of magnesium, Mg^{24} (α, n) Si^{27}. A 15-Mev alpha-beam from the Purdue cyclotron was used. Magnesium has three stable isotopes of mass numbers 24, 25, 26 with abundances of about 77, 12, 11 percent, respectively. Alpha-bombardment of magnesium 25, and 26 gives rise to the activities of 2.4 minutes and 6.7 minutes, respectively,[6] which form the background of the activity curve shown in Fig. 2. Analysis of this curve yields a value of 4.92 ± 0.1 sec. for the half-life of Si^{27} in agreement with the Princeton value of 4.9 ± 0.2 seconds.

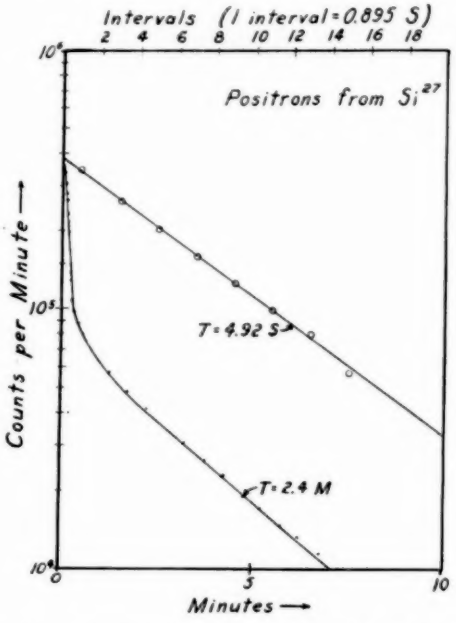

FIG. 2. Decay curve of S^{27} produced by $_{12}Mg^{24}$ (α, n) $_{14}Si^{27}$.

No energy measurements were made for Si^{27} in this laboratory.

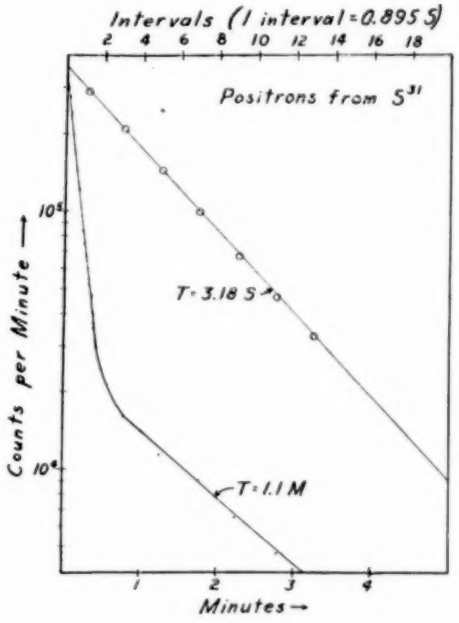

FIG. 3. Decay curve of S^{31} produced by $_{14}Si^{28}$ (α, n) $_{16}S^{31}$.

$_{16}S^{31}$

S^{31} was produced by alpha-bombardment of Si in the form of quartz according to the reaction Si^{28} (α, n) S^{31}.[5] Quartz was used because of its high purity. The oxygen in the quartz causes no difficulty, for bombardment of oxygen by a 15-Mev alpha-beam produces no activity. No attempt was made to eliminate the air recoils in this case, thus accounting for the 1.1-minute

[6] H. A. Bethe and W. J. Henderson, Phys. Rev. **56**, 1060 (1939).

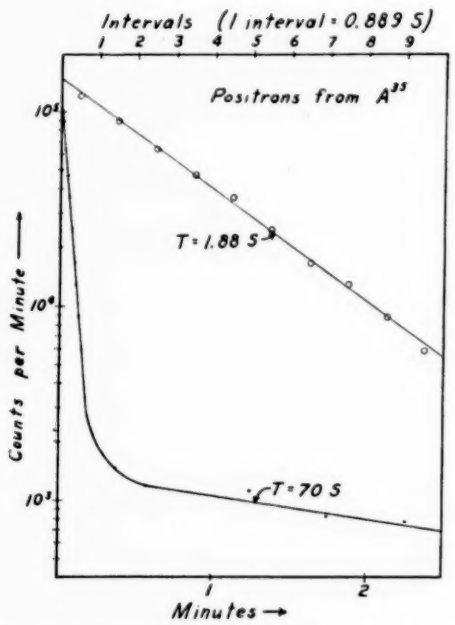

FIG. 4. Decay curve of S^{35} produced by $_{16}S^{32}$ (α, n) $_{18}A^{35}$.

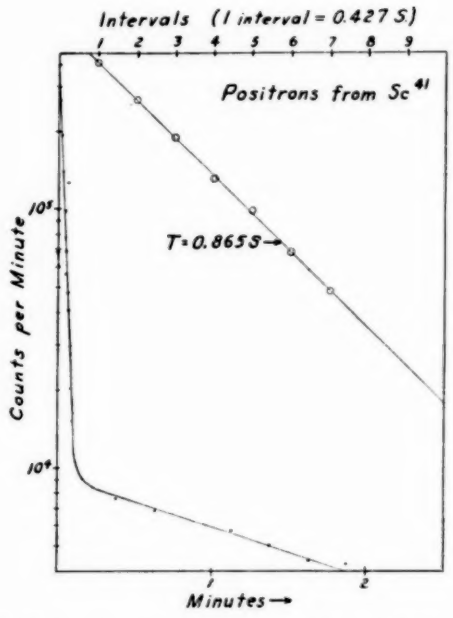

FIG. 5. Decay curve of Sc^{41} produced by $_{20}Ca^{40}$ (d, n) Sc^{41}.

period shown in Fig. 3. The assignment of the 3.18 ± 0.04-second period to S^{31} seems quite certain. In the first place, all other nuclei from probable alpha-reactions have been assigned with certainty. Also the Rochester group (private communication) and the Princeton group[7] have obtained the same half-life (3.2 ± 0.2 seconds) by proton bombardment of P^{31}.

The Princeton group report a value of 3.85 ± 0.07 Mev for the upper limit of the positron spectrum. This is to be compared with our value of 3.87 ± 0.15 Mev.[8] Both measurements were obtained by cloud-chamber methods.

$_{18}A^{35}$

A^{35} was obtained by the bombardment of sulphur with 15-Mev alphas.[5,8] Sulphur samples were prepared by melting flowers of sulphur by gentle heat until a thin straw-colored liquid was obtained, and then pouring it into a clean iron mold and allowing it to set. The value of 1.9 ± 0.1 seconds was obtained for the half-life. Because this was in disagreement with the value of 2.2 ± 0.2 sec. published later by the Princeton group,[7] the measurement of the half-life was repeated and a value of 1.88 ± 0.04 seconds was obtained (see Fig. 4). This time a filter of $\frac{1}{8}''$ Al was placed between the active sample and the counter, in order to reduce the low energy com-

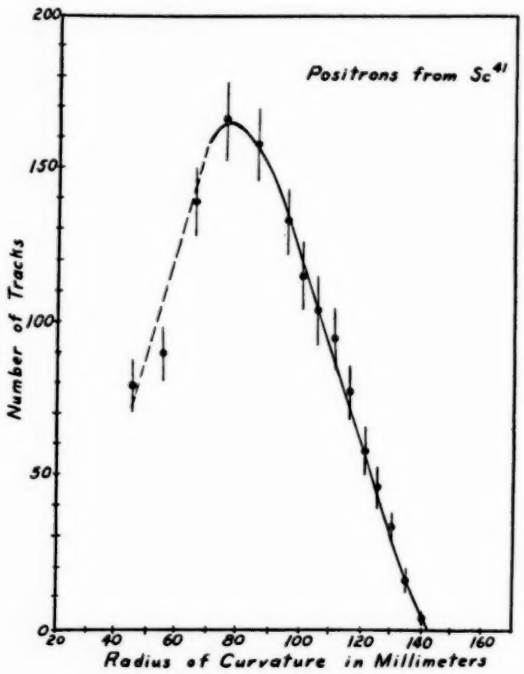

FIG. 6. Positrons from Sc^{41}. Maximum energy 4.94 ± 0.07 Mev, half-life 0.87 ± 0.03 second.

[7] White, Creutz, Delsasso, and Wilson, Phys. Rev. **59**, 63 (1941).
[8] D. R. Elliott and L. D. P. King, Phys. Rev. **59**, 403 (1941).

ponents of the background. The background correction for the resulting activity curve changed the initial slope by less than two percent.

The value of 4.38 ± 0.07 Mev obtained by the Princeton group for the energy of the upper limit of the positron spectrum of A^{35} compares well with our value of 4.41 ± 0.09 Mev.[8]

$_{21}Sc^{41}$

The production of Sc^{41} was obtained by deuteron bombardment of calcium according to the reaction Ca^{40} (d, n) Sc^{41}. The samples used consisted of calcium metal turnings waxed to small brass supports, so that no part of the support was exposed to the deuteron beam. Measurement of the half-life yielded a value of 0.87 ± 0.03 second. (See Fig. 5.) A $\frac{1}{8}''$ aluminum filter placed between the active sample and the counter suppressed all other periods so that their combined effect was reduced from twenty-five percent to less than two percent of the initial activity. Because Sc^{41} cannot be reached by any other of the usual nuclear reactions its identification is mostly one of elimination. All other probable Ca $(d, -)$ reactions have been investigated carefully.[9] Further identification of the 0.87-second period with Sc^{41} is given also by the fact that both the value of the period and the value of the upper energy limit of the positrons are in accord with the values obtained for these quantities by extrapolation from other members of the series $Z-1=\pm1$ (see Figs. 7, 8, and 9).

Energy measurements made by a cloud chamber gave a value of 4.94 ± 0.07 Mev[8] for the upper energy limit of the positron spectrum (see Fig. 6). The unusually high value of the positron energy eliminates the possibility that impurities are effecting the value of the upper energy limit. The complete absence of a "tail" may indicate that, in many cases, the presence of a "tail" in a distribution curve is caused by an impurity. Because of the changing geometry of the experimental set-up for different energy particles and the increased chance of stray tracks at lower energies it would be difficult to compare the entire curve with the theoretical Fermi curve even if an attempt had been made to count all

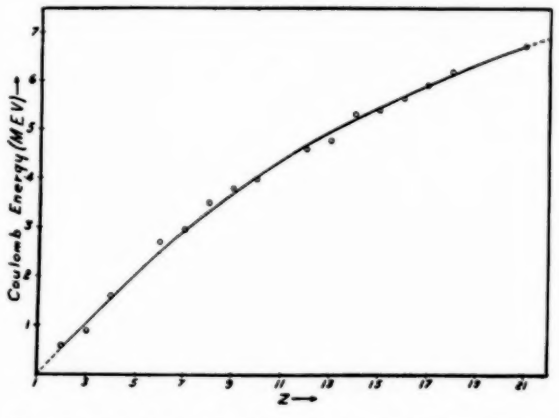

FIG. 7. Experimental values of the Coulomb energy of the "last" proton calculated by Eq. (1) for nuclei with one more proton than neutron, plotted as a function of atomic number. $E_c=E_{max}+1.78$.

[9] G. T. Seaborg, Chem. Rev. **27**, 199 (1940).

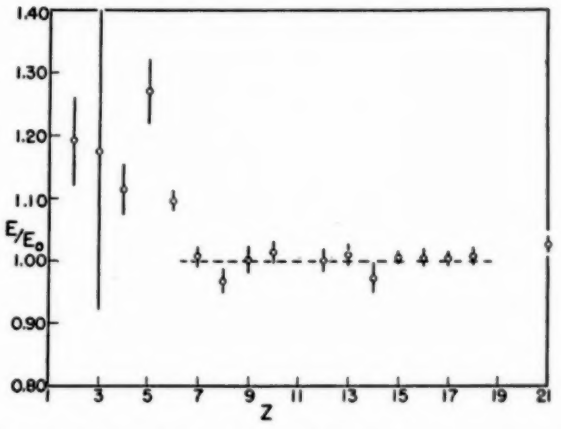

FIG. 8. Ratio of the calculated Coulomb energy to the experimental values. $E=0.592(A-1)/A^{\frac{1}{3}}$.

TABLE I. *Calculation of Coulomb energies, "core" model.*

Z	a	b	ρ	R_0	$f(\rho)$	E (MEV)
2	6.65	1.118	0.618	1.80	0.289	0.70
4	7.65	0.92	0.374	2.46	0.324	1.70
5	1.85	1.84	0.689	2.67	0.280	1.80
6	12.35	0.704	0.244	2.90	0.347	2.57
7	5.3	1.065	0.348	3.06	0.328	2.77
8	11.6	0.715	0.222	3.22	0.352	3.30
9	4.5	0.145	0.341	3.35	0.330	3.40
10	11.0	0.73	0.210	3.49	0.355	3.95
11	8.0	0.852	0.236	3.61	0.350	4.18
12	13.0	0.669	0.180	3.73	0.361	4.59
13	7.5	0.877	0.228	3.84	0.351	4.72
14	11.9	0.696	0.117	3.94	0.362	5.14
15	8.9	0.803	0.191	4.03	0.359	5.38
16	12.9	0.667	0.162	4.12	0.365	5.63
17	9.6	0.772	0.183	4.22	0.361	5.89
18	9.6	0.772	0.180	4.30	0.361	6.14
21	10.0	0.75	0.166	4.53	0.364	6.92

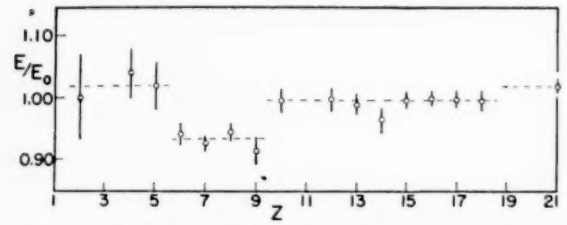

FIG. 9. Ratio of the Coulomb energy calculated by the central core model to the experimental values. $E=4.31(Z/R_0)f(\rho)$.

low energy tracks. However, the high energy end has a shape predicted by the Fermi theory.

CALCULATION OF COULOMB ENERGY

The experimental values of the Coulomb energy of the "last proton" calculated by Eq. (1) are shown in Fig. 7 as a function of atomic number. From this it is seen that the Coulomb energies of this series can be represented by a smooth function of the atomic number plus small local variations which seem to be quite random in their occurrence. However, in some cases, these variations are several times larger than the probable error of the measurements.

It has been pointed out[1,2] that the smooth curve is easily explained from the assumption that the nucleus is a homogeneous sphere the volume of which is proportional to the number of particles. This assumption leads to the following expression for the Coulomb energy of the last proton:

$$E_c=0.6(A-1)e^2/r_0A^{\frac{1}{3}},$$

where A is the mass number of the nucleus, $r_0A^{\frac{1}{3}}$ the volume of the nucleus, and e the electronic charge. If r_0 is determined from the Coulomb energy of the "extra proton" of P^{29} (5.41 Mev), this gives

$$E_c=0.592(A-1)/A^{\frac{1}{3}}\ \text{Mev} \quad \text{and}$$
$$r_0=1.47\times10^{-13}\ \text{cm}.$$

Figure 8 shows the ratios of the calculated Coulomb energies to the experimental values. It is seen that the theoretical and experimental results agree for $Z\geqslant 6$, therefore our assumption that the volume of the nucleus is proportional to the number of particles must be satisfied. However, for $Z\leqslant 6$ the curve indicates that the volume occupied per particle increases with decreasing atomic number.

Bethe[2] has proposed a model to account for the local deviations of the Coulomb energies by taking into account the extension of the wave function of the "extra proton." For this he assumes that the nucleus consists of a homogeneous core of radius R_0 and an "extra proton," the wave function of which is assumed to be a constant inside the core and to satisfy the force-free wave equation outside the core.

In the above references several approximations were made which led to quite large errors in some cases. A direct calculation leads to the following formula for the Coulomb energy of the "extra proton,"[10]

$$E_c=3Z_0e^2f(\rho)/R_0 \qquad (2)$$

$$\rho=b/R_0 : b=\hbar/2(2M\epsilon)^{\frac{1}{2}} : R_0 = r_0[A_0+1/(1+3\rho)]^{\frac{1}{3}},$$

where Z_0 is the atomic number of the "core," A_0 the number of "core" particles, ϵ is the binding energy of the "extra neutron," and f is a slowly varying function of its argument (see Fig. 10). If b, and R_0 are measured in units of 10^{-13} cm, and the parameter r_0 determined to give the observed value of the Coulomb energy of the "extra proton" of P^{29}

$$E_c=4.31Z_0f(\rho)/R_0\ \text{Mev}. \qquad (3)$$

Table I shows the values of the various variables appearing in Eqs. (2) and (3). Here

TABLE II. *Coulomb energies.*

ATOMIC NUMBER	HOMOGENEOUS NUCLEUS MODEL	HOMOGENEOUS CORE MODEL	EXPERIMENTAL VALUES
2	0.822	0.689	0.70
3	1.39	—	0.80
4	1.86	1.70	1.81
5	2.28	1.80	1.84
6	2.66	2.57	2.73
7	3.03	2.77	2.98
8	3.37	3.30	3.50
9	3.69	3.40	3.70
10	4.0	3.95	3.98
11	4.30	4.18	—
12	4.59	4.59	4.60
13	4.86	4.72	4.77
14	5.14	5.14	5.32
15	5.41	5.38	5.41
16	5.66	5.63	5.65
17	5.91	5.89	5.91
18	6.16	6.14	6.18
21	6.88	6.92	6.73

[10] This calculation has been carried out somewhat differently from that of Bethe.[2] See Appendix for details.

$Z_0=Z-1$, $A_0=2Z-1$, and $r_0=1.32$. The values of ϵ were taken from Barkas' table of masses.[11] Table II lists the observed coulomb energies together with the values calculated by each of these models.

Figure 9 shows the ratio of the values of the Coulomb energy calculated by the central core model to the experimental values. This graph has an altogether different character than the graph shown in Fig. 8, derived from the homogeneous model of the nucleus. There is no definite uptrend for the lighter nuclei and instead of the seemingly unrelated deviations of points from the average, they fall into four definite groups as shown by the dotted lines. At first one might be inclined to think that the group character of the points in Fig. 9, as well as the relatively large separations between groups, might be due to an over-correction of the model, the roughness of which cannot be denied. However, examination of Table I shows that the values of ϵ for the elements of even atomic number $Z=6$ to $Z=14$ are all about the same, and much more than the values of ϵ of their odd neighbors. If large errors are present in the model due to over-correction, then the average of the points corresponding to even Z should lie definitely apart from the average for odd Z. Although there seems to be a slight tendency toward such an effect between the elements $Z=6$ and $Z=9$, the large separation between $Z=9$ and $Z=10$ cannot be explained on this basis. Therefore, it appears that the "cores" of these elements vary in some regular manner. The "core" affects Eq. (3) only through its radius R_0, so that Fig. 9 indicates that elements having "cores" of 10, 12, 14, and 16 particles have radii smaller than given by Eqs. (2). This means that the "cores" of these elements are more tightly bound than those having, for example, 2, 6, or 8 particles in the "core." Although this is in agreement with the low binding energies of H^2, Li^6, Be^8, too much weight must not be given to the corresponding values of the nuclear radius of these elements, because the above model cannot be expected to be reliable for so few nuclear particles. However, this objection is not present for the higher mass numbers and the grouping can be attributed to abrupt changes in the average volume occupied by a neutron or proton in the "core." The fact that one of these transitions occurs after a "core" of 16 particles and the other somewhere between 36 and 40 particles is in agreement with the shell structure of nuclei predicted from the Hartree model.[11, 12]

The authors are indebted to Professor Bethe for first suggesting this research and to Professor Weisskopf for further encouragement. We wish to thank also Dr. R. G. Sachs for discussions and suggestions concerning some of the theoretical aspects.

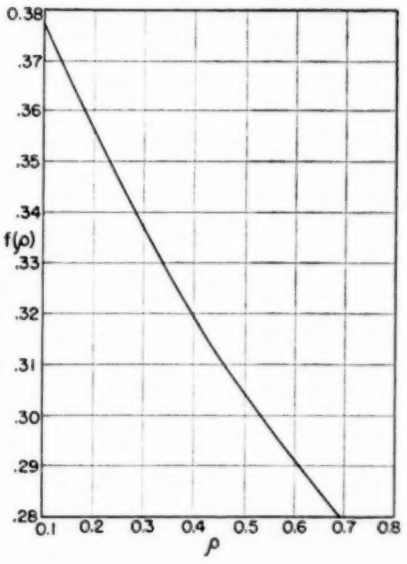

FIG. 10. Values of the function $f(\rho)=[0.4+I(\rho)]/(1+3\rho)$.

APPENDIX

According to Bethe[2] the wave function of the "extra neutron" is

$$U_r=(a/r)\exp[-(r-R_0)/2b] \quad r\geq R_0,$$
$$U_r=a/R_0 \quad r\leq R_0,$$

where $b=\hbar/2(2M\epsilon)^{\frac{1}{2}}$, and ϵ is the binding energy of the "extra neutron," to be taken from experiment, and M is the reduced mass of the system.

The normalization condition

$$\int U^2 dv=1$$

gives

$$a^2=1/4\pi(b+R_0/3).$$

If, now, the "extra neutron" is replaced by a proton, it is assumed that the wave function of the proton is the same as that of the neutron, the Coulomb energy of the

[11] W. H. Barkas, Phys. Rev. **55**, 691 (1939).

[12] H. A. Bethe and R. F. Bacher, Rev. Mod. Phys. **8**, 173 (1936).

"extra proton" is given by[2]

$$E_c=\frac{Ze^2}{b+R_0/3}\left[\frac{2}{5}+\int_{R_0}^{\infty}\frac{dr}{r}\exp\left(\frac{-(r-R_0)}{b}\right)\right]. \quad (4)$$

If we let

$$\rho=b/R_0,$$

$$I(\rho)=\int_{-R_0}^{\infty}\frac{dr}{r}\exp\left(\frac{-(r-R_0)}{b}\right),$$

and

$$f(\rho)=\frac{0.4+I(\rho)}{1+3\rho},$$

Eq. (4) becomes

$$E_c=3Z\epsilon^2 f(\rho)/R_0.$$

If b is measured in units of 10^{-13} cm then

$$b=\frac{2.36}{\epsilon^2}\left(\frac{A_0+1}{A_0}\right)^{\frac{1}{3}},$$

where ϵ is expressed in m.m.u., and $f(\rho)$ is shown plotted in Fig. 10.

It is now assumed that the volume of the core is proportional to the number of core particles A_0 plus the fraction of the "extra neutron" within the sphere of radius R_0. Therefore,

$$R_0^3=r_0^3\left(A_0+\int_0^{R_0}U^2dv\right)$$

or

$$R_0=r_0[A_0+1/(1+3\rho)]^{\frac{1}{3}}.$$

OCTOBER 1, 1941 PHYSICAL REVIEW VOLUME 60

A Rotational Analysis of Some CS_2 Bands in the Near Ultraviolet System*

L. N. LIEBERMANN
Ryerson Physical Laboratory, University of Chicago, Chicago, Illinois

(Received July 7, 1941)

Six bands in the λ3100 system of CS_2, photographed in absorption on a 30-foot grating spectrograph, have been analyzed and B values are given for their initial and final states. The band structure is of the simple PR branch type, all of the observed bands originating from $^1\Sigma^+_u-{}^1\Sigma^+_g$ transitions. The bands at λ3468, λ3501, and λ3535 originate in the normal state, giving a value $r_0=1.548$A for the normal carbon-sulphur separation. A partial vibrational analysis shows that for the bending vibration, $2\nu_2''=802$ cm^{-1}. Two progressions, $v_2''=0$ and $v_2''=2$, indicate that $\nu_2'=270$ cm^{-1}. Two bands, λ3501 and λ3601, have their common upper $^1\Sigma^+_u$ state perturbed by a $^1\Pi_u$ state. A perturbation analysis gives constants which are in good agreement with observation and in addition gives the B value for the perturbing $^1\Pi_u$ state. Evidence is presented which indicates that the excited electronic state of CS_2 is bent. It is shown that, even if the molecule is bent to 125°, the P and R series may still be represented by a simple quadratic formula exactly as for a linear molecule, for J values less than 25. The state nomenclature used ($^1\Sigma^+_u$, $^1\Pi_u$, etc.) is that corresponding to the vibronic (electronic-vibrational) states of a linear molecule.

Introduction

THE analysis of the carbon disulphide spectrum has been of considerable interest to the band spectroscopist. Measurements on the Raman spectrum[1] of the liquid and on the infrared spectrum of the gas[2–4] have determined the fundamental vibration frequencies in the normal state. Recent improvements in the resolving power of infra-red spectrometers have made possible a rotational analysis of the $\nu_1+\nu_3$ band. The analysis showed it to be of the parallel type with $B''=0.112$ and $B'=0.111$.[5]

An investigation of vibrational structures in the far ultraviolet absorption spectrum has been made by Price and Simpson.[6] They were unable to make a definite assignment of vibrational frequencies of the molecule in the excited states, but reported possible series.

The first reported attempt to analyze the well-known ultraviolet absorption system near

* Assistance in the preparation of the materials was furnished by the personnel of Works Project Administration Official Project No. 665-54-3-87.

[1] S. C. Sirkar, Ind. J. Phys. **10**, 189 (1936).
[2] C. R. Bailey and A. B. D. Cassie, Proc. Roy. Soc. **A132**, 236 (1931).
[3] D. M. Dennison and N. Wright, Phys. Rev. **38**, 2077L (1931).
[4] C. R. Bailey, Nature **140**, 851 (1937).
[5] J. A. Sanderson, Phys. Rev. **50**, 209 (1936).
[6] W. C. Price and D. M. Simpson, Proc. Roy. Soc. **A165**, 272 (1936).

λ3200 was that of Wilson[7] who photographed the bands under various conditions of temperature and pressure with a low dispersion instrument. Jenkins[8] attempted a rotational analysis of some of these bands, but, with the 21-foot grating spectrograph used, he was unable to resolve them sufficiently for an analysis. He was, however, able to report that the band structures resembled those of a diatomic molecule. Watson and Parker[9] attempted a vibrational analysis of this system and reported a possible vibrational frequency of 270 cm^{-1} which has also been observed here (see below). Herzberg[10] has also attempted to analyze these bands.

Kusch and Loomis[11] have obtained magnetic rotation spectra of this same band system on a 21-foot grating spectrograph and reported possible vibrational series. In addition, they observed doublets separated by about 17 cm^{-1} in the magnetic rotation spectrum. In the present work[12] the same bands have been rephotographed with higher resolving power and six of them have been analyzed. The analysis shows that the Kusch-Loomis doublets agree with the *P* and *R* branches of the bands, the low frequency component being the *P* branch, the high frequency, the *R* branch.

Experimental

A series of absorption photographs was made varying both the length of the column and the pressure of the vapor. Two Pyrex tubes of lengths 1 and $2\frac{1}{2}$ meters, and diameter 4 cm, having quartz windows cemented on with De Khotinsky cement, were employed. Liquid carbon disulphide was introduced into a small bulb attached to one end of the tube. In order to make the low gas pressure in the tube accurately reproducible, it was controlled by immersing the bulb into baths of known constant temperature. Vapor pressures of 4 mm and 1.0 cm were obtained by immersing the bulb into melting chloroform (−63.5°C) and melting chlorbenzene (−45°C), respectively. Higher pressures were found to be sufficiently accurately reproducible by cooling the bulb to −78°C and then allowing it to warm up slowly; when a mercury manometer attached to the tube showed that the desired pressure was attained, the bulb was sealed off. Since carbon disulphide has a vapor pressure of 28 cm at room temperature, a large range of gas pressures could be obtained without the necessity of heating the absorption tube. The vapor in the tube was changed once every hour by evacuating the tube and repeating the above process. This was done in order to avoid possible contamination by the by-products of the photo-decomposition of CS_2.

A hydrogen lamp was utilized as a source of continuum for the region 2900A to 3350A. This lamp was constructed of Pyrex in the conventional manner, with two large electrodes and a 30-cm water-cooled capillary and two quartz windows. A palladium valve was permanently fixed in the lamp so that any loss of hydrogen could be replaced without admitting air into the lamp. The lamp was operated at 0.8 ampere at 2500 volts.

A tungsten filament lamp served as a source for the continuum in the region 3350A to 3700A. The lamp, which was specially designed for this purpose, used a heavy tungsten ribbon which could be considerably overloaded to give a high intensity in this spectral region. The filament was operated at 110 amperes and about 18 volts. At an estimated temperature of about 3600°K, the filament had a lifetime of 10–20 hours. Beutler and Metropolis[13] later improved the design and investigated some of the characteristics of this lamp.

The spectra analyzed were obtained in the second order of an aluminized, 30-foot radius grating having 30,000 lines per inch, and a useful surface of $5\frac{1}{2}$ inches. The grating was ruled by Professor H. G. Gale in the Ryerson Laboratory. The resolving power attained on the plates is very near to 300,000.

Exposure times of 30 hours with the hydrogen lamp and 10–15 hours with the tungsten lamp were required. Such long exposure times were unavoidable in using a high dispersion grating and a very narrow slit (12 microns). This fact

[7] E. D. Wilson, Astrophys. J. **69**, 34 (1929).
[8] F. A. Jenkins, Astrophys. J. **70**, 191 (1929).
[9] W. W. Watson and A. E. Parker, Phys. Rev. **37**, 1484 (1931).
[10] G. Herzberg, unpublished work.
[11] P. Kusch and F. W. Loomis, Phys. Rev. **55**, 850 (1939).
[12] Some of these results have been given in (a) Phys. Rev. **58**, 183L (1940); (b), Phys. Rev. **59**, 106A (1941).
[13] H. Beutler and N. Metropolis, J. Opt. Soc. Am. **30**, 115 (1940).

TABLE I. *Band at λ3468, $\nu_0 = 28{,}816.35$.*

J	Wave Numbers of Observed Lines $R(J)$	$P(J)$	$\Delta_2F''(J+1) = R(J) - P(J+2)$	$\Delta_2F'(J) = R(J) - P(J)$
0	28,816.63			
2	17.10		1.59	
4	17.54	28,815.51	2.43	2.03
6	18.03	15.11	3.30	2.92
8	18.58	14.73	4.19	3.85
10	19.08	14.39	5.02	4.69
12	19.62	14.06	5.86	5.56
14	20.26	13.76	6.77	6.50
16	20.85	13.49	7.65	7.36
18	21.48	13.20	8.53	8.28
20	22.11	12.95	9.38	9.16
22	22.78	12.73	10.27	10.05
24	23.44	12.51	11.13	10.93
26	24.14	12.31	12.01	11.83
28	24.79	12.13		12.66
30	25.49			
32	26.22			
34	26.92			
36	27.65			
38	28.37			
40	29.10			

TABLE II. *Band at λ3501, $\nu_0 = 28{,}548.83$.*

J	Wave Numbers of Observed Lines $R(J)$	$P(J)$	$\Delta_2F''(J+1) = R(J) - P(J+2)$	$\Delta_2F'(J) = R(J) - P(J)$
0	28,549.10*		0.73*	
2	49.52	28,548.37*	1.54	1.15*
4	50.00	47.98	2.42	2.02
6	50.52	47.58	3.29	2.94
8	51.06	47.23	4.15	3.83
10	51.61	46.91	5.04	4.70
12	52.19	46.57	5.90	5.62
14	52.79	46.29	6.76	6.50
16	53.04	....	7.63	7.39
	53.42	46.03		
18	53.80	....	8.50	8.31
	54.10	45.79		
20	54.54	....	9.43*	9.25
	54.85	45.60		
22	55.27	45.42*		10.20*
	55.62			
24	55.99			
	56.41			
26	56.71			
28	57.45			
30	58.18			
32	58.94			
34	59.70			
36	60.49			
38	61.28			
40	62.09			
42	62.89			
44	63.69			
46	64.50			
48	65.32			
50	66.12			
52	66.96			
54	67.80			
56	68.63			
58	69.41			
60	70.26			
62	71.06			
64	71.87			
66	72.67			
68	73.48			
70	74.29			

* Indicates blended or weak lines.

provided the chief difficulty in obtaining satisfactory photographs, since the barometric pressure rarely remained constant during these long exposures. A change in pressure of only 0.3 inch is sufficient with this high resolving power to shift detectably the spectrum lines. The most favorable conditions for observation of the bands were as follows:

Region (in A)	Gas Pressure (in mm)	Column Length (in m)
3050–3150	4	1
3250–3350	10	1
3350–3450	60	1
3450–3550	120	1
3550–3700	240	2½

These conditions were determined by first photographing the spectrum under small dispersion.

DATA

The most intense bands are located at 3100A with the system extending symmetrically on each side for about 600A. The system consists of an unusually large number of bands. Consequently, few bands are to be found free from overlapping.

High dispersion photographs of the spectrum show that the bands are simple in appearance, resembling those of a diatomic molecule. Practically all of the bands are of the *PR* branch type. A few, whose structure is too overlapped to permit an analysis to be made, may possibly be of the *PQR* branch type.

Six of the bands were found to be sufficiently free from overlapping to permit a rotational analysis to be made. In spite of the high resolving power attained, the bands were not completely resolved in the neighborhood of the head. The wave numbers of those lines of each band which were capable of measurement are listed in Tables I–VI. Lines which are weak or which consist of unresolved blends are designated by an asterisk (*). Those lines which are not so designated are estimated to be accurate to plus or minus 0.01 cm^{-1}. It will be noted that some *R* lines in the bands at λ3601 and λ3501 consist of

TABLE III. *Band at λ3535, $\nu_0 = 28{,}273.74$.*

J	Wave Numbers of Observed Lines $R(J)$	$P(J)$	$\Delta_2F''(J+1) = R(J) - P(J+2)$	$\Delta_2F'(J) = R(J) - P(J)$
0	28,274.03*		0.66*	
2	74.43*	28,273.37*	1.48*	1.06*
4	74.95*	72.95	2.36*	2.00*
6	75.42*	72.59	3.22*	2.83*
8	76.00	72.20	4.15	3.80*
10	76.58*	71.85*	5.03	4.73
12	77.21	71.55	5.94	5.66
14	77.79	71.27	6.73	6.52
16	78.47	71.06	7.65	7.41
18	79.10	70.82	8.53	8.28
20	79.79	70.57	9.39	9.22
22	80.53	70.40		10.13
24	81.23			
26	81.99			
28	82.77			
30	83.55			
32	84.37			
34	85.20			
36	86.05			
38	86.92			
40	87.79			
42	88.70			
44	89.62			
46	90.58			
48	91.53			
50	92.50			
52	93.48			
54	94.46			
56	95.48			
58	96.51			
60	97.55			
62	98.58			
64	99.67			
66	28,300.74			
68	01.87			

* Indicates blended or weak lines.

TABLE IV. *Band at λ3601. $\nu_0 = 27{,}746.94$.*

J	Wave Numbers of Observed Lines $R(J)$	$P(J)$	$\Delta_2F''(J+1) = R(J) - P(J+2)$	$\Delta_2F'(J) = R(J) - P(J)$
0				
2	27,747.65*		1.57*	
4	48.12	27,746.08	2.42	2.04*
6	48.63	45.70	3.31	2.93
8	49.14	45.32	4.16	3.82
10	49.68	44.98	5.04	4.70
12	50.25	44.64	5.91	5.61
14	50.84	44.34	6.78	6.50
16	51.44	44.06	7.65	7.38
18	51.81	....	8.55*	8.32
	52.11	43.79		
20	52.50	....	9.55*	9.23*
	52.79	43.56		
22	53.18	....		10.31*
	53.55	43.24*		
24	53.88			
26	54.57			
28	55.26			
30	55.98			
32	56.67			
34	57.38			
36	58.12			
38	58.86			
40	59.60			
42	60.33			
44	61.08			
46	61.80			
48	62.57			
50	63.30			
52	64.04			

* Indicates blended or weak lines.

pairs with the same J value. These lines are the result of a perturbation which will be discussed below.

Rotational Analysis

The carbon disulphide molecule is expected to obey Bose-Einstein statistics because the sulphur atom (mass 32) has an even number of protons and neutrons. This means that the total wave function should be symmetric in the nuclei. Since the spins of the sulphur atoms are zero, only symmetric rotational functions are to be expected. Consequently, alternate lines should be missing in Σ to Σ and Σ to Π transitions.

The notation (Σ, Π, and so on) here and below is that corresponding to the vibronic,[14] i.e., electronic-vibrational states of a linear molecule. It is in general the vibronic rather than merely the electronic states involved which determine the structure of any band in a polyatomic molecule's spectrum.

Figure 1 shows a microphotometer trace of the band at λ3501. As is seen from the figure, the first P line is separated from the first R line by $1\frac{1}{2}$ spacings, thus indicating missing alternate lines.[15] A consideration of the relative intensities (see Fig. 1) of the first few lines of the P and R branches shows that even J values are present in the lower state. Similar considerations show that five of the six measured bands have even J values in their lower states, which are designated $^1\Sigma^+_g$, and upper states which must then according to the selection rules for linear molecules and in view of the PR band structure, be $^1\Sigma^+_u$. The other band at λ3468 *apparently* has a Q branch and an analysis was first reported assuming this to be correct.[12a] However, the B values calculated from this band were then found to differ markedly from the other five bands. Also few, if any, other bands in this system have Q

[14] R. S. Mulliken, J. Phys. Chem. **41**, 168 (1937).

[15] R. S. Mulliken, Rev. Mod. Phys. **3**, 150 (1931), Fig. 33.

TABLE V. *Band at λ3637, $\nu_0 = 27{,}471.96$.*

J	Wave Numbers of Observed Lines $R(J)$	$P(J)$	$\Delta_2F''(J+1) = R(J) - P(J+2)$	$\Delta_2F'(J) = R(J) - P(J)$
0				
2		27,471.51		
4	27,473.14	71.12	2.39*	2.02
6	73.64	70.75	3.26	2.89
8	74.19	70.38	4.16	3.81
10	74.75	70.03	5.05	4.72
12	75.32	69.70	5.91	5.62
14	75.92	69.41	6.80	6.51
16	76.54	69.12	7.67	7.42
18	77.19	68.87	8.57	8.32
20	77.85	68.62	9.43	9.23
22	78.53	68.42	10.31	10.11
24	79.21	68.22		10.99
26	79.92			
28	80.66			
30	81.42			
32	82.20			
34	82.97			
36	83.75			
38	84.58			
40	85.43			
42	86.22			
44	87.08			
46	87.94			
48	88.83			
50	89.74			
52	90.64			
54	91.53			
56	92.46			
58	93.40			
60	94.38			

* Indicates blended or weak lines.

TABLE VI. *Band at λ3673, $\nu_0 = 27{,}190.08$*

J	Wave Numbers of Observed Lines $R(J)$	$P(J)$	$\Delta_2F''(J+1) = R(J) - P(J+2)$	$\Delta_2F'(J) = R(J) - P(J)$
0				
2	27,190.67*		1.50*	
4	91.17*	27,189.17*	2.41	2.00*
6	91.67*	88.76*	3.30	2.91*
8	92.23	88.37	4.18	3.86*
10	92.71	88.05	5.02	4.66
12	93.26	87.69	5.91	5.57
14	93.83	87.35	6.82	6.48
16	94.41	87.01	7.67	7.40
18	95.01	86.74	8.55	8.27
20	95.62	86.46	9.42	9.16
22	96.25	86.20	10.30	10.05
24	96.89	85.95	11.18	10.94
26	97.56	85.71	12.05	11.85
28	98.23	85.51	12.91	12.72
30	98.92	85.32	13.81	13.60
32	99.62	85.11		14.51
34	27,200.34			
36	01.07			
38	01.81			
40	02.60			
42	03.38			
44	04.19			
46	04.98			
48	05.80			
50	06.60			
52	07.42			
54	08.31			
56	09.13			
58	10.02			
60	10.92			

* Indicates blended or weak lines.

branches (see above). Hence this band has been re-analyzed, assuming that it also is of the type $^1\Sigma^+_u - {}^1\Sigma^+_g$ and that the apparent Q branch is simply the overlapping head of another band. The new analysis gives (see below) Δ_2F'' values which are the same as those of λ3501 and λ3535, and hence is probably correct.

The CS_2 molecule is well known to be linear in its normal state. The rotational term values should then be given by the formula

$$E/hc = \text{const.} + BJ(J+1) + DJ^2(J+1)^2, \quad (1)$$

where $B = h/8\pi^2Ic$ and D is the centrifugal expansion term.

Mulliken[16] has suggested that CS_2 is triangular in the excited electronic state of the bands discussed here. The molecule then becomes an asymmetrical top. If, however, the apex angle 2α is not too small, the rotational term formula can be expanded in an expression very similar to that of a symmetrical top with a symmetry axis parallel to the line joining the two sulphur atoms and with angular momentum $Kh/2\pi$ around this axis. For $K=0$ the terms are given by

$$E/hc = \text{const.} + BJ(J+1) - (D+S)J^2(J+1)^2 + \cdots, \quad (2)$$

where $B = h/16\pi^2c(1/I_C + 1/I_B)$, and where I_C and I_B are the largest and the middle moment of inertia. The coefficient D (centrifugal expansion parameter) is extremely complicated for the asymmetrical top and cannot be evaluated here. The coefficient S may be considered as a parameter giving the deviations of the energy of a rigid asymmetrical top from that given by the usual symmetrical top formula. By using Eq. (10) of Wang's[17] expression for the energy of an asymmetrical top, and by making the approximation that the large moment of inertia is equal to the middle moment of inertia, S can be shown to be

[16] R. S. Mulliken, J. Chem. Phys. **3**, 720 (1935).

[17] S. C. Wang, Phys. Rev. **34**, 243 (1929).

(for $K=0$):

$$S=\frac{h\mu^3\cot^6\alpha}{2048I_C m^3\pi^2 c}, \tag{2a}$$

where α is the half-apex angle; $\mu=2mM/2m+M$, where m = atomic weight of sulphur and M the atomic weight of carbon; I_C is the large moment of inertia.

Referring to Eqs. (1) and (2), it is seen that the forms of the expression for E/hc are essentially the same (for $K=0$) whether the molecule is linear or bent in the upper state. It seems reasonable to assume[18] that the selection rules $\Delta J=\pm 1$, for $\Delta K=0$, also hold. Hence the usual procedure for the evaluation of rotational constants for linear or diatomic molecules may be followed. Further, in this case it is convenient to adopt the conventional symbols for the vibronic states of a linear molecule for the upper state designations, even though the molecule may be bent in these states.

The following combination relations were used to evaluate the molecular constants:

$$F'(J+1)-F'(J-1)\equiv\Delta_2F'(J)=R(J)-P(J). \tag{3a}$$

$$F''(J+2)-F''(J)\equiv\Delta_2F''(J-1)=R(J)-P(J+2). \tag{3b}$$

The values of $\Delta_2F'(J)$ and $\Delta_2F''(J+1)$ obtained from six measured bands are listed in the tables. They are related to the coefficients B, D, and S in the following manner:

$$\Delta_2F''(J+1)=4B''(J-\tfrac{1}{2})-8D''(J-\tfrac{1}{2})^3. \tag{4a}$$

$$\Delta_2F'(J)=4B'(J+\tfrac{1}{2})-8(D'+S)(J+\tfrac{1}{2})^3. \tag{4b}$$

D for the linear molecule has been shown by Shaffer[19] to be of the same form as for a diatomic molecule, namely:

$$D=4B^3/\nu_1^2 \tag{5}$$

where B is the coefficient in (1) and ν_1 is the totally symmetrical normal frequency of the molecule. From (5) with $B''=0.109$ cm^{-1} (see below) and $\nu_1=655$ cm^{-1}, D'' is found to be 1.21×10^{-8} cm^{-1}. D' is not known, but even if it were ten times D'', which seems a safe upper limit, terms in D in Eqs. (4a) and (4b) would be negligible up to $J=30$. Substitution of numerical magnitudes in Eq. (2a) shows that, even if the apex angle is as small as 125°, the term in S in Eq. (4a) may be neglected, compared with errors of measurement, for J less than 25.

The B values were obtained, by use of Eqs. (4), from the Δ_2F values. Because of blending near the head of the P branch, the Δ_2F values extend only up to J values of 20 or 30, although R lines can be extended up to $J=70$ in some cases. Each B value listed in Table VII represents the weighted mean of all the separately calculated B values for the state. The probable error was calculated from the usual statistical formula for a small number of samples.

The moment of inertia, I'', and the carbon-sulphur distance, r'', given in Table VII were calculated in the usual manner for the lower states, in which the molecule is linear. It seems quite certain (see below) that the bands at λ3535, λ3501, and λ3468 come from the vibrationless state. The corresponding value $r_0''=1.548$A (see Table VII) may be compared with $r_0''=1.54\pm0.03$A given by electron diffraction experiments.[20]

I', calculated in the same manner as I'', is an effective moment of inertia as is shown in the following formula (see Eq. (2)):

$$(1/I')=1/2(1/I_C+1/I_B).$$

The moments of inertia and r' could be calculated from I' if the apex angle were known. For example, if the apex angle is 180°, r' for λ3501 is 1.522A, while if 2α is 125°, r' is 1.735A. The fact that I' is slightly smaller than I'' may be taken as evidence that the molecule is bent in the

FIG. 1. A microphotometer trace of the origin of the band at λ3501. The numbers above each peak are proportional to the intensities calculated from the formula $I\propto(J'+J''+1)$.

[18] R. S. Mulliken, Phys. Rev. **60**, 506 (1941) (this issue, following paper).

[19] W. H. Shaffer, unpublished work.

[20] P. P. Debye, Physik. Zeits. **40**, 404 (1939).

TABLE VII. *Summary of results of rotational analyses.*

BANDS	B (cm^{-1})	I (g cm^2 $\times 10^{40}$)	r in A	STATE
	Lower States			
λλ3468, 3501, 3535	0.1092±0.0001	253.2	1.548	$^1\Sigma_g^+$
λλ3601, 3637, 3673	0.1096±0.0001	252.3	1.545	$^1\Sigma_g^+$
	Upper States			
λ3673	0.1116±0.0001	247.7		$^1\Sigma_u^+$
λλ3637, 3535	0.1124±0.0002	245.9		$^1\Sigma_u^+$
λλ3601, 3501	0.1121±0.0001	246.6		$^1\Sigma_u^+$
(corrected for perturbation)				
perturbing state of				
λλ3501, 3601	0.1138±0.0002	242.9		$^1\Pi_u$
λ3468	0.1117±0.0002	247.4		$^1\Sigma_u^+$

TABLE VIII. *Verification of some combination relations.*

J	$R_{3501}(J)-R_{3601}(J)$	$R_{3535}(J)-R_{3637}(J)$	DIFFERENCE	$R_{3501}(J)-R_{3535}(J)$	$R_{3601}(J)-R_{3637}(J)$	DIFFERENCE
4	801.88	801.81	0.07	275.05	274.98	0.07
12	801.94	801.89	0.05	274.98	274.93	0.05
16	801.98	801.93	0.05	274.95	274.90	0.05
30	802.20	802.13	0.07	274.63	274.56	0.07
38	802.42	802.34	0.08	274.36	274.28	0.08
50	802.82	802.76	0.06	273.62	273.56	0.06

upper state. For a linear molecule one would expect $r'>r''$, since the excited electron in all probability goes to an anti-bonding state[16] and this requires $I'>I''$. However, if the molecule is bent, the observed $I'<I''$ is possible even if $r'>r''$.

As can be seen in Tables I–VI, most of the P branches are unresolved beyond $J=24$, so it is not possible to form combination differences involving lines of higher J value. If the P branch were resolved to $J=40$ or 50, it would be possible to form combination differences which would depend appreciably on the J^3 terms. According to Eq. (4b) the coefficient of $(J+\frac{1}{2})^3$ can be expressed as a function of the apex angle by using the results of Shaffer and Nielsen.[21] Hence, if combination differences for high enough J values were available, the apex angle might be determined. An attempt is being made to obtain some information from the R branch alone for which lines with much higher J values can be observed.

VIBRATIONAL ANALYSIS

Tables I–VI show that many of the bands have, within experimental error, identical Δ_2F values and, therefore, have states in common. The following agreements are found: (a) The Δ_2F' values are the same for λ3501 and λ3601. This is confirmed by an identical perturbation in these two bands (see below). (b) The Δ_2F' values are the same for λ3535 and λ3637. (c) The Δ_2F'' values are the same for λ3601, λ3637, and λ3673. (d) The Δ_2F'' values are the same for λ3501, λ3468, and λ3535. The following combination relations must *also* hold if some of the foregoing Δ_2F agreements are correct:

$$R_{3501}(J)-R_{3535}(J)=R_{3601}(J)-R_{3637}(J)$$
$$=F_B'(J+1)-F_A'(J+1),$$

where A and B refer to two of the upper state vibrational levels. Also,

$$R_{3501}(J)-R_{3601}(J)=R_{3535}(J)-R_{3637}(J)$$
$$=F_B''(J)-F_A''(J).$$

It will be noted in Table VIII, which was made from a few lines chosen at random, that the agreement predicted by the above combination relations is fulfilled except for one thing, namely, in each set the $R_{3501}(J)-R_{\text{other}}(J)$ are all higher by nearly a constant amount, 0.05–0.08 cm^{-1}, than the $R_{\text{other}}(J)-R_{3637}(J)$. This can be reasonably explained by errors in the absolute

[21] W. H. Shaffer and H. H. Nielsen, Phys. Rev. **56**, 188 (1939).

values of the wave-lengths which are unavoidable because of an insufficient number of wave-length standards in this spectral region.

The bands at λ3501 and λ3601, which have been shown above to have a common upper state, have their origins separated by 801.89 cm^{-1}. A consideration of the normal state fundamental vibrations, $\nu_1=655$ cm^{-1}, $\nu_2=397$ cm^{-1}, $\nu_3=1523$ cm^{-1}, shows that the only reasonable explanation of the above separation is that 801.89 $cm^{-1}=2\nu_2''$. The fact that $2\nu_2$ obtained here is somewhat more than twice the value of ν_2 obtained from Raman spectra data may be explained by an expected vibrational perturbation of $2\nu_2$ by ν_1, analogous to the well-known perturbation in CO_2.[22] Also ν_2 for liquid CS_2, which was used in obtaining the Raman spectra, may be different from the vapor. It is interesting to note that the B value for the level $2\nu_2$ is greater than for the ground level (cf. Table VII). The same relation has been found in CO_2. It is just what would be expected for a bending vibration of a linear molecule.

The bands at λ3468, λ3501, and λ3535, which have a common lower state, as is shown above, form a progression whose difference is about 270 cm^{-1}. Similarly, the bands at λ3637, λ3673, and λ3601 form another progression whose difference is also about 270 cm^{-1} (see Table IX). This frequency has been noted by Wilson,[7] Watson and Parker,[9] and recently by Kusch and Loomis.[11] The latter using both absorption and magnetic rotation data reported four progressions, one of which was found to fit partially with the present scheme. The agreement is not exact since Kusch and Loomis' measurements were made on the band heads while the present work lists the band origins. Band head measurements are not given in the tables here because higher resolution shows that some of the bands do not converge to a head. A comparison of the present results with those of Kusch and Loomis is given in Table IX. It will be noted that the inclusion of 27,467.1 and 27,741 in the Kusch and Loomis progression disagrees with the present work.

Kusch and Loomis[11] have suggested that the 270 cm^{-1} vibration is probably ν_1'. However, intensity measurements made by varying the vapor pressure in the tube show that the bands in the $\nu_2''=0$ progression are about 5 times as strong as those in the $\nu_2''=2$ progression, whereas the Boltzmann factor would predict that the $\nu_2''=0$ progression should be about 50 instead of 5 times stronger. Obviously, the bands of the $\nu_2''=2$ progression must have a higher transition probability. It is likely, therefore, that it is the ν_2' vibration of a bent molecule which is excited. Hence it is concluded that ν_2' is about 270 cm^{-1}.

In order to ascertain if the lowest of the observed vibrational states is the normal state, a search was made for bands approximately 800 cm^{-1} to the violet of the bands at λ3501, λ3535, and λ3468. One fairly intense band was found 790 cm^{-1} from λ3501, but it does not show the characteristic perturbation which it should have if its upper state were in common with λ3501 (see below). No other possibilities were found. Hence it is fairly certain that the lowest observed state is the normal state.

Band Perturbations

The bands at λ3501 and λ3601 show a perturbation which is the same in both bands. The maximum perturbation occurs at the eleventh line of both the P and R branches. In view of the J numbering established in Fig. 1 and given in Table II, this shows that it is the upper state

Table IX. *A comparison of a progression given by Kusch and Loomis with those of the present work.*

Kusch and Loomis*	$\nu_2''=0$ Progression†‡		$\nu_2''=2$ Progression	
27,467.1 (4)				
273.9				
27,741				
246.1				
27,987.1 (4)	27,987.1 KL (6)		*797*	27,190.08 (2)
282.8	*286.6*			*281.88*
28,269.9 (7)	28,273.74 (7)		*801.78*	27,471.96 (2)
273.6	*275.09*			*274.98*
28,543.5 (10)	28,548.83 (10)		*801.89*	27,746.94 (3)
272.3	*267.52*			
28,815.8 (8)	28,816.35 (10)			
265.1	*264.6*			
29,080.9 (10)	29,080.9 KL (10)			
255.7	*255.7*			
29,336.6 (8)	29,336.6 KL (8)			
268.7	*268.7*			
29,605.3 (8)	29,605.3 KL (7)			

* Data taken from Kusch and Loomis.
† Frequencies designated KL taken from column one; note that these refer to heads.
‡ Absorption intensities, determined from a microphotometer trace, are given in parentheses.

[22] G. Placzek, *Handbuch der Radiologie*, Vol. 6, Part 2, p. 328.

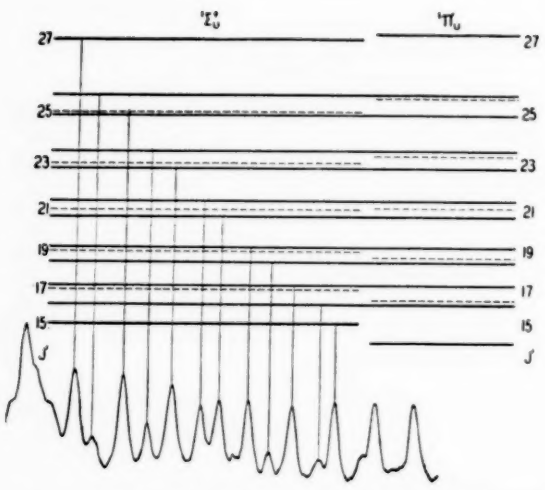

FIG. 2. The analysis of the perturbation in λ3501. The broken lines represent the unperturbed levels. The perturbed $^1\Sigma^+_u$ and $^1\Pi_u$ levels are connected to indicate a mixing of the wave functions of the two states. The curve given below is a reproduction of a microphotometer trace of the band at λ3501. It will be noted that the stronger component of each pair of lines comes from the level which is closest to the unperturbed $^1\Sigma^+_u$ level.

which is common to both. Also the Δ_2F' values for the two bands are found to be the same (see above). This perturbation must be caused by a neighboring state whose rotational levels have approximately the same energy as the observed state, and in addition satisfy the Kronig rules for perturbations. These state that only levels of identical rigorous symmetry type (+ or −, *s* or *a*) and equal J can perturb one another. For a linear or triangular CS_2 molecule which is not too much bent, $\Delta K=0, \pm1$ may be expected.[23]

If we let T_1 and T_2 be the actual term values for any J value of the perturbed and perturbing states, and T_1^0 and T_2^0 be the values they would have if they had not perturbed each other, we may write:

$$T_1^0=A_1+B_1J(J+1)-\cdots,$$
$$T_2^0=A_2+B_2J(J+1)-\cdots.$$

Following Dieke's discussion for diatomic molecules[24] let us define δ, a, and b as follows:

$$\delta\equiv T_2^0-T_1^0=(A_2-A_1)+(B_2-B_1)J(J+1)\equiv a+bJ(J+1). \quad (6)$$

The perturbed levels T_2 and T_1 are given by:

$$T_2,\ T_1=\tfrac{1}{2}(T_2^0-T_1^0)\pm[S_{12}^2+\delta^2/4]^{\frac{1}{2}}. \quad (7)$$

[23] R. S. Mulliken, Phys. Rev., **59**, 873 (1941).
[24] G. H. Dieke, Phys. Rev. **47**, 870 (1935).

For a perturbation of class A, ($\Delta\Lambda=\pm1$ for the diatomic case)

$$S_{12}^2=\alpha^2J(J+1), \quad (7a)$$

while for class B perturbations S_{12} is independent of the J value. The + sign goes with T_2 or T_1 according as δ is positive or negative. The sign of δ reverses as one goes through the maximum of the perturbation. Extra lines in the band involve the T_2 levels, while the regular or main lines involve the T_1 levels. As can be seen from Eq. (7), the interval from any main line to the corresponding extra line is

$$|T_2-T_1|\equiv\Delta\nu=(4S_{12}^2+\delta^2)^{\frac{1}{2}}. \quad (8)$$

Intensities of the main lines and extra lines may be calculated in the usual manner. Letting I_1 be the intensity of the main line arising from the transition to the T_1 level and I_2 be the intensity of the extra line arising from the transition to the T_2 level, it is found that

$$I_1/I_2=(\Delta\nu+\delta)/(\Delta\nu-\delta). \quad (9)$$

The microphotometer trace in Fig. 2 of the perturbed part of the R branch of λ3501 shows that the lines at $J'=21$, which are separated by 0.30 ± 0.005 cm^{-1}, have practically equal intensity. Hence, from Eq. (9), δ must be nearly zero for these lines. However, the lines at $J'=19$, whose intensities are in the ratio 2 : 1, are also separated by 0.30 ± 0.01 cm^{-1}. From this intensity ratio Eq. (9) shows that, in this case, δ must be about 0.1 cm^{-1}. Hence it is seen from Eq. (8) that S_{12} is not constant, which means that these perturbations most likely are of the class A type, i.e., the $^1\Sigma^+_u$ state is perturbed by a $^1\Pi_u$ state. It must be pointed out, however, that the above reasoning depends rather critically on the measured value of $\Delta\nu$. For example if the lines at $J'=19$ are separated by 0.32 cm^{-1} instead of 0.30 cm^{-1}, the class B equations are satisfied. However, it is found that these equations then give poor agreement for the perturbations at other J' values, so it seems safe to conclude that the perturbation is of class A.

From a careful study of the five measured $\Delta\nu$'s (for $J'=17$, 19, 21, 23, 25), α^2 and $\delta(J)$ of (7) have been determined. From Eq. (8), α^2 was found to be 4.87×10^{-5} cm^{-1}. The numerical

form for Eq. (6) was found to be

$$\delta = -0.712 + 0.00157J(J+1). \quad (10)$$

Equations (7a) and (8) with the above constants yield good agreement with observation for the five $\Delta\nu$'s. Also, the intensities calculated from (9) agree quite well with those measured from the microphotometer trace. The B value for the perturbing $^1\Pi_u$ state as given by Eq. (6), and the constants in (10), is 0.1138 cm^{-1}.

It is also possible to compute, with the aid of the above constants, the deviations ϵ between the actual and the unperturbed positions of the main lines from the relation

$$T_1 - T_1^0 \equiv \epsilon = \pm\tfrac{1}{2}(|\Delta\nu| - |\delta|), \quad (11)$$

with the sign of ϵ always opposite to that of δ. (The same formula but with opposite choice of sign also holds for $T_2 - T_2^0$ for the "extra" lines.) The theoretical ϵ's, computed according to Eq. (11), in which δ from Eq. (10) and Eqs. (7a), (8) with $\alpha^2 = 4.87 \times 10^{-5}$ are used, are shown by the continuous curves in Fig. 3. The "observed" points in Fig. 3 represent the deviations of the observed lines from the quadratic,

$$\nu = 28{,}548.83 + 0.2211M + 0.00278M^2, \quad (12)$$

where $M = J'' + 1$ for the R branch and $M = -J''$ for the P branch. This equation was obtained by fitting a few of the low numbered P and R lines, and also the midpoint of the two strongly perturbed R lines at $J' = 21$, to a quadratic of this form. It will be noted that the agreement of observed and calculated ϵ's is good for J' values up to the maximum of the perturbation. The increasing deviations beyond this point are apparently due to the fact that the quadratic Eq. (12) is a poor approximation for high J values, where J^3 and J^4 terms evidently become important. Similar large deviations from a quadratic form are also found in some of the other bands where no perturbation is present.

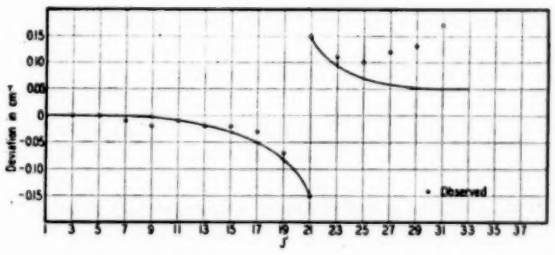

FIG. 3. The perturbation in λ3501. The deviations (calculated minus observed) of the observed lines from the positions predicted by Eq. (12) are shown, for the R branch, by the circles. The continuous curves give the *theoretical* deviations ϵ computed from Eq. (11), with δ from Eq. (10) and by using Eqs. (7a), (8) with $\alpha^2 = 4.87 \times 10^{-5}$. It will be noted that, according to the theoretical curves, a constant deviation of 0.05 cm^{-1} should remain after the perturbation. Actually, larger deviations are observed.

In conclusion, I wish to express my gratitude to Professor R. S. Mulliken, who suggested this problem and whose many suggestions and criticisms have proved invaluable. I also wish to thank Dr. H. G. Beutler for his generous assistance with the experimental problems.

Correlation of Energy Levels of Linear and Bent Triatomic Molecules, and the Ultraviolet CS_2 Absorption Spectrum

ROBERT S. MULLIKEN
Ryerson Physical Laboratory, University of Chicago, Chicago, Illinois
(Received July 7, 1941)

A set of vibronic levels for a $^1\Sigma^+_g$ and a $^1\Pi_g$ electronic state of linear AB_2 is shown in a diagram, together with gyrovibronic levels of the corresponding electronic states (a $^1A_1$ and a $^1B_2$ and a $^1A_2$) of bent AB_2; and a correlation is set up between the sets of gyrovibronic levels of the two cases. This diagram is then used in a discussion of the near-ultraviolet absorption bands of carbon disulfide, where the molecule is linear in the $^1\Sigma^+_g$ ground state. The band types and structures for such a transition are discussed; the structures should be practically identical in character whether the upper state is linear or bent. Vibrational intensities, and their relation to a strong allowed electronic transition at shorter wave-lengths, are also discussed. It is concluded that the near-ultraviolet system is an electronic-allowed transition to a $^1B_2$ bent molecule upper state related to a $^1\Pi_g$ linear molecule state.

I. Correlation of Gyrovibronic States of Linear and Bent AB_2

IN a preceding paper,[1] the species classification and rotational energy level patterns of nonlinear triatomic molecules AB_2 have been discussed. If, for any such molecule, we imagine the ABA apex angle to be increased continuously to 180°, the energy level system must go over somehow into that of linear AB_2. Since, however, the type of electronic and vibrational quantization is very different in the two cases, it is evident that in the transition region radical and complicated transformations must occur in the wave functions and in the arrangement of levels. In the first three sections of this paper, the matter of bridging this region is considered by using a qualitative correlation scheme relating the energy level patterns of linear and bent AB_2. In the last section, electronic transitions from *linear* to *linear or bent* molecular states, and their band structures, are considered, and the results are applied to the interpretation of the near-ultraviolet absorption spectrum of carbon disulfide.

If the bending of any AB_2 molecule is small or moderate,[1] the rotation approximates rather closely to that of a symmetric top, with quantum number K_η for the rotation about the least moment of inertia axis η. K_η becomes an increasingly good quantum number with approach to linearity. At the same time, however, a strong vibration-rotation interaction must set in, essentially between the deformation vibration mode ν_2 and the K_η rotation, whose quanta become larger and larger as the molecule straightens out and the moment of inertia I_η decreases. This interaction points toward the situation in linear AB_2, where there is a two-dimensional vibration mode ν_2 with quantum numbers v_p (radial) and l (azimuthal).

At the same time, strong electronic-rotational interactions may develop, leading to an electronic angular momentum around the axis with quantum number Λ. In the linear molecule, K is in general the sum of Λ and l. During the change from bent to linear AB_2, we normally expect K_η to become K, although since K_η is not quite rigorous, occasional deviations from this correlation are possible.

Linear AB_2, like diatomic B_2, is a prolate symmetrical-top rotator, but, because of the zero equilibrium moment of inertia around the symmetry axis, the wave functions and energy level patterns differ considerably from those of nonlinear symmetrical top molecules. In particular, $K>0$ is possible in linear molecules only by the excitation of vibronic angular momentum (i.e., Λ and/or l), and K here forms an integral part of the vibronic as well as of the rotational species classification.

The wave functions reflect these differences. Thus we have:[1]

Moderately bent AB_2, $\psi_{evr}=\psi_r\psi_{ev}+\psi'_{evr}$,
with

$$\psi_r \approx S_{JKM}=2^{-\frac{1}{2}}(\psi^{\times}_{JKM}+(-1)^{\gamma}\psi^{\times}_{J-KM}), \quad (1)$$

[1] R. S. Mulliken, Phys. Rev. **59**, 873 (1941).

but

Linear AB_2,

$$\psi_{evr}=2^{-\frac{1}{2}}(\psi^{\times}_{JKM}\psi^{K}_{ev}+(-1)^{\delta}\psi^{\times}_{J-KM}\psi^{-K}_{ev}), \quad (2)$$

with $\delta=0$ or 1. (Recall that $K=|k|$, so that $+K$ and $-K$ represent two values of k differing in sign only.) It is characteristic of linear AB_2 that the combination of $k=+K$ and $k=-K$ cannot occur until the ψ_{evr} stage, instead of within the ψ_r factor as in bent AB_2. Thus for linear AB_2 no rotational functions S_{JKM} classifiable under asymmetric-top species exist as they do[1] for bent AB_2.

In Section V of the preceding paper[1] the concept of gyrovibronic species was defined for moderately bent AB_2; this corresponds to gyrovibronic wave functions

$$\psi_{evk}=(2\pi)^{-\frac{1}{2}}e^{ik\phi}\psi_{ev}, \quad (3)$$

the factor $(2\pi)^{-\frac{1}{2}}e^{ik\phi}$ having been borrowed from the rotational function ψ_{JkM}. There are two wave functions ($k=\pm K$) for each gyrovibronic state; in the complete ψ_r or ψ_{evr}, these are combined as in Eq. (1) and give rise to K doubling. Similarly for linear AB_2,

$$\psi_{evk}=(2\pi)^{-\frac{1}{2}}e^{ik\phi}\psi^{k}_{ev}; \quad (4)$$

here ψ_{evk} really differs from ψ^{k}_{ev} only in the way of measuring the internal angular coordinates ϕ_i. The ϕ_i are part of a set of cylindrical coordinates for the electrons and nuclei; this type of coordinates is especially convenient for linear molecules. Let the top axes x, y, z be chosen to coincide, respectively, with ζ, ξ, η of Fig. 3 of the preceding paper[1] (A nucleus in xz plane), and let ϕ be measured from the line of nodes to the x axis. Further, let a ϕ_i be similarly defined for each electron. If also we define the *relative* coordinates $\Phi_i=\phi_i-\phi$ for the electrons, then ψ_{evk} in Eq. (4) is a function of the ϕ_i's and ψ^{k}_{ev} is the corresponding function of the Φ_i's.

Because of this simple relation between ψ_{evk} and ψ^{k}_{ev}, the gyrovibronic species classification for linear AB_2 is identical with the vibronic species classification. The latter, in turn, is formally the same as the electronic species classification for symmetrical diatomic molecules, being based, like the latter, on the symmetry group $D_{\infty h}$. We can, therefore, conveniently adopt the well-known diatomic species definitions and symbolism: Σ, Π, Δ, etc., for $K=0$, 1, 2, etc. (K in the diatomic case is called Λ), with subscript g or u to denote behavior under inversion of the internal axis-system x, y, z, and superscript $+$ or $-$ for Σ states to denote behavior for reflection of the axis-system in any plane through the symmetry axis. To distinguish electronic, vibrational, and vibronic species, one can, if necessary, add a superscript e, v, or ev at the left of the species symbol: for example, ${}^{e}{}^{3}\Sigma^{+}_{g}$, ${}^{v}\Sigma^{+}_{g}$, ${}^{ev}{}^{3}\Sigma^{+}g$.[2]

For moderately bent AB_2, a gyrovibronic species classification is obtained by merely giving K value and vibronic species.[1] Each gyrovibronic species of bent AB_2 shows a characteristic pattern with respect to over-all species character of rotational levels as a function of J; and comparison with the similar sets of level patterns for linear AB_2 leads to the setting up of a correspondence between the gyrovibronic species of bent and linear AB_2.[3] This correspondence, already embodied in Fig. 6 of the preceding paper,[1] furnishes the desired scheme for qualitatively bridging the gap between the energy levels of linear and bent AB_2. As the figure shows, there is a one-to-one correspondence for $K=0$, a two-to-one correspondence (two gyrovibronic species of bent AB_2 to one of linear AB_2) for $K>0$.

It may be noticed that gyrovibronic species such as Π_u, Φ_u (or any odd K) have qualitatively identical over-all species patterns in Fig. 6 of the preceding paper; similarly with sets like Δ_g, Γ_g. The members of such a set are distinguished only by their K values. Since, however, the K classification is not quite a rigorous property of ψ_{evr}, especially for bent AB_2, perturbations may occur between members of any such set; and if two gyrovibronic levels belonging to one set tend to cross during a correlation, this crossing will, technically though usually not in a practical sense, be avoided.

[2] Cf. R. S. Mulliken, J. Phys. Chem. **41**, 159 (1937).

[3] The over-all species patterns for various electronic states of symmetrical diatomic molecules are well known (cf., e.g., G. Herzberg, *Molecular Spectra and Molecular Structure. I. Diatomic Molecules* (Prentice-Hall, 1938), pp. 261–2). It is easily seen that exactly the same patterns must occur for like-named electronic states of linear AB_2, and, further, for like-named vibronic states of linear AB_2.

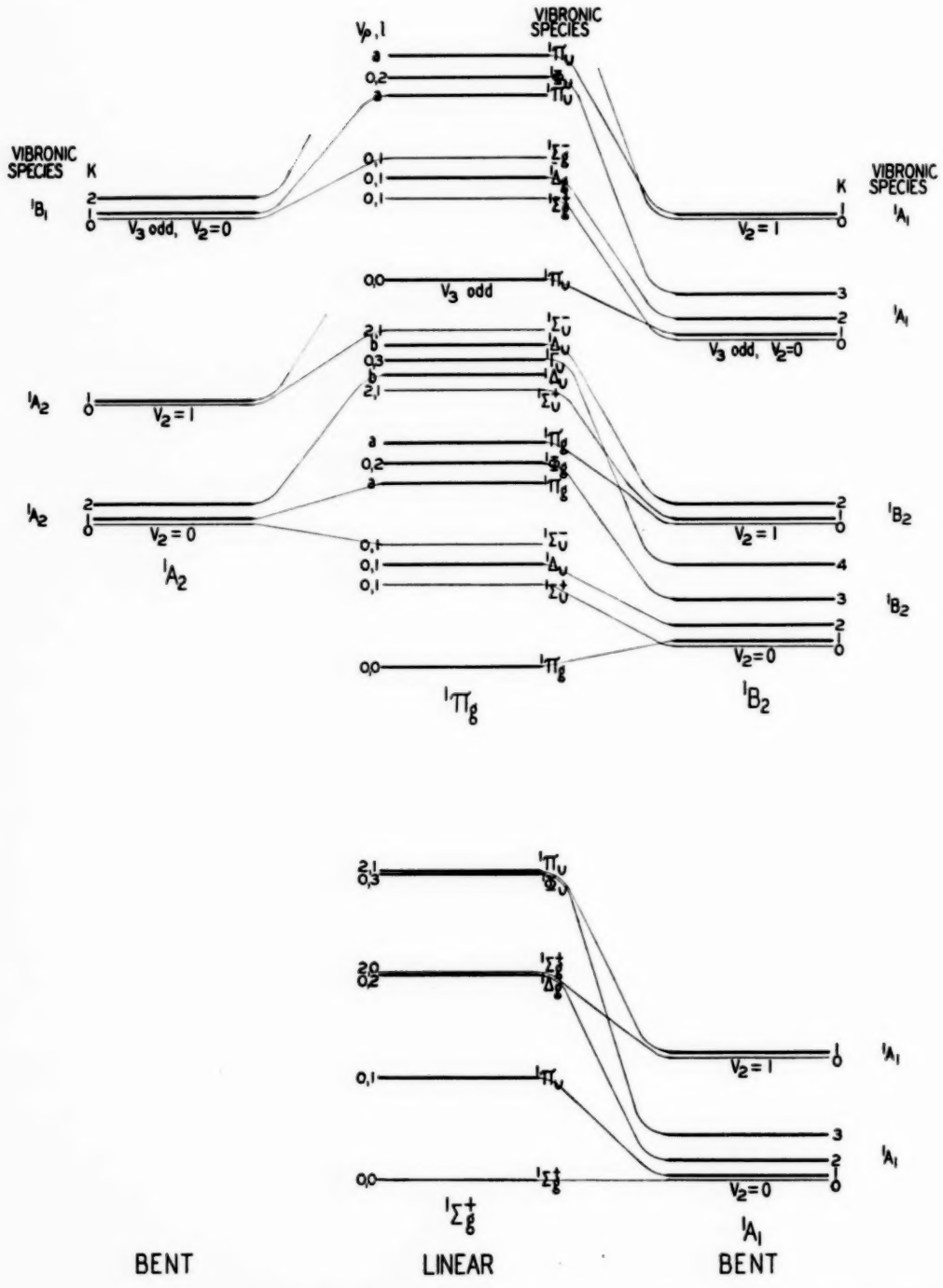

FIG. 1. Correlation between (gyro)vibronic levels of a $^1\Sigma_g^+$ and a $^1\Pi_g$ electronic state of linear AB_2 (middle section of diagram) and gyrovibronic (i.e., vibronic and K) levels of corresponding electronic states ($^1A_1$, $^1A_2$ and $^1B_2$) of bent AB_2 (outer sections of diagram). The diagram covers various states of excitation of the deformation frequency (quantum numbers v_p and l in linear AB_2, v_2 in bent AB_2). It assumes no excitation of the antisymmetrical frequency (quantum number v_3), except at the top of the diagram; and it ignores additional levels, and other complications, corresponding to excitation of the symmetrical valence frequency. For the levels marked a and b, definite v_p, l values cannot be given; a refers to levels whose wave functions are mixtures of 2, 0 and 0, 2, b to mixtures of 0, 3 and 2, 1. Each "level" of Fig. 1 represents actually a whole set of rotational levels, whose characteristics can be obtained by reference to Fig. 6 of reference 1. (A slight error has been made in the drawing in that the correlation lines coming from the left to the levels $K=0$ and 1 of $v_2=1$ of the $^1B_2$ state *should cross*.)

Still more generally, Σ^+_u and Σ^-_u can perturb Π_u states, Π_u can perturb Δ_u, Σ^+_g and Σ^-_g can perturb Π_g, and so on. In general, however, these effects should be no larger than ordinary perturbations in diatomic spectra. Between levels belonging to g and u gyrovibronic species, no appreciable interactions can occur.

II. Vibrational and Vibronic States of Linear AB_2

Before proceeding further, it is desirable to review the modes of vibration of linear AB_2. These may be classified, like the ψ_{evk}'s, as species of the group $D_{\infty h}$, where however, small instead of capital letters are used for the species symbols.[2] There are the symmetrical mode ν_1, species σ_g, the antisymmetrical mode ν_3, species σ_u, and the degenerate pair of deformation modes ν_2, species π_u. The two deformation degrees of freedom are best taken as a radial and an azimuthal, with quantum numbers v_p and l ($v_p+|l|=v_2$). The possible values of v_p and $|l|$ for a given v_2 are $v_p=0$, $|l|=v_2$; $v_p=2$, $|l|=v_2-2$; and so on.

For the complete ψ_v, the species is respectively Σ^+_g, Π_u, Δ_g or Φ_u according as $|l|=0, 1, 2$, or $3\cdots$. if v_3 is even; for v_3 odd, the g and u subscripts are reversed. If the electronic state ψ_e is $^1\Sigma^+_g$, then the ψ_{vrk} species is the same as the vibrational species, except for addition of the multiplicity symbol. Figure 1 (lowest section of middle column) shows the vibronic levels and their species symbols for a $^1\Sigma^+_g$ electronic state with $v_3=v_1=0$ but v_2 ranging from 0 to 3.

In general, if we let $\pm\Lambda h/2\pi$ represent (as in the diatomic case) the *electronic* orbital angular momentum around the symmetry axis, the total orbital angular momentum $kh/2\pi=\pm Kh/2\pi$ around this axis is given by

$$K=|\Lambda+l|. \tag{5}$$

Taking K and Λ as always positive, it is necessary to let l in Eq. (5) assume either positive or negative values, the + sign when the l vector is parallel to $\pm\Lambda$, the − sign when it is antiparallel. For a given Λ and $|l|$, there are, in general, two K values $\Lambda+|l|$ and $|\Lambda-|l||$, each (if $K\neq 0$) having a pair of wave functions obtained from $\delta=0$ and $\delta=1$ in Eqs. (2).

The vibronic states resulting from the combination of any given type of electronic and vibrational state can be determined, since ψ_e, ψ_v, and ψ_{evk} species are all classified under $D_{\infty h}$, by species multiplication according to well-known group-theoretical procedure. The vibronic levels are illustrated in the middle section of the middle column of Fig. 1 for a $^1\Pi_g$ electronic state with $v_1=0$ and $v_3=0$ (or an even number), and v_2 ranging from 0 to 3. Above, in the top section, are illustrated a further set of vibronic levels for $v_3=1$ (or any odd value). The vibronic levels in the middle section of Fig. 1 are spaced approximately like those of an actual linear AB_2 molecule, except that certain levels with $v_1>0$, which actually would come in the energy ranges covered, are omitted. In practice, these would cause marked complications (the reader may recall the well-known perturbations in CO_2 resulting from the approximate equality of $2\nu_2$ and ν_1).

For each value of $v_2>0$, there are two or more vibronic levels. These differ very little in energy if $\Lambda=0$ and if there is no perturbation by excited v_1 levels. If $\Lambda=1$, the Renner effect should, in general, cause relatively large energy differences between the different levels for a given v_2,[4] and the $^1\Pi_g$ levels in Fig. 1 have been drawn in qualitative accordance with this expectation.

III. Correlation of Levels of Linear and Bent AB_2

We now have, in Fig. 1, typical sets of gyrovibronic levels for two different types of electronic states of linear AB_2, and wish to correlate these with corresponding levels of bent AB_2. Before doing this, two steps remain: (a) to determine what relations exist between electronic species of linear and bent AB_2; (b) to add to

TABLE I. *Correlation of electronic states of linear* AB_2 *(symmetry* $D_{\infty h}$*) with those of bent* AB_2 *(symmetry* C_{2v}*). Cf. reference 5 regarding the derivation.*

Linear AB_2	Bent AB_2	Linear AB_2	Bent AB_2
Σ^+_g	A_1	Π_u, Δ_g, or Φ_u	A_1+B_1
Σ^-_g	B_1		
Σ^+_u	B_2	Π_g, Δ_u, or Φ_g	A_2+B_2
Σ^-_u	A_2		

[4] R. Renner, Zeits. f. Physik **92**, 172 (1934).

Fig. 1 gyrovibronic levels of the proper bent AB_2 electronic states.

If we consider the electronic wave functions by themselves, as if the nuclei were fixed, the way in which the various species of electronic states of linear AB_2 go into those of bent AB_2 can be determined by familiar methods,[5] with results as given in Table I. Thus the $^{e1}\Sigma^+_g$ state of linear AB_2 corresponds to an $^{e1}A_1$ state of bent AB_2, while the $^{e1}\Pi_g$ state must split into an $^{e1}A_2$ and an $^{e1}B_2$ state, the magnitude of the splitting increasing with the bending.

Gyrovibronic levels for bent AB_2 corresponding to those shown for linear AB_2 have been drawn at the left and right of Fig. 1. For each vibrational state shown, a few gyrovibronic levels have been added, spaced according to CK^2. The spacings of the vibrational levels of both bent and linear AB_2 in Fig. 1 have been chosen so as to be related roughly as for an actual molecule like CO_2 or NO_2. Levels with $v_1>0$ have been omitted for the sake of simplicity for bent AB_2 just as for linear AB_2.

By using Fig. 6 of the preceding paper,[1] correlation lines can now be drawn connecting corresponding gyrovibronic states of linear and bent AB_2 in Fig. 1. The results are interesting. If we look first at the $^{e1}\Sigma^+_g$ state and correlate with $^{e1}A_1$, Fig. 1 shows a systematic correlation of vibrational levels in such a way that v_2 (bent AB_2) $=\frac{1}{2}v_p$ (linear AB_2).

On considering the $^{e1}\Pi_g$ state, for $v_3=v_1=0$ (similar results are expected for $v_1>0$, $v_3=$ even), some of the gyrovibronic levels are found to connect with those of $^{e1}B_2$, others with those of $^{e1}A_2$. It is particularly interesting that the two lowest vibrational levels of $^{e1}\Pi_g$ cross each other in going over to the lowest two K levels of $^{e1}B_2$. In particular, the $^{e1}\Pi_g$ level with $v_3=v_1=v_2=0$, where $K=1$ is purely electronic angular momentum, goes over into the second K level of $v_3=v_1=v_2=0$ of $^{e1}B_2$, where $K=1$ is purely nuclear top angular momentum. K is conserved, but the carrier of the angular momentum changes completely, and the wave function must be radically transformed. A detailed study of the changes in the gyrovibronic wave functions in the correlation between $^{e1}\Pi_g$ and $^{e1}A_2$ plus $^{e1}B_2$ shows several types of interesting transformations, but these will not be discussed here. For the vibrational wave functions also, radical changes have to occur, as is shown by the rule v_2 (bent) $=\frac{1}{2}v_p$ (linear), which holds in the same way here as for the $^{e1}\Sigma^+_g$ state.

When levels with $v_3=1$ are considered, a correlation rule v_3 (bent) $=v_3$ (linear) is seen to be fulfilled. It is apparent also that there is a tendency for v_1 (bent) $=v_1$ (linear), but that this must be modified in practice by strong interactions between excited v_1 and v_p levels (linear AB_2) or between v_1 and v_2 levels (bent AB_2). These interactions must also, in practice, interfere more or less with the smoothness of the correlations v_2 (bent) $=\frac{1}{2}v_p$ (linear). For strongly vibrating states, many vibrational interferences of various sorts will enter to upset the simplicity of the correlations.

Although Fig. 1 shows directly only the correlation behavior for $^{e1}\Sigma^+_g$ and $^{e1}\Pi_g$ states of linear AB_2, it illustrates how these may be constructed in general.

IV. Selection Rules and Band Structures for Electronic Transitions from Linear AB_2 to Linear or Bent AB_2 States; with Applications to the Ultraviolet Carbon Disulfide Absorption Spectrum

In the ultraviolet absorption spectrum of carbon disulfide vapor there is a region near λ3000 containing a great number of bands. The molecule is linear in the lower electronic state, which is $^1\Sigma^+_g$.[6] If it were linear in both states, not more than one series of bands of any considerable intensity would be expected, but the large number of observed bands can be understood if we use the Franck-Condon principle and if the equilibrium configuration of the molecule is non-linear in the upper state. A study of the electronic structures of CO_2, CS_2 and related molecules makes it rather probable that the latter is a $^1\Pi_g$ state if the molecule is linear;[6] if it is bent, this $^1\Pi_g$ should be replaced by two corresponding states, a $^1A_2$ and a $^1B_2$ (cf. Table I), perhaps

[5] Cf. R. S. Mulliken, Phys. Rev. **43**, 293 (1933), Table III. Although the results now needed are not given (cf. footnote *a* of the table), they can be obtained by the method given there.

[6] R. S. Mulliken, J. Chem. Phys. **3**, 739 (1935).

TABLE II. *Survey of permitted gyrovibronic transitions for a transition between an* $^3\Sigma^+_g$ *and an* $^3\Pi_g$ *state of linear* AB_2, *and between* $^3\Sigma^+_g$ *of linear and* $^3B_2$ *and* $^3A_2$ *of bent* AB_2. ($^3B_2$ *and* $^3A_2$ *of bent correspond to* $^3\Pi_g$ *of linear* AB_2—*see Table I.*) *Only the transitions marked in bold-face type are allowed by electronic selection rules. Polarization: p means perpendicular,* (ξ *and* ζ), η *parallel, to the axis of linear* AB_2 (*axes* ξ, η, ζ *as in Fig. 3 of reference 1*). *In the first two sections of the table,* Σ^+_g *and so on indicate (gyro)vibronic states.*

			$^3\Pi_g$								$^3B_2$								$^3A_2$							
			Even v_3				Odd v_3				Even v_3; $K=$				Odd v_3; $K=$				Even v_3; $K=$				Odd v_3; $K=$			
			Σ^+_u	Σ^-_u	Π_g	Δ_u	Φ_g	Σ^+_g	Σ^-_g	Π_u	Δ_g	Φ_u	0	1	2	3	0	1	2	3	0	1	2	3	0	1	2	3
$^3\Sigma^+_g$		Σ^+_g	η						p				**n**						ζ						ξ			
	v_3 even:	Π_u		η				p	p		p			**n**				ζ		ζ		η			ξ		ξ	
		Δ_g			η					p		p			**n**				ζ		ζ		η			ξ		ξ
		Φ_u				η					p					**n**				ζ				η			ξ	
	v_3 odd:	Σ^+_u		p				η									**n**					ξ						

rather near together. Reasons why a bent upper state is likely have been given earlier.[6]

In connection with Liebermann's analysis of some of the bands of this system,[7] it was desirable to determine what selection rules and band structures are expected for (a) linear $^{e1}\Sigma^+_g \rightarrow$ linear $^{e1}\Pi_g$; (b) linear $^{e1}\Sigma^+_g \rightarrow$ bent $^{e1}A_2$ and $^{e1}B_2$. The results of this study are also of general interest.

Kusch and Loomis's observation of bands of this system in the form of a magnetic rotation spectrum[8] indicated the existence of a magnetic moment along the figure axis in the upper electronic state. This would call for a P, Q, R band structure, however. Since the bands actually have P, R structure, the magnetic moment must be directed along the J vector, and must be of secondary origin, like that in the visible iodine bands. The existence of magnetic rotation is, therefore, not decisive as to the linearity or non-linearity of the molecule in the upper state. Hence let us consider the two possibilities in succession.

The transition $^{e1}\Pi_g$, $^{e1}\Sigma^+_g$ in a *linear* molecule is forbidden by the electronic selection rules, but its appearance with rather low intensity (such as is observed) would not be unreasonable. Any well-developed bands must, however, obey the vibronic selection rules. Table II (sections 1–2) shows all the allowed kinds of bands, with their polarization, for various types of upper and lower vibronic states. Parallel (η) and perpendicular (p) bands are both possible. They should have, respectively, the same structures as like-designated diatomic molecule bands.

[7] L. Liebermann, Phys. Rev. **60**, 496 (1941), (this issue, preceding paper).

[8] P. Kusch and F. W. Loomis, Phys. Rev. **55**, 850 (1939).

At room temperature, the most prominent absorption bands should arise from the vibrationless lower state, of vibronic species $^1\Sigma^+_g$. Parallel bands ($\Delta J = \pm 1$) going to $^1\Sigma^+_u$ upper vibronic states, and perpendicular bands ($\Delta J = 0, \pm 1$) going to $^1\Pi_u$ upper states, are here possible (see Table II). For the former, the most probable upper states are those with $v'_3 = 0$, $v'_\rho = 0$, $l' = 1$, for the latter, those with $v'_3 = 1$, $v'_\rho = l' = 0$. Changes in v_1 should be governed by the Franck-Condon principle. Weak bands involving multiples of $2\nu_2$ and $2\nu_3$ are also possible.

Less prominent absorption bands should arise from vibrating lower states. For the lowest such state ($v''_3 = v''_1 = v''_\rho = 0$, $l'' = 1$), of vibronic species $^1\Pi_u$ (cf. Fig. 1), the most favored upper vibronic states should be the $^1\Pi_g$ states with $v'_3 = v'_\rho = l' = 0$ in the case of parallel bands ($\Delta J = 0, \pm 1$), and the $^1\Sigma^+_g$, $^1\Sigma^-_g$, and $^1\Delta_g$ states with $v'_3 = 1$, $v'_\rho = 0$, $l' = 1$ in the case of perpendicular bands.

The right-hand half of Table II corresponds to a *bent* upper state. Here some of the vibronic transitions with η polarization, belonging to $^{e1}B_2$, $^{e1}\Sigma^+_g$, may be called electronic-allowed, although strictly this is justified only in emission where the initial state is bent, but not in absorption where it is linear. There are also several types of electronic-forbidden transitions, of both the parallel (η) and perpendicular (ξ or ζ) kinds, going to both $^{e1}B_2$ and $^{e1}A_2$ upper states.

Table II and Fig. 1 form a useful guide in the attempt to interpret the observed CS_2 absorption bands. In connection with Fig. 1, it is to be noted that if the upper equilibrium configuration is bent, the two upper electronic states $^1A_2$ and $^1B_2$ must differ in equilibrium dimensions and energy.

Unpublished considerations on the electronic structure of CS_2 indicate, for that molecule, somewhat greater bending at equilibrium and a lower energy minimum for the $^1B_2$ than for the $^1A_2$, and Fig. 1 has been constructed accordingly.

For a bent upper state, the most probable transitions from the vibrationless lower state, on the basis of Table II and the Franck-Condon principle, are parallel transitions to levels $v'_3=0, K'=0$ of $^{e1}B_2$ and perpendicular transitions to $v'_3=1$, $K'=1$ of $^{e1}B_2$ and $^{e1}A_2$. The most probable values of v'_2 should be large. Only one value of K'' and K' is involved for each band. Hence, unlike typical symmetrical-top bands where both J and K structures are present, each band should show only a structure due to J. Since, even for a considerably bent CS_2 molecule, there is little deviation from the linear-molecule rotational energy formula $BJ(J+1)+\cdots$,[7] the band structures should be practically indistinguishable from those of linear or diatomic molecules.

In the case that $K'=1$, there should be an appreciable splitting of the upper rotational levels due to asymmetry, so as to give effectively two values of B', one for the Q branch, the other for the P and R branches, as in Λ-doubling in diatomic molecules. For an adequately resolved structure, the sign and magnitude of the difference in the two B''s could be obtained. The *sign* would show whether the transition is to $^{e1}A_2$ or $^{e1}B_2$ (cf. Fig. 6 of preceding paper,[1] for $K=1$); the *magnitude*, in conjunction with energy formulas of asymmetric-top theory, would show (provided perturbations between $^eA_2$ and $^eB_2$ are small enough) just how much the molecule is bent.

For bands arising from a vibrating lower state (cf. Table II), there is again just one value of K'' and of K' for each band, and the structures should again be practically identical with those of linear molecules; or at most there are two values of K', which should give an appearance like two linear-molecule bands close together or overlapping. From the lowest vibrating state ($K''=1$, $^1\Pi_u$ vibronic state), parallel-type transitions can occur to $^{e1}B_2$ and $^{e1}A_2$ levels with $K'=1$, $v'_3=0$ (or v'_3 even). Perpendicular bands can also occur, going to levels $K'=0$ and 2, $v'_3=1$ (or odd), of the $^eB_2$ and $^eA_2$ states.

All of the analyzed CS_2 bands are parallel bands of the P, R branch type ($K'=K''=0$). Within the errors of measurement, the structures of all these bands agree with what is expected for the case of a linear upper state; but as Liebermann has shown, the asymmetric-top corrections are so small for $K'=0$ that the data are equally consistent with an upper state with apex angle as small as 125°. There is no definite evidence of perpendicular bands in the spectrum. (It should, however, be kept in mind that only bands in the weak long wave-length end of the spectrum have been studied as yet.)

The simplest interpretation of the observed spectrum is that it actually corresponds chiefly to the allowed electronic transition $^1B_2-{}^1\Sigma^+_g$. This is confirmed by several features in the vibrational structure. In the long wave-length part of the spectrum, the Franck-Condon principle for a bent upper level favors transitions from states in which ν_2 is initially excited; and in fact Liebermann has analyzed three such bands, arising from the level $2\nu_2$; these bands are much stronger than the Boltzmann factor for $2\nu_2$, alone, would permit. Further, a long vibrational progression with $\Delta\nu$ about 270 cm^{-1}, observed by various authors and clarified by Liebermann, can hardly be interpreted otherwise than as a ν'_2 progression of a bent molecule. For 270 cm^{-1} is definitely too small for ν'_1, in view of the fact (cf. Eqs. (6), (7)) that only one electron has jumped while eight bonding electrons remain; and a possible identification of 270 cm^{-1} with $2\nu'_2$ of a linear molecule is incompatible with the Franck-Condon principle, since the 270 cm^{-1} progression is too long, and has an intensity maximum.[7] The large total number of observed bands in the spectrum can now reasonably be attributed to extensive progressions in both ν'_1 and ν'_2 and combinations of these, assuming a bent upper state. As Liebermann has shown, the observed values of B' correspond to a considerable increase of r' over r'' *provided* the molecule is considerably bent in the upper state. The Franck-Condon principle would then call for extensive excitation of ν'_1. Thus an allowed $^1B_2$, $^1\Sigma^+_g$ electronic transition to a bent upper state seems to be established.

This is in agreement with the writer's earlier expectations. These, however, call for additional, presumably weaker, vibronic-allowed transitions

to the $^1B_2$ and to a closely adjacent $^1A_2$ upper electronic state. These and other electronic-forbidden bands may well be present among the very numerous bands not yet analyzed.

It is interesting to inquire somewhat into the factors governing the intensity of the observed electronic transition $^1B_2$, $^1\Sigma^+_g$. The normal electron configuration and state of CS_2 may be written as follows:[9]

$$\cdots(\sigma s\sigma, \sigma_g)^2(\sigma 0\bar{\sigma}, \sigma_u)^2(\pi\pi\pi, \pi_u)^4(\pi 0\bar{\pi}, \pi_g)^4 \times(\sigma\bar{s}\sigma, \sigma_g)^0(\bar{\sigma}\sigma\sigma, \sigma_u)^0(\pi\bar{\pi}\pi, \pi_u)^0,\ ^1\Sigma^+_g. \quad (6)$$

The *MO*'s with superscript zero are unoccupied but capable of being occupied in excited states. We shall be interested in two such electronic states:

$$(\pi 0\bar{\pi})^3(\sigma\bar{s}\sigma)^1,\ ^1\Pi_g;\quad (\pi 0\bar{\pi})^3(\pi\bar{\pi}\pi)^1,\ ^1\Sigma^+_u. \quad (7)$$

In (7) all *MO*'s not mentioned are supposed to be populated in the same way as in (6).

For a linear molecule, the electronic transition to the $^1\Pi_g$ of (7) is forbidden, but that to the $^1\Sigma^+_u$ is allowed, and *strongly* so, since it is easily seen that the transition involved ($\pi 0\bar{\pi}\rightarrow\pi\bar{\pi}\pi$) has $N\rightarrow V$ characteristics.[10] (The strong CS_2 bands near λ2000 are, perhaps, to be identified with this transition.)

Now consider, for a linear molecule, vibrating states of the $^{e1}\Pi_g$ state such as to give $^1\Sigma^+_u$ vibronic states. (Such a state can be obtained, for example, if one quantum of ν_2 is excited.) These $^1\Sigma^+_u$ vibronic states will be perturbed by the $^1\Sigma^+_u$ electronic state of (7). Vibronic perturbations such as these will overcome the complete forbiddenness of the $^1\Pi_g$, $^1\Sigma^+_g$ electronic transition, giving *P*, *R* bands which might even have considerable intensity and explain the observed CS_2 bands.

However, suppose the molecule is bent in its upper electronic state. The $^{e1}\Pi_g$ then splits into $^{e1}B_2$ and $^{e1}A_2$ and the $^{e1}\Sigma^+_u$ becomes $^{e1}B_2$. As the molecule becomes bent, the two $^{e1}B_2$ wave functions begin to mix, and thus the transition to the $^{e1}B_2$ derived from $^{e1}\Pi_g$ becomes more and more allowed. [Of course other higher $^{e1}B_2$ wave functions also mix in, but it is improbable that any of them are important for the intensity.] It is easily shown, using perturbation theory, that the extent of mixing should be proportional to the amount of bending. However, as a result of the fact that the molecule is linear in its lower electronic state, it is found that the *total* absorption intensity for an upper state of the kind here considered should be just the same whether the equilibrium configuration of the upper state is bent or linear. Thus in either case our analysis indicates that the intensity of the observed bands may be attributed mainly to the influence of the $^{e1}\Sigma^+_u$ state of (7).

The Franck-Condon principle can now be applied. For an upper state with bent equilibrium configuration, the usual Franck viewpoint applies and predicts that the strongest bands should involve excitation of ν'_2, together with perhaps a few quanta of ν'_1, with enough energy to carry the excited molecule from its bent equilibrium state up to a practically linear configuration[11] (not quite linear, when one corrects for the forbiddenness of the transition in an exactly linear molecule). Further, the *total* intensity of all the absorption bands from any given initial vibrational state should increase strongly (with of course some shift in the intensity distribution among upper vibrational states) if the bending vibration is excited in the lower state. A preliminary examination of the intensity integrals involved indicates proportionality of the total intensity to v''_2+1. [Experimental confirmation of this prediction would not, however, give evidence for or against a bent upper equilibrium state, since the *same* prediction is found to be valid for a linear upper state.]

[9] This is based on Eqs. (16a), (17) of reference 6, with some simplication in the *LCAO* notation.

[10] Cf. R. S. Mulliken, J. Chem. Phys. **7**, 20 (1939), in regard to $N\rightarrow V$ transitions.

[11] That is, the Franck principle would say that, at the first instant after the transition, the molecule should be linear. This would then have to correspond to the large angle phase of a violent angular vibration. It is to be noted that such a motion, if $K>0$, would involve very strong rotation-vibration interaction, leading to an irregular arrangement of energy levels (cf., earlier parts of this paper).

Finite Self-Energies in Radiation Theory. Part II

ALFRED LANDÉ AND LLEWELLYN H. THOMAS
Mendenhall Laboratory, Ohio State University, Columbus, Ohio

(Received July 9, 1941)

The "cutting-off method" proposed in Part I is equivalent to a field theory based on Maxwell's equations supplemented by Yukawa's equations, both fields having the same point charges as sources. The chief result is a finite self-energy $W=e^2/2r_0$ and a modified Coulomb potential $(e/r)[1-\exp(-r/r_0)]$, also derivable from a Hamiltonian in Fourier form. For accelerated motions the field theory yields a finite force of inertia $(-m\ddot{x})$ together with the universal damping term in first approximation. Small additional terms reflect the "structure" of the electron. Radiation and self-force of a vibrating electron are discussed, and the perturbation problem is formulated. The exact integration of Yukawa's field equation is given in Section 9. Our results are related to Born-Infeld's unitary field theory and Dirac's theory of the classical electron, in particular with respect to waves of velocity larger than c. The electronic mass m is the result of photons of rest mass *zero* and mesons of rest mass $M=m\cdot 2\cdot 137=274m$.

1. INTRODUCTION

IN Part I we discussed a "cutting-off method"[1] for obtaining finite self-energies of charged particles. We started from the physical consideration that the natural line breadth $\Delta\lambda=4\pi e^2/3mc^2$ allows to determine the position of an electron only within a range of order $\Delta\lambda$ since the electron does not react to the phase of an external field at its exact position but rather to the phase averaged over the range $\Delta\lambda$. More precisely, its vibrational energy is reduced, as compared with the energy without damping, by the damping factor $R=[1+(\nu\Delta\lambda/c)^2]^{-1}$. In Part I we then proposed to reduce the Fourier terms in Fermi's theory of radiation by the same factor R made invariant by Doppler correction for particles in motion. This reduction led to a finite electrostatic self-energy $W=e^2/2r_0$ and a modified Coulomb potential $(e/r)[1-\exp(-r/r_0)]$ where $r_0=\Delta\lambda/2\pi=2e^2/3mc^2$.

In Part II we start from the remark that this potential is the difference of Maxwell and Yukawa potentials as solutions of two separate sets of invariant field equations with the same point charges as sources. The special value $r_0=2e^2/3mc^2$ was chosen in Part I so that the Fourier reduction factor R_ν equals the former damping factor R. This led to an electromagnetic mass $\frac{3}{4}$ of the total mass. However, the special choice of r_0 is not essential. It would seem even more reasonable to choose the parameter $k=1/r_0$ of the field theory so as to have a *unitary field theory* in which the mass of the field equals the total mass, by virtue of the formula $W=e^2/2r_0=ke^2/2=mc^2$, or vice versa $r_0=e^2/2mc^2$. Whether this choice is correct can only be decided by experiments with extremely short waves. In view of the existence of neutral particles it has become doubtful whether one should insist on a purely electromagnetic origin of the electronic mass. On the other hand the combination of Maxwell's and Yukawa's field equations is already a deviation from the pure electromagnetic theory.

Our method offers a consistent and invariant scheme of formulae for calculating the properties of electronic charges without infinities. However, from a physical point of view it is hard to understand why the resulting potential, the resulting radiation of energy, etc., should be the *difference* rather than the sum of the two independent fields of Maxwell and Yukawa. A similar objection could be raised against Dirac's[2] *difference* of advanced and retarded potentials. We are using *retarded* potentials only, although the retarded Yukawa potential is given a negative sign. Apart from the lack of "physical understanding" of this negative sign, our method may at least be considered as an invariant formal way of avoiding infinities in classical point charges. The Fourier representation of Section 7 shall

[1] A. Landé, Phys. Rev. **60**, 121 (1941).

[2] P. A. M. Dirac, Proc. Roy. Soc. **167**, 148 (1938).

prepare the way to a future application of *quantum theory* to our classical scheme.

2. Field Equations

Already in Part I we remarked that the modified electrostatic potential resulting from the Fourier method is the difference of two separate potentials

$$V = V'' - V' = (e/r) - (e/r)\exp(-r/r_0). \quad (1)$$

V' and V'' are solutions of the differential equations

$$\Box V'' = -4\pi\rho, \quad \Box V' = -4\pi\rho + k^2 V', \quad (2)$$

to be supplemented by two equations for vector potentials

$$\Box A'' = -4\pi j/c, \quad \Box A' = -4\pi j/c + k^2 A'. \quad (2')$$

ρ and j vanish everywhere except on the world lines of point particles. The field derived from $V''A''$ is an ordinary Maxwell field. The field of meson type derived from the potential V', A' is

$$E' = -\nabla V' - \dot{A}'/c, \quad H' = \operatorname{curl} A', \qquad \operatorname{div} A' + \dot{V}'/c = 0. \quad (3)$$

Together with (2) (2') this is equivalent with the field equations

$$\operatorname{curl} E' = -\dot{H}'/c, \quad \operatorname{div} H' = 0,$$
$$\operatorname{curl} H' = \dot{E}'/c + 4\pi j/c - k^2 A', \qquad (4)$$
$$\operatorname{div} E' = 4\pi\rho - k^2 V', \quad \operatorname{div} j + \dot{\rho} = 0.$$

Multiplying by H' and E', and subtracting we arrive at

$$-(c/4\pi)\int ds\{[E'H']_n + k^2 A_n'\} = (1/8\pi)(d/dt)$$
$$\times \int dv\{E'^2 + H'^2 + k^2(V'^2 + A'^2)\} + \int E' j dv. \quad (5)$$

The stress-energy-momentum tensor T' therefore has the components

$$-T_{44}' = w' = (1/8\pi)\{E'^2 + H'^2 + k^2(V'^2 + A'^2)\}, \quad (6)$$
$$-iT_{41}' = g' = (1/4\pi c)\{[E'H'] + k^2 V'A'\},$$

representing density of energy and momentum. Condensing three rows and columns to one we can write for the tensor T'

$$T' = \begin{Vmatrix} p'_{mn} & iS'/c \\ iS'/c & -w' \end{Vmatrix} + \frac{k^2}{4\pi}\begin{Vmatrix} A'_m A'_n & iA'V' \\ iA'V' & -V'^2 \end{Vmatrix} - \frac{k^2}{8\pi}\begin{Vmatrix} (A'^2 - V'^2)_{nm} & 0 \\ 0 & (A'^2 - V'^2) \end{Vmatrix}, \quad (7)$$

where p', S', w' are the usual expressions for Maxwell's tensor, Poynting's vector, and energy density in terms of E' and H'.

Corresponding equations with $k=0$, called (3') to (7'), hold for the Maxwell field E'', H''. Since the potentials V'' and V' are supposed to be subtractive the same applies to the field components $E''-E'=E$, $H''-H'=H$. But it also applies to the tensor components $T''-T'=T$. This can be learned from the fact that the last term in (5) is to be subtracted from the last term in (5') in order to give the total mechanical work $\int E\cdot j dv = \int (E''-E')j dv$.

Integration of the wave equations (2) leads to the following general solution (see Section 9) for the potential of a point charge at $xyzt$:

$$V'' - V' = ck\int\int\int\int R^{-1}J_1(kR)\rho d\xi d\eta d\zeta d\tau, \quad (8)$$

where $\rho(\xi\eta\zeta\tau)$ is the density, and R is the 4-distance

$$R^2 = (c\tau - ct)^2 - (\xi - x)^2 - (\eta - y)^2 - (\zeta - z)^2. \quad (8')$$

The integral extends over τ from $-\infty$ to t and over values $\xi\eta\zeta$ belonging to real values of R for the respective value of τ (*retarded potential*). In case of point charges e the integration over $\xi\eta\zeta$ yields a factor e so that (8) simplifies to a sum over the point charges:

$$V'' - V' = \sum eck\int R^{-1}J_1(kR)d\tau = \sum eck\int_0^\infty R^{-1}J_1(kR)(-\partial\tau/\partial R)dR. \quad (9)$$

Replacing ρ by j/c and j by $e\xi$ for point charges one obtains the vector potential

$$A'' - A' = \sum ek\int_0^\infty R^{-1}J_1(kR) \times \xi(\tau)(-\partial\tau/\partial R)dR. \quad (9')$$

The proof of the fundamental formula (9) is given in Section 9.

V' and V'' can always be supplemented by solutions of the homogeneous Maxwell and Yukawa equations. The latter are solved by plane waves λ whose frequency is

$$\nu^* = [\nu_0^2 + (c/\lambda)^2]^{\frac{1}{2}} \quad \text{where} \quad \nu_0 = kc/2\pi,$$

so that the phase velocity $c^* = \nu^*\lambda$ is larger than c:

$$c^* = [c^2 + (\nu_0\lambda)^2]^{\frac{1}{2}}.$$

A similar velocity larger than c occurred also in Dirac's theory of the classical point electron[2] and does not interfere with invariance. ν_0 is the minimum frequency of Yukawa waves.

3. Applications. Uniform Motion

(I) As our first example we consider an electron at rest at the zero point $\xi\eta\zeta = 0$. At $t = 0$ and at the distance $r^2 = x^2 + y^2 + z^2$ we have from (8′)

$$R^2 = (c\tau)^2 - r^2, \quad \partial c\tau/\partial R = -R(R^2 + r^2)^{-\frac{1}{2}},$$

the root with minus sign since $\tau < t$. According to (9) we obtain

$$\begin{aligned} V'' - V' &= ek \int_0^\infty J_1(kR)(R^2 + r^2)^{-\frac{1}{2}} dR \\ &= (e/r)[1 - \exp(-kr)]. \end{aligned} \tag{10}$$

In particular for $r = 0$ we have $(V'' - V')_0 = ek$, that is, the modified Coulomb potential of Part I and the starting point of Part II. Instead of k we may write $1/r_0$.

The electrostatic self-energy of an electron at rest is

$$W_{\text{rest}} = (1/8\pi) \int dv \{E''^2 - (E'^2 + k^2 V'^2)\},$$

where

$$E'' = e/r^2, \quad V' = (e/r) \exp(-kr), \quad E' = -\partial V'/\partial r.$$

Integration gives

$$W_{\text{rest}} = e^2 k/2. \tag{10′}$$

The same result could have been obtained by the simpler formula

$$W_{\text{rest}} = \tfrac{1}{2} e(V'' - V')_0 = e^2 k/2.$$

The electromagnetic rest mass is therefore

$$m = e^2 k/2c^2, \text{ vice versa } k = 2mc^2/e^2, \tag{10″}$$

k determines the ratio e^2/m, where the "mass m" is defined as the factor of c^2 in the self-energy, and the "charge e" is defined as the factor of $1/r$ in the mutual energy. The corresponding meson mass is

$$M = h\nu_0/c^2 = kh/2\pi = 2m(hc/2\pi c^2) = m \cdot 2 \cdot 137.$$

(II) If the electron moves uniformly with velocity $v_x/c = \beta$ we have

$$\xi = \beta c\tau, \quad \eta = \zeta = 0,$$

$$R^2 = (c\tau - ct)^2 - (\beta c\tau - x)^2 - y^2 - z^2,$$

$$\partial c\tau/\partial R = -R(1 - \beta^2)^{-\frac{1}{2}}(R^2 + a^2)^{-\frac{1}{2}},$$

where

$$a^2 = (1 - \beta^2)^{-1}[r^2 - 2\beta ctx + \beta^2(c^2t^2 + x^2 - r^2)],$$

so that

$$\begin{aligned} V''' - V' &= ek(1 - \beta^2)^{-\frac{1}{2}} \int_0^\infty J_1(kR)(R^2 + a^2)^{-\frac{1}{2}} dR \\ &= e[a(1 - \beta^2)^{\frac{1}{2}}]^{-1}[1 - \exp(-ak)]. \end{aligned} \tag{11}$$

It can easily be shown geometrically that

$$a(1 - \beta^2)^{\frac{1}{2}} = d \cdot (1 - \beta \cos\alpha)$$

where d is the distance between $xyzt$ and the position ξ of the particle at the retarded time τ so that $d = c(t - \tau)$, whereas α is the angle between d and the velocity. Therefore the first part of (11) agrees with the Lienard-Wiechert potential of a point charge V''', whereas the second part represents the Yukawa potential V'. The vector potential is

$$A_x'' - A_x' = (V''' - V')(v_x/c).$$

In particular, on the moving electron itself ($a = 0$) we have

$$\begin{aligned} V_0 &= (V''' - V')_0 = ek(1 - \beta^2)^{-\frac{1}{2}}, \\ A_0 &= (A'' - A')_0 = ek\beta(1 - \beta^2)^{-\frac{1}{2}}. \end{aligned} \tag{12}$$

Energy and momentum of the field of the moving electron are therefore

$$\begin{aligned} W &= eV_0/2 = mc^2(1 - \beta^2)^{-\frac{1}{2}}, \\ G &= eA_0/2c = mv(1 - \beta^2)^{-\frac{1}{2}}, \end{aligned} \tag{12′}$$

agreeing with relativity. An explicit proof of (12′) is given in (29) Section 8. When two like (unlike) point charges approach to the distance *zero* the finite work $e^2k=2mc^2$ is spent (gained).

4. Acceleration. Self-Force

Next we consider an electron moving along the x-axis with coordinates

$$\xi=u\tau+\tfrac{1}{2}f\tau^2+\tfrac{1}{6}g\tau^3, \quad \eta=\zeta=0. \tag{13}$$

The meaning of u, f, g is seen from the values at $\tau=0$:

$$u=(d\xi/d\tau)_0, \quad f=(d^2\xi/d\tau^2)_0, \quad g=(d^3\xi/d\tau^3)_0.$$

At an external point $r^2=x^2+y^2+z^2$ at time t we have from (8′)

$$R^2=(c\tau-ct)^2-(u\tau+\tfrac{1}{2}f\tau^2+\tfrac{1}{6}g\tau^3-x)^2-y^2-z^2.$$

For the field on the particle itself at $\tau=0$ consider t and r as small so that r^2 can be neglected altogether. Also neglecting second orders of u, f, g we obtain approximately

$$c\tau=ct-R+xR^{-1}(u\tau+\tfrac{1}{2}f\tau^2+\tfrac{1}{6}g\tau^3).$$

In the same approximation we can on the right replace τ by $(t-R/c)$, hence

$$\begin{aligned} cd\tau/dR=&-1-xR^{-2}\{u(t-R/c)\\ &+\tfrac{1}{2}f(t-R/c)^2+\tfrac{1}{6}g(t-R/c)^3\}\\ &-xR^{-1}c^{-1}\{u+f(t-R/c)+\tfrac{1}{2}g(t-R/c)^2\}. \end{aligned} \tag{14}$$

There are two special cases of (14). If $t=0$ and r is small we obtain

$$cd\tau/dR=-1+\tfrac{1}{2}xf/c-\tfrac{1}{3}xgR/c^3. \tag{14′}$$

If t is small and $r=0$ hence $x=0$ we have

$$cd\tau/dR=-1. \tag{14″}$$

We are now prepared to calculate V near the electron at $t=0$ for small r. Substituting (14′) in (9) we obtain

$$\begin{aligned} V''-V'&=(1-\tfrac{1}{2}xf/c^2)ek\int_0^\infty J_1(kR)R^{-1}dR\\ &\quad+(xge/3c^3)\int_0^\infty J_1(kR)d(kR)\\ &=(1-\tfrac{1}{2}xf/c^2)ek+xge/3c^3, \end{aligned} \tag{15}$$

since both integrals are unity. Therefore

$$-\partial V/\partial x=\tfrac{1}{2}fek/c^2-eg/3c^3.$$

Substituting (14″) and $\xi=u+f\tau+\frac{1}{2}g\tau^2$ in (9′) we arrive at

$$\begin{aligned} A''-A'&=(ek/c)\int_0^\infty[u+f(t-R/c)\\ &\quad+\tfrac{1}{2}g(t-R/c)^2]J_1(kR)R^{-1}dR,\\ -(\partial A/\partial ct)_{t=0}&=(ek/c)\int_0^\infty(-f+gR/c)J_1(kR)R^{-1}dR\\ &=-ekf/c+ge/c^2. \end{aligned}$$

The magnetic field H vanishes on the electron so that the self-force $F=eE=-e\partial V/\partial x-e\partial A/\partial ct$ at $t=0$ becomes

$$\begin{aligned} F&=-(e^2k/2c^2)\cdot f+(2e^2/3c^3)\cdot g,\\ &=-m(d^2\xi/d\tau^2)+(2e^2/3c^3)(d^3\xi/d\tau^3). \end{aligned} \tag{16}$$

where m is the mass due to the two fields, see (10″). If the whole mass of the electron is due to the fields, the various field centers (point charges) move *according to the field equations alone* in such a way that "the total field force is zero" on every single particle.

Charges with different masses and radii could be accounted for by extending the sums (9) (9′) over terms with different individual values of k.

The self-force (16) at $t=0$ is composed of retarded contributions of the whole path (13) during $\tau<0$. But only the immediate past matters in producing the two terms of (16). In case of a more general path

$$\xi=u\tau+\tfrac{1}{2}f\tau^2+\tfrac{1}{6}g\tau^3+\tfrac{1}{24}h\tau^4+\cdots \quad \text{for } \tau<0$$

it turns out that the higher terms contribute also with their remote past to the self-force at $t=0$. In connection with the fact that the velocity ξ on such a path would be larger than c in the remote past, each higher term furnishes an infinite contribution to F. Even if an infinite series in τ should represent a physically possible path $\xi(\tau)$ (vibrating electron) an integration by terms is not possible.

It would be an interesting problem to find an accelerated path such that the self-force vanishes at all times. As long as the acceleration is small this path will coincide with that derived by Dirac[2] from the difference of advanced and retarded Maxwell potentials.

5. Vibrating Electron. Radiation

An electronic point shall vibrate about the zero point with coordinates

$$\xi = a \sin(\omega\tau), \quad \eta = 0 = \zeta.$$

The amplitude a shall be small compared with the wave-length $2\pi c/\omega$ and with the electronic radius $r_0 = 1/k = c/\omega_0$ so that a^2 can always be neglected. At distance $r^2 = x^2+y^2+z^2$ we have (8′)

$$R^2 = c^2(\tau - t)^2 + 2ax \sin(\omega\tau) - r^2,$$

hence in the same approximation

$$c\tau = ct - (R^2+r^2)^{\frac{1}{2}} + (R^2+r^2)^{-\frac{1}{2}} ax \sin(\omega\tau)$$

with the argument $\omega\tau = \omega t - (R^2+r^2)^{\frac{1}{2}}\omega/c$ when neglecting a^2. Thus

$$\begin{aligned} -R^{-1}\partial(c\tau)/\partial R = {} & (R^2+r^2)^{-\frac{1}{2}} \\ & + (ax\omega/c)(R^2+r^2)^{-1} \cos(\omega\tau) \\ & + ax(R^2+r^2)^{-\frac{1}{2}} \sin(\omega\tau) \end{aligned} \tag{17}$$

consisting of three terms. For large r (wave zone) the second term alone contributes to V, and the first term alone to A. With $d\xi/d\tau = a\omega \cos(\omega\tau)$ we obtain from (9) (9′)

$$\begin{aligned} V'' - V' &= (eax\omega/c) \int_0^\infty J_1(kR)(R^2+r^2)^{-1} \\ &\quad \times \cos[\omega t - (R^2+r^2)^{\frac{1}{2}}\omega/c] d(kR), \\ A'' - A' &= (ea\omega/c) \int_0^\infty J_1(kR)(R^2+r^2)^{-\frac{1}{2}} \\ &\quad \times \cos[\omega t - (R^2+r^2)^{\frac{1}{2}}\omega/c] d(kR). \end{aligned} \tag{18}$$

In the limit of small ω one can replace (R^2+r^2) by r^2 not only for small R but also for large R since the integrals give negligible contributions for large R if ω is small. In this case (18) simplifies to

$$\begin{aligned} V = V'' - V' &= (ea\omega/c)(x/r^2) \cos[\omega(t - r/c)], \\ A = A'' - A' &= (ea\omega/c)(1/r) \cos[\omega(t - r/c)], \end{aligned} \tag{18′}$$

that are the well-known Lorentz potentials. But for larger ω one has to use the complete integrals (18); we have not been able to evaluate them. From what is learned in (20′) about the self-force of a vibrating electron the Lorentz potentials (18′) are valid up to $\omega = \omega_0$, and a decrease of the emitted potential will occur only for $\omega > \omega_0$ in connection with the fact that Yukawa waves have a minimum frequency $\omega_0 = kc$ (Section 2). This result is confirmed by the Fourier method, Section 8, III.

6. Vibrating Electron. Self-Force

In order to find the self-force of a vibrating electron at time t it is convenient to have the electron in the zero point $r = 0$ at time t. We therefore consider the position

$$\xi = a \sin(\omega\tau) - a \cdot s, \quad \eta = \zeta = 0,$$

where the parameter s will later be equated to $\sin(\omega t)$. With small r and neglection of r^2 we now have

$$c\tau = ct - R + xaR^{-1}[\sin(\omega\tau) - s].$$

On the right we can replace τ by $(t - R/c)$ if a is small. Then

$$\begin{aligned} \partial c\tau/\partial R = {} & -1 - xaR^{-2}[\sin(\omega t - \omega R/c) - s] \\ & - (xa\omega/Rc) \cos(\omega t - \omega R/c). \end{aligned}$$

Substituting in (9) (9′) and neglecting a^2 we obtain

$$\begin{aligned} \partial V/\partial x &= eka \int_0^\infty J_1(kR)\{R^{-3}[\sin(\omega t - \omega R/c) - s] \\ &\quad + (\omega/R^2c) \cos(\omega t - \omega R/c)\} dR, \\ \partial A/\partial ct &= -eka(\omega/c)^2 \int_0^\infty J_1(kR) R^{-1} \\ &\quad \times \sin(\omega t - \omega R/c) dR. \end{aligned}$$

We now put $s = \sin(\omega t)$. In the self-force

$$F = -e\partial V/\partial x - e\partial A/\partial ct,$$

we separate terms with factors $\sin(\omega t)$ and $\cos(\omega t)$. Writing

$$-\omega^2 a \sin(\omega t) = d^2\xi/d\tau^2, \quad -\omega^3 a \cos(\omega t) = d^3\xi/d\tau^3,$$

and using the abbreviations $kR = u$, $\omega R/c = qu$ with

$$e^2k/2c^2 = m, \quad ck = c/r_0 = \omega_0, \quad \omega/\omega_0 = q, \tag{19}$$

we obtain

$$F=-m(d^2\xi/d\tau^2)f(q)+(2e^2/3c^3)(d^3\xi/d\tau^3)g(q),$$

$$f(q)=2\int_0^\infty J_1(u)u^{-1}\{\cos(qu)-(qu)^{-1}\sin(qu)+(qu)^{-2}[1-\cos(qu)]\}du, \tag{20}$$

$$g(q)=\tfrac{3}{2}\int_0^\infty J_1(u)\{(qu)^{-1}\sin(qu)+(qu)^{-3}[(qu)\cos(qu)-\sin(qu)]\}du.$$

For small $q=\omega/\omega_0$ the factors f and g reduce to *unity* so that F has the classical form (16). In general F can be found with help of auxiliary formulae in two cases $0\leqslant q\leqslant 1$ and $q\geqslant 1$, respectively:

$$\int_0^\infty J_1(u)\frac{\sin(qu)}{(qu)}du=\begin{cases}1\\1-(1-q^{-2})^{\frac{1}{2}},\end{cases}$$

$$\int_0^\infty J_1(u)\frac{\sin(qu)}{(qu)}\frac{du}{u}=\begin{cases}\frac{1}{2}[(1-q^2)^{\frac{1}{2}}+q^{-1}\sin^{-1}q]\\(\pi/4)q^{-1},\end{cases}$$

$$\int_0^\infty J_1(u)\cos(qu)\frac{du}{u}=\begin{cases}(1-q^2)^{\frac{1}{2}}\\0.\end{cases}$$

Also

$$(qu)^{-2}[1-\cos(qu)]=(qu)^{-1}\int_0^1\sin(pqu)dp,$$

$$(qu)^{-2}[(qu)\cos(qu)-\sin(qu)]=-\int_0^1\sin(pqu)pdp.$$

With these formulae we obtain in (20)

$$f(q)=\begin{cases}(1/3q^2)[1-(1-q^2)^{\frac{1}{2}}]\\\qquad+q^{-2}[(1-q^2)^{\frac{1}{2}}-1]+(1-q^2)^{\frac{1}{2}}\\\qquad-(2/3q^2)\end{cases}$$

$$g(q)=\begin{cases}1\\1-(1-q^{-2})^{\frac{1}{2}},\end{cases} \tag{20'}$$

for $0\leqslant q\leqslant 1$ and $q\geqslant 1$, respectively. For large frequencies $q\gg 1$ both f and g tend toward zero as though inertia and damping were fading out with increasing ω. The amplitude a shall always be small compared with c/ω. If we should consider frequencies $\omega\sim\omega_0$ and yet amplitudes a not small compared with the electronic radius $r_0=\omega_0/c$ the result would be quite different. The dependence of the "scattering cross section" on the amplitude for frequencies of order ω_0 could be used for checking the classical theory if this effect were not completely overshadowed by quantum effects just at these high frequencies.

It is quite significant that the decrease of the factor $g(q)$ begins only at the characteristic frequency ω_0 itself. Since the damping term with $(2e^2/3c^3)\cdot g(q)$ is the counterpart of long distance radiation, this means that up to $\omega=\omega_0$ only Maxwell radiation is emitted, in agreement with the fact (Section 2) that Yukawa waves have a minimum frequency $\omega_0=kc$. We learn from (20') that for $\omega>\omega_0$ the ratio of Maxwell to Yukawa radiated energy is 1 to $(1-q^{-2})^{\frac{1}{2}}$. The same result can be obtained directly by the Fourier method.

7. Fourier Method. Hamiltonian

For particles at rest the field theory is equivalent with the Fourier reduction method of Part I. For particles in motion the field theory gives results differing from the Doppler correction of Part I, but consistent with relativity.

Similar to Fermi we expand the Yukawa potential $V'(r,t)$ into a Fourier series of standing waves of direction α_s in a large space Ω (for details compare with Fermi[3]):

$$V'(r,t)=c(8\pi/\Omega)^{\frac{1}{2}}\textstyle\sum_s Q_s'(t)\cos\Gamma_{sr},\qquad \Gamma_{sr}=(\omega_s/c)(\alpha_s\cdot r)+\text{phase}. \tag{21}$$

Substitution into Eq. (2) gives the following differential equation for Q_s'

$$d^2Q_s'/dt^2+(\omega_s^2+k^2c^2)Q_s'=c(8\pi/\Omega)^{\frac{1}{2}}\textstyle\sum_i e_i\cos\Gamma_{si} \tag{21'}$$

[3] E. Fermi, Rev. Mod. Phys. **4**, 87 (1932).

in case of point charges. For uniform motions where r_i in Γ_{si} changes with time (21) is solved by

$$Q_s'(t)=c(8\pi/\Omega)^{\frac{1}{2}}\sum_i e_i\cos\Gamma_{si}[\omega_s^2(1-\beta_i^2\cos^2\vartheta_{si})+\omega_0^2]^{-1}. \tag{22}$$

ϑ_{si} is the angle between the wave normal α_s and the direction of β_i, and ω_0 is written for kc. The dependence of t is contained in r_i in Γ_{si}. Corresponding Fourier series for the Maxwell potential V'' lead to

$$Q''(t)=c(8\pi/\Omega)^{\frac{1}{2}}\sum_i e_i\cos\Gamma_{si}[\omega_s^2(1-\beta_i^2\cos^2\vartheta_{si})]^{-1}. \tag{22'}$$

(22) and (22') can be augmented by solutions of the homogeneous differential equations. The Fourier coefficient $Q_s=Q_s''-Q_s'$ of the resulting potential $V=V''-V'$ can be written

$$Q_s(t)=c(8\pi/\Omega)^{\frac{1}{2}}\sum_i e_i\cos\Gamma_{si}\omega_s^{-2}(1-\beta_i^2\cos^2\vartheta_{si})^{-1}R_{si} \tag{23}$$

and contains the "reduction factor"

$$R_{si}=[1+(1-\beta_i^2\cos^2\vartheta_{si})\omega_s^2/\omega_0^2]^{-1}. \tag{24}$$

For $\beta_i=0$ this is the factor used in Part I for particles at rest.

Corresponding calculations can be applied to the vector potential $A=A'-A''$:

$$A(r,t)=c(8\pi/\Omega)^{\frac{1}{2}}\sum_s[\alpha_s\chi_s(t)+A_sq_s(t)]\sin\Gamma_{sr}$$

with $\alpha_s=$longitudinal, $A_s=$transversal unit vector. (3') is equivalent to $\omega_s\chi_s'+\dot{Q}_s'=0$. The Fourier coefficients $\chi_s=\chi_s''-\chi_s'$ and $q_s=q_s''-q_s'$ are

$$\begin{matrix}\chi_s\\ q_s\end{matrix}(t)=c(8\pi/\Omega)^{\frac{1}{2}}\sum_i e_i\beta_i\begin{matrix}\cos\\ \sin\end{matrix}(\vartheta_{si})\sin\Gamma_{si}\omega_s^{-2}(1-\beta_i^2\cos^2\vartheta_{si})^{-1}R_{si} \tag{25}$$

with the same factor R_{si}. In all cases one may add solutions of the homogeneous equation (21') etc.

The *Hamiltonian* of the resulting field is $H=H''-H'$, *viz.*

$$\begin{aligned}H=&\sum_i m_ic^2+\sum_i(\dot{r}_i(p_i^{\text{kin}}+p_i^{\text{pot}}))+c(8\pi/\Omega)^{\frac{1}{2}}\sum_i e_i\sum_s(Q_s''-Q_s')\cos\Gamma_{si}\\ &-c(8\pi/\Omega)^{\frac{1}{2}}\sum_i(e_i/c)\sum_s(\dot{r}_i,\alpha_s(\chi_s'-\chi_s')+A_s(q_s''-q_s'))\sin\Gamma_{si}\\ &+\tfrac{1}{2}\sum_s[(p_s''^2+\xi_s''^2-P_s''^2)+\omega_s^2(q_s''^2+\chi_s''^2-Q_s''^2)]\\ &-\tfrac{1}{2}\sum_s[(p_s'^2+\xi_s'^2-P'^2)+(\omega_s^2+\omega_0^2)(q_s'^2+\chi_s'^2-Q_s'^2)]\end{aligned} \tag{26}$$

with coordinates $Q_s'Q_s''q_s'q_s''\chi_s'\chi_s''$ and momenta $P_s'P_s''p_s'p_s''\xi_s'\xi_s''$ and with $\omega_0=kc$. (26) is verified by the canonical equations

$$\dot{Q}_s'=\partial H/\partial P_s'=-P_s',\quad \dot{P}_s'=-\partial H/\partial Q_s', \tag{26'}$$

etc., that agree with the differential equations (21) etc., for Q_s', Q_s'' etc., (compare with Fermi, reference 3, p. 129).

The first sum in (26) is the *mechanical* rest energy, the second sum contains the *mechanical* kinetic energy. In a unitary theory with $k=2mc^2/e^2$ these two terms are to be omitted. The sum over $(\dot{r}_ip_i^{\text{pot}})$ is identical with the whole second line of (26) so that these sums cancel one another. The energy reduces to the two last lines of (26).

8. APPLICATIONS OF THE FOURIER METHOD

(I) First we consider a system of electrons *at rest*. Here (22) simplifies to

$$Q_s' = c(8\pi/\Omega)^{\frac{1}{2}} \sum_i e_i \cos\Gamma_{si} (\omega_s^2 + \omega_0^2)^{-1},$$
$$\dot{Q}_s' = P_s' = p_s' = \xi_s' = q_s' = \chi_s' = 0$$

and similar formulae for Q_s'' etc., without ω_0^2. The second line in (26) turns out to be half as large as, and of opposite sign as the third line, so that H reduces to

$$H = \tfrac{1}{2} c^2 (8\pi/\Omega) \sum_i \sum_j e_i e_j \sum_s \cos\Gamma_{si} \cos\Gamma_{sj} \times [(\omega_s^2)^{-1} - (\omega_s^2 + \omega_0^2)^{-1}],$$

obviously a difference of Maxwell and Yukawa terms. Instead we may write

$$H = \tfrac{1}{2} c (8\pi/\Omega) \sum_i \sum_j e_i e_j \sum_s \cos\Gamma_{si} \cos\Gamma_{sj} \times \omega_s^{-2} [1 + (\omega_s/\omega_0)^2]^{-1}, \quad (27)$$

that is, Fermi's expression "reduced" by a factor $R = [1 + (\omega_s/\omega_0)^2]^{-1}$ as in Part I. Replacing the summation $\sum_s$ by an integration with Jeans' factor $(\Omega/2\pi^2 c^3)\omega_s^2 d\omega_s$ one arrives (see Part I) at

$$H = \sum_i (e_i \omega_0/2c) + \sum_i \sum_j (e_i e_j/r)[1 - \exp(-r\omega_0/c)] \quad (27')$$

in agreement with (10) (10'), representing finite self-energies and modified Coulomb energies.

(II) Our second example shall be *one* electron in uniform motion with velocity $\dot{r}_i = \beta_i c$. Here we have to substitute the complete expressions (22) into the last two lines of (26). In addition we have

$$P_s' = -\partial H/\partial P_s' = -\dot{Q}_s'$$
$$= c(8\pi/\Omega)^{\frac{1}{2}} e_i \sin\Gamma_{si} \omega_s \beta_i \cos\vartheta_{si} \times [\omega_s^2 (1 - \beta_i^2 \cos^2\vartheta_{si}) + \omega_0^2]^{-1}$$

and corresponding expressions for the other momenta. First we sum over all directions ϑ_{si} by integrating with factor $\frac{1}{2} d(\cos\vartheta)$ from -1 to 1, and replace $\sin^2\Gamma_{si}$ and $\cos^2\Gamma_{si}$ by $\frac{1}{2}$ because of irregular phases. The second line of (26) then gives

$$c^2(8\pi/\Omega)(e^2/2) \sum_s \{\omega_s^{-2} \beta_i^{-1} \operatorname{tgh}^{-1}\beta_i - (\omega_s\beta_i)^{-1} (\omega_s^2 + \omega_0^2)^{-\frac{1}{2}} \operatorname{tgh}^{-1}(\omega_s\beta_i(\omega_s^2 + \omega_0^2)^{-\frac{1}{2}})\}, \quad (28)$$

obviously a difference of Maxwell and Yukawa terms. The latter are small compared with the former for $\omega_s \ll \omega_0$. The last line of (26) gives

$$-\tfrac{1}{2} c^2 (8\pi/\Omega)(e^2/2) \times \sum_s \{(\omega_s^2)^{-1} - [\omega_s^2 + (\omega_0^2/(1-\beta_i^2))]^{-1}\}. \quad (28')$$

The tgh^{-1} in (28) can be expanded in powers of β_i and then integrated term by term with Jeans' factor $(\Omega/2\pi^2 c^3)\omega_s^2 d\omega_s$. The result is a series that condenses to the simple expression $(e^2\omega_0/c)(1-\beta_i^2)^{-\frac{1}{2}}$. On the other hand (28') can be integrated directly with the result $-\frac{1}{2}(e^2\omega_0/c)(1-\beta_i^2)^{-\frac{1}{2}}$ just half as large as (28). The balance is

$$H = (e^2\omega_0/2c)(1-\beta_i^2)^{-\frac{1}{2}} = mc^2(1-\beta_i^2)^{-\frac{1}{2}}, \quad (29)$$

agreeing with (12') and verifying the invariance of the method in Fourier form.

(III) The Fourier method can also be applied to the *radiation* emitted by a vibrating electron similar to Heitler's method.[4] The result is quoted at the end of Section 6.

Our invariant "cutting-off method" consists in using the Hamiltonian $H = H'' - H'$ rather than H'' alone.

The *perturbation problem* of the classical Hamiltonian is this. The electrons may first move with prescribed *constant* velocities $\dot{r}_i$. The corresponding "electronic" field coordinates $Q_s'(t)$, etc., are given in (22), etc., augmented by solutions of the homogeneous equations (21') representing the initial "pure field." Between t_1 and t_2 the electrons shall move on prescribed accelerated path [$r_i(t)$ in Γ_{si} on the right of (21') prescribed]. The equation of motion (21') together with the initial value $Q_s'(t_1)$ determines the final value $Q_s'(t_2)$. Its continuation for $t > t_2$ can again be separated into an "electronic field" of type (22) and a "pure field" if the electrons move with constant velocities after t_2. Such a separation is not possible during the time of radiation $t_1 < t < t_2$. The prescribed path ought to be such that the total force (no matter whether it can be separated into external and self-force) vanishes on every electron.

[4] W. Heitler, *Quantum Theory of Radiation* (Oxford, 1936), p. 54.

9. Appendix. Exact Integration of Yukawa's Equation

The exact solution (V'', A'') of the Maxwell equations produced by charges ρ, j is well known. The exact solution of the combined Maxwell-Yukawa problem shall be given here. The exact solution of the Yukawa problem alone might be of value for the discussion of meson problems, irrespective of the present field theory.

In order to solve the differential equation

$$\nabla^2 V' - \partial^2 V'/\partial c^2 t^2 = -4\pi\rho + k^2 V' \qquad (30)$$

we use the Fourier transformation

$$u'(A, B, C; t) = \int\int\int V'(x, y, z; t) \times \exp[-2i\pi(Ax+By+Cz)]dxdydz,$$

$$\sigma(A, B, C; t) = \int\int\int \rho(x, y, z; t) \times \exp[-2i\pi(Ax+By+Cz)]dxdydz.$$

Their inversion substituted in (30) yields for u' the equation

$$-4\pi^2(A^2+B^2+C^2)u' - \partial^2 u'/\partial c^2 t^2 = -4\pi\sigma + k^2 u'. \qquad (31)$$

With the abbreviation

$$p^2 = c^2[k^2 + 4\pi^2(A^2+B^2+C^2)], \qquad (32)$$
$$q^2 = c^2 4\pi^2(A^2+B^2+C^2),$$

(31) reduces to

$$p^2 u' + \partial^2 u'/\partial t^2 = 4\pi c^2 \sigma.$$

The solution for vanishing u' and $\partial u'/\partial t$ at $t = -\infty$ is

$$u'(A, B, C, t) = \int_{-\infty}^{t} \sin[p(t-\tau)]p^{-1} 4\pi c^2 \times \sigma(A, B, C; \tau)d\tau. \qquad (33)$$

Reversing the Fourier transformation we obtain

$$V' = \int\int\int dAdBdC \exp[2i\pi(Ax+By+Cz)] \times \int_{-\infty}^{t} d\tau \sin[p(t-\tau)]p^{-1}4\pi c^2 \times \int\int\int d\xi d\eta d\zeta \rho(\xi, \eta, \zeta; \tau) \times \exp[-2i\pi(A\xi+B\eta+C\zeta)]. \qquad (34)$$

Changing the order of integration we arrive at

$$V'(xyzt) = 4\pi c^2 \int\int\int\int_{-\infty}^{t} \rho(\xi\eta\zeta\tau) \times K'(x-\xi, \cdots, t-\tau)d\xi d\eta d\zeta d\tau \qquad (35)$$

with the kernel function

$$K'(x, y, z, t) = \int\int\int \sin\eta pt) p^{-1} \times \exp[+2i\pi(Ax+By+Cz)]dAdBdC. \qquad (36)$$

The same considerations applied to the Maxwell field (with $k=0$) result in a corresponding formula for V'' with kernel K'' in which p is replaced by q of (32). The resulting potential is

$$V'' - V' = 4\pi c^2 \int\int\int\int_{-\infty}^{t} \rho(\xi\eta\zeta\tau) \times (K''-K')d\xi d\eta d\zeta d\tau. \qquad (37)$$

The kernel $K''-K'$ can be evaluated in polar coordinates. With

$$x^2+y^2+z^2 = r^2, \quad A^2+B^2+C^2 = D^2$$

we obtain

$$K''-K' = 2\int_0^\infty \sin(2\pi rD)r^{-1} \times [\sin(pt)p^{-1} - \sin(qt)q^{-1}]DdD, \qquad (38)$$

in which $p^2 = c^2(k^2+4\pi^2D^2)$ and $q^2 = c^2 4\pi^2 D^2$. Writing

$$p = ck\cosh\theta, \quad q = ck\sinh\theta, \quad 2\pi D = k\sinh\theta,$$

we have

$$K''-K' = (k^2/4\pi^2)2\int_0^\infty \sin(kr\sinh\theta)r^{-1} \times [\sin(ckt\cosh\theta)(ck\cosh\theta)^{-1} - \sin(ckt\sinh\theta)(ck\sinh\theta)^{-1}] \times \sinh\theta\cosh\theta d\theta. \qquad (39)$$

(39) has two forms according to $ct > r$, or $ct < r$. If $ct > r$ we write

$$ckt = \lambda\cosh\alpha, \quad kr = \lambda\sinh\alpha, \quad \lambda^2 = k^2(c^2t^2 - r^2).$$

Associating and dissociating sines and cosines we arrive after some transformations at the simple value of (39):

$$K''-K'=(k^2/4\pi c\lambda)J_1(\lambda).$$

If $ct<r$ we write

$$ckt=\lambda' \sinh\alpha, \quad kr=\lambda' \cosh\alpha,$$
$$\lambda'^2=k^2(r^2-c^2t^2)=-\lambda^2.$$

Here λ is imaginary, and the result is

$$K''-K'=0.$$

(37) thus yields the exact solution

$$V''-V'=ck^2\int_{-\infty}^{t}\int\int\int J_1(\lambda)\lambda^{-1}\rho(\xi\eta\zeta\tau)d\tau d\xi d\eta d\zeta, \tag{40}$$

where

$$\lambda^2=k^2[(ct-c\tau)^2-(x-\xi)^2-(y-\eta)^2-(z-\zeta)^2].$$

The $\xi\eta\zeta$-integral is extended over values that make λ real.

Subtracting $V''-V'$ from the well-known Maxwell solution V'' with the same charges as sources one obtains the exact solution of the Yukawa equation.

OCTOBER 1, 1941 PHYSICAL REVIEW VOLUME 60

Intensities in Perturbations

G. H. DIEKE
Johns Hopkins University, Baltimore, Maryland

(Received August 2, 1941)

Quantitative formulae for the intensities of lines from a pair of interacting states to a common lower state are applied to perturbations in band spectra. It appears that rotational and vibrational perturbations show quite a different behavior. In the former there is a direct superposition of intensities of the two interacting states whereas in the latter interference effects give an entirely different picture. The general formulae are applied to a few cases in the H_2 spectrum.

THE so-called perturbations in molecular spectra are a special case of interaction between a pair of quantum-mechanical states. So far the energy shifts due to the perturbations have been well studied but very little definite information is available in the literature about the intensities except some general qualitative statements. The perturbations are often of great importance for the interpretation of complex spectra and the intensities may be just as helpful as the frequency shifts.

In the present paper the general theory of the intensities in perturbations is given which follows directly from the general quantum-mechanical treatment of interaction of states, and is then applied to a few special cases.

§1. General Theory

Assume that ψ_1 and ψ_2 are the wave functions of two states satisfying

$$H^0\psi_n=W_n{}^0\psi_n, \quad n=1, 2,$$

and that ψ_a and ψ_b are the corresponding wave functions of the perturbed problem[1]

$$(H^0+H^1)\psi_m=(W_1{}^0+E_m)\psi_m, \quad m=a, b.$$

We assume further that only the interaction between ψ_1 and ψ_2 is appreciable. This is an assumption very well realized in most molecular perturbations,[2] and means that the problem can be treated without further approximations. We shall drop this restriction in certain cases later on in this paper. We can express the neglect of the other interactions by assuming all matrix elements of the perturbation matrix to be zero[3]

[1] Throughout this paper indices 1 and 2 will refer to the unperturbed and a and b to the perturbed states. ψ_a corresponds to ψ_1 and ψ_b to ψ_2 in the sense that ψ_1 furnishes the largest contribution to ψ_a, etc.

[2] We leave the influence of the electron spin out of consideration. The results are then strictly applicable only to singlets and to those multiple terms where the multiplet separation is small compared to the distance of the interacting states. The considerations can easily be expanded to the more general case.

[3] This does not necessarily mean that the other matrix elements are actually small compared to H'_{12}. Even if they

except H'_{12} and H'_{21} and we call

$$H'_{12}=\bar{H}'_{21}=S \quad \text{and} \quad S=Re^{i\alpha}. \tag{1}$$

We take in general ψ_1 to belong to the lower of the two unperturbed levels and ψ_a the lower of the two perturbed states. The correlation between the perturbed and unperturbed states is then perfectly defined except when $W_1^0=W_2^0$ when it does not matter. If the distance between the unperturbed states is

$$2\delta=W_2^0-W_1^0$$

we have

$$E_{a,b}=\delta\mp(R^2+\delta^2)^{\frac{1}{2}}. \tag{2}$$

The absolute value of the shift for either level is

$$\epsilon=|E_a|=E_b-2\delta=(R^2+\delta^2)^{\frac{1}{2}}-\delta. \tag{3}$$

The perturbed wave functions are

$$\psi_a=\frac{R}{(R^2+\epsilon^2)^{\frac{1}{2}}}\left(\psi_1-\frac{\epsilon}{R}e^{-i\alpha}\psi_2\right), \tag{4a}$$

$$\psi_b=\frac{R}{(R^2+\epsilon^2)^{\frac{1}{2}}}\left(\psi_2+\frac{\epsilon}{R}e^{i\alpha}\psi_1\right). \tag{4b}$$

ϵ/R lies between zero and one. If $R\ll\delta$, $\epsilon/R=R/2\delta$.

If both ψ_1 and ψ_2 can combine with the same final state ψ'' then the intensities of the two resulting lines are[4]

$$I_1=|q_1|^2, \quad I_2=|q_2|^2,$$

where the amplitudes are

$$q_n=\int\bar{\psi}_n q\psi''d\tau, \quad n=1, 2. \tag{5}$$

q is proportional to one of the components of the dipole moment if we are concerned with dipole radiation to which we shall restrict ourselves. The results for quadrupole radiations are analogous if we substitute for q the various components of the quadrupole moment. If q is proportional to x, I_1 is the radiation polarized in the x direction, etc.

The perturbed amplitudes can be expressed in terms of the unperturbed ones because of (4) and (5)

$$q_a=\frac{R}{(R^2+\epsilon^2)^{\frac{1}{2}}}\left(q_1-\frac{\epsilon}{R}e^{-i\alpha}q_2\right), \tag{6a}$$

$$q_b=\frac{R}{(R^2+\epsilon^2)^{\frac{1}{2}}}\left(q_2+\frac{\epsilon}{R}e^{i\alpha}q_1\right), \tag{6b}$$

from which it follows that the intensities are

$$I_a=\frac{R^2}{R^2+\epsilon^2}\left[I_1+\frac{\epsilon^2}{R^2}I_2-\frac{2\epsilon}{R}(I_1I_2)^{\frac{1}{2}}\cos(\alpha-\beta)\right], \tag{7a}$$

$$I_b=\frac{R^2}{R^2+\epsilon^2}\left[I_2+\frac{\epsilon^2}{R^2}I_1+\frac{2\epsilon}{R}(I_1I_2)^{\frac{1}{2}}\cos(\alpha-\beta)\right], \tag{7b}$$

in which β is the phase difference between ψ_2 and ψ_1. This phase difference is entirely arbitrary, as the phases of the wave functions are not determined by the wave equation and the boundary and normalization condition, and no physical quantity should depend on it. The dependence of the intensities on it is only apparent, for if we increase β by an arbitrary amount γ the perturbation matrix element

$$H_{12}'=\int\bar{\psi}_1H'\psi_2d\tau=Re^{i\alpha}$$

is multiplied by $e^{+i\gamma}$, i.e., α increased by γ. $\alpha-\beta$ which occurs in (7) is therefore completely independent of the phases of the wave function as it should be.

We shall call the terms in (7) containing the cosine the interference terms.

A direct consequence of (7) is that

$$I_a+I_b=I_1+I_2. \tag{8}$$

The sum of the intensities of two lines due to the combination of two levels with a common lower level is independent of the interaction between the two initial states.

are not small their influence is negligible if the levels lie far away from W_1^0 and W_2^0. Furthermore by assuming $H'_{11}=H'_{22}=0$ we do not restrict the generality of the problem as these terms have only a trivial influence on the result and do not affect the interaction. Treatment of the intensities in a more complicated case in He_2 is given by Kronig and Fujioka, Zeits. f. Physik **63**, 168, 175 (1930).

[4] If the q_i are proportional to the coordinates then $I\sim\nu^4|q_i|^2$, where the proportionality factor now contains only general constants. In general the perturbed and unperturbed lines lie so close together that the factor ν^4 is a constant and can be left out. In comparing the intensities of lines in different wave-length regions, however, the factor ν^4 would become important. In order to avoid carrying this factor in all the formulae we use in this paper quantities which are proportional to the real intensities divided by ν^4.

The formulae (7) apply to any interacting pair of levels in any atomic or molecular system. A special case, for example, is furnished by the Raman effect of CO_2 treated by Fermi.[5]

When both I_1 and I_2 are different from zero, the phase α of the perturbation element is very important. (We take the arbitrary phase difference β to be zero which corresponds to the conventional form of the wave functions in almost all cases), and we shall see that the two different types of perturbations usually recognized in spectra of diatomic molecules to which we shall restrict ourselves from now on differ fundamentally in this respect.

When $I_2=0$, the interference term always is absent and we have

$$I_a=\frac{R^2}{R^2+\epsilon^2}I_1, \quad I_b=\frac{R^2}{R^2+\epsilon^2}I_1.$$

We get the so-called extra line with the intensity I_b but as the intensities are entirely independent of the phases in this case, we cannot draw any conclusions regarding the type of interaction from the intensities.

As the intensities depend on ϵ/R we can have considerable intensity anomalies even for small wave-length perturbations, provided ϵ and R are both small. This will happen when two very feebly interacting states lie very close together.

In the approximate treatment of a molecule certain terms are left out of the Hamiltonian. Some of these terms can be interpreted as interaction between electronic motion and rotation, and the perturbations caused by them are called *rotational* or type A perturbations. Type B or *vibrational* perturbations are caused by terms which express the interaction between electronic motion and vibration. In a typical perturbation of either kind the usual manifestation of the perturbation is an irregularity in the spacing of the *rotational* levels. From this point of view the terms "rotational" and "vibrational" perturbation are somewhat misleading, but there can be no ambiguity if they are used in the above sense.

The two types of perturbations differ in many of their properties[6] and we shall see that they are quite radically different in the behavior of their intensities.

§2. Rotational (Type A) Perturbations

The interaction function for rotational perturbations is[6]

$$H^{(3)}=Bi\Big[\operatorname{ctg}\theta(M_\xi+iM_\eta M_\zeta+iM_\zeta M_\eta)+2\operatorname{cosec}\theta M_\eta\frac{\partial}{\partial\varphi}+2M_\xi\frac{\partial}{\partial\theta}\Big],$$

where ξ, η, ζ are Cartesian coordinates fixed to the molecule and θ and ϕ the angles which determine the orientation of the molecule. M_ξ, M_η, $M_\zeta=\Lambda h$ are the components of the electronic angular momentum and $B=h^2/8\pi^2mr^2$. The matrix element for the interaction between the states $\psi_1(\Lambda\pm1, K, m)$ and $\psi_2(\Lambda, K, m)$ is (all others are zero)

$$S=2(\Lambda\pm1\,|\,BM_\eta\,|\,\Lambda)\times[(K+\tfrac{1}{2}-\Lambda\mp\tfrac{1}{2})(K+\tfrac{1}{2}+\Lambda\pm\tfrac{1}{2})]^{\frac{1}{2}}.$$

With the conventional choice of coordinates and wave functions $(\Lambda\pm1\,|\,BM_\eta\,|\,\Lambda)$ is purely imaginary,[7] which means that the interference term in (7) disappears and we get for the perturbed intensities

$$I_a=\frac{R^2}{R^2+\epsilon^2}\left(I_1+\frac{\epsilon^2}{R^2}I_2\right), \tag{9a}$$

$$I_b=\frac{R^2}{R^2+\epsilon^2}\left(I_2+\frac{\epsilon^2}{R^2}I_1\right). \tag{9b}$$

This has a well-known elementary interpretation. The perturbed states can be regarded as mixtures of the unperturbed states, and the properties of the perturbed states are accordingly mixtures of the properties of the unperturbed

[5] E. Fermi, Zeits. f. Physik **71**, 250 (1931).

[6] J. H. Van Vleck, Phys. Rev. **33**, 467 (1929). See also G. H. Dieke, Phys. Rev. **47**, 870 (1935). The notation of the latter paper is followed closely in this article.

[7] $$M_\xi\pm iM_\eta=he^{i\chi}\left(\pm\frac{\partial}{\partial\psi}-\frac{i}{\sin\theta}\frac{\partial}{\partial\chi}\right)$$
has only real elements, if the connection between the Cartesian coordinates ξ, η, ζ and the polar coordinates ρ, ψ, χ is in the usual form
$$\xi=\rho\sin\psi\cos\chi, \text{ etc.}$$
and the dependence on the cyclic variable χ is in the form $\exp(\pm i\Lambda\chi)$. It is easily seen that nothing is changed if the dependence on χ is taken in the form $\cos\Lambda\chi$ and $\sin\Lambda\chi$ which is more suitable for molecular levels. From this it follows that the elements of M_ξ are real and those of M_η purely imaginary.

states. The perturbed intensities are weighted averages of the unperturbed ones and the weight factors are the probabilities with which the unperturbed states occur in the perturbed state. It must be noted, however, that we get this simple result only because the interference term is absent.

If the interaction terms are small but the interacting levels close together we call the effect perturbations proper. For larger values of the interaction with the interacting levels at a great distance we have Λ-doubling. If the levels are close together and interact strongly we get l-decoupling. In the latter case our results are only valid for a p-complex as, for d- and higher complexes, the interaction of more than two levels has to be considered.

There are many cases known where anomalous intensities have been observed in band spectra perturbations but quantitative measurements of such anomalies are scarce. The interpretation of such measurements, even when they exist, is complicated by the fact that the actual intensities of the lines depend often in a complicated way on the discharge conditions so that it is difficult to know what the unperturbed intensities should be. Ratios of intensities of lines coming from the same upper level have more significance. Such a pair of lines in a band are $R(K-1)$ and $P(K+1)$ and the ratio

$$f(K)=I_{R(K-1)}/I_{P(K+1)}$$

has a definite value for the different types of bands, e.g., for

$\Sigma\rightarrow\Sigma$	$\Pi\rightarrow\Sigma$	$\Sigma\rightarrow\Pi$	$\Pi\rightarrow\Pi$	
$\frac{K}{K+1}$	$\frac{K+1}{K}$	$\frac{K-1}{K+2}$	$\frac{(K-1)(K+1)^2}{K^2(K+2)}$	etc.

Let us call these ratios f_1 and f_2 for the unperturbed lines, then

$$f_a=\frac{f_1+(\epsilon^2/R^2)A^2f_2}{1+(\epsilon^2/R^2)A^2}=\frac{f_1+\alpha^2f_2}{1+\alpha^2}, \qquad (10a)$$

$$f_b=\frac{f_2+(\epsilon^2/AR^2)f_1}{1+(\epsilon^2/AR^2)}, \qquad (10b)$$

where

$$\alpha=(\epsilon/R)A, \quad A^2=I_2{}^P/I_1{}^P. \qquad (11)$$

These values lie between f_1 and f_2. If the perturbation is only small $f_a\sim f_1$ and $f_b\sim f_2$. It may be noted that these simple relations are only true if the perturbation element is imaginary. Otherwise f_a and f_b might have any value between 0 and ∞.

TABLE I. *Values of the ratio* f_a.

K	f_1	f_2	Observed f_a $0\rightarrow0$	$1\rightarrow1$	$2\rightarrow2$	$3\rightarrow3$
1	2.00	0.50			1.55	1.51
2	1.50	0.67		1.35	1.08	1.00
3	1.33	0.75				0.84
4	1.25	0.80	0.85		0.82	
5	1.20	0.83				
6	1.17	0.86	0.74			

§3. Example in the H_2-spectrum

A test of these relations is generally of value only for small values of K as otherwise the f_u values are so close to one that they cannot be distinguished experimentally. There are quantitative measurements of the f_a quantities in the Fulcher bands of hydrogen[8] which are summarized in Table I. The Fulcher bands are a $\Pi\rightarrow\Sigma$ transition and the f values for this transition are given in column f_1. The initial $3p^3\Pi$ state is known to be perturbed by the $3p^3\Sigma$ state and the f values of the $\Sigma\rightarrow\Sigma$ transition are given in column f_2. We see that the observed f_a values all lie between f_1 and f_2 except the somewhat doubtful value for $K=6$ of the $0\rightarrow0$ band. (Kapuscinski and Eymers give 0.92 for this value.)

Whereas this qualitative result agrees with what we expect, we find serious discrepancies in the quantitative results. The magnitude of the perturbation is expressed in the Λ-doubling and from it follows[9] that the value of $\epsilon/R=0.041\times[K(K+1)]^{\frac{1}{2}}$. The order of magnitude of $A^2=I_2/I_1$ is less than 10. Under these circumstances we would expect only a very slight departure from f_1. (For $K=1$ and $A=10$ we would obtain $f_a=1.95$ instead of the observed 1.53.)

The reason for the discrepancy can be either that the experimental values are wrong or that the calculations do not represent the true picture.

As far as the experimental values are concerned, it is immediately obvious that the only source of errors responsible for the anomalous values can

[8] N. Ginsburg and G. H. Dieke, Phys. Rev. **59**, 632 (1941).
[9] G. H. Dieke, Phys. Rev. **48**, 610 (1935).

be the calibration of the plate for different wave-lengths. This involves the calibration of the standard comparison lamp. As the measurements referred to were made with all reasonable care and agreed besides quite well with those of Kapuscinski and Eymers[10] which were made under entirely different circumstances, though with essentially the same method, there is very little doubt that the discrepancy cannot be due to experimental errors.

If the anomalous values for the R/P ratios cannot arise from the interaction with the $3p^3\Sigma$ state which gives rise to the regular Λ-doubling, we must look for other interactions which, though giving rise to unnoticed wave-length perturbations, may affect the intensities strongly. We have seen earlier that the possibility for such perturbations exists. The perturbing state can be only a $^3\Sigma$ state, as a $^3\Delta$ state, although capable of giving rise to strong wave-length perturbations, cannot produce anomalies of the intensity ratios in a $\Pi\rightarrow\Sigma$ transition, as a $\Delta\rightarrow\Sigma$ transition does not exist. It is easy to convince oneself that the higher vibrational states of $3p^3\Sigma$ cannot be responsible. Other $^3\Sigma$ states in the immediate vicinity of $3p^3\Pi$ are not known. There certainly can not be another $^3\Sigma$ state with the right symmetry in a suitable position, with the possible exception of states with both electrons excited about the position of which we know nothing.

The other remaining possibility is that the abnormal intensity ratios do not arise from the interaction with only one state but by the cooperating influence of several states, and we have to investigate this possibility next.

§4. Interaction with Several Levels

If more than a pair of states interact, the calculations become much more complicated. However, when the influence of the other states on state one is small, their contributions are additive and we obtain in first-order approximation according to (4)

$$\psi_a = N\left(\psi_1 - \sum_n \frac{\epsilon_n}{R_n}\exp(-i\alpha_n)\psi_n + \sum_m \frac{\epsilon_m}{R_m}\exp(i\alpha_m)\psi_m\right),$$

where N is the normalizing factor

$$N^2 = [1+\sum_{n,m}(\epsilon_l^2/R_l^2)]^{-1}$$

and the first sum extends over all states below and the second over all states above ψ_1.

Let us take a state ψ_1 with a definite value of Λ. Then the interacting states can either have $\Lambda_n=\Lambda-1$ or $\Lambda_n=\Lambda+1$. In the former case $\exp(-i\alpha_n)=i$, which makes $\exp(i\alpha_m)=-i$. For $\Lambda_n=\Lambda+1$ the signs are exactly reversed so that we have

$$\psi_a = N\left(\psi_1 \mp i\sum\frac{\epsilon_n}{R_n}\psi_n\right),$$

where the summation extends now over all states and the minus sign refers to the states with $\Lambda-1$ and the plus sign to those with $\Lambda+1$. Only for $\Lambda\rightarrow\Lambda$ transitions do we have to consider both terms for the R/P ratios.

We have

$$I_a = N^2\left[I_1+\left(\sum\pm\frac{\epsilon_n}{R_n}A_n\right)^2\right]. \tag{12}$$

This makes the ratio

$$\frac{I_R}{I_P}=f_a=\frac{f_1+[\sum\pm(\epsilon_n/R_n)A_n f_n^{\frac{1}{2}}]^2}{1+[\sum\pm(\epsilon_n/R_n)A_n]^2},$$

where, as before, $A^2{}_n=I_n/I_1$ for the P lines. All the values of f_n belonging to a given sign are identical, so that we can write also

$$f_a=\frac{f_1+(\alpha f_2^{\frac{1}{2}}-\beta f_3^{\frac{1}{2}})^2}{1+(\alpha-\beta)^2}, \tag{13}$$

where

$$\alpha=\sum(\epsilon_n/R_n)A_n, \quad f_2=I_2{}^R/I_2{}^P, \tag{14}$$

for the states with $\Lambda_n=\Lambda-1$ and β and f_3 the corresponding values for the states with $\Lambda_n=\Lambda+1$. If only one type of states needs to be considered, as, e.g., for a $\Pi\rightarrow\Sigma$ transition, we have

$$f_a=(f_1+\alpha^2 f_2)/(1+\alpha^2),$$

which is identical with (10a) except for the more general definition (14) of α.

These relations also hold when the perturbing states are continuous. In that case we have with the proper normalization of the wave functions

$$\alpha = I_1^{-\frac{1}{2}}\int\frac{R_v}{2\delta_n}|q_v|\,dv.$$

[10] W. Kapuscinski and J. G. Eymers, Proc. Roy. Soc. **A122**, 58 (1929).

$\int |q_\nu^2| d\nu$ is the total intensity[4] of the continuous spectrum originating from transitions between the state ψ'' and the continuous states. A fairly accurate numerical calculation of α can be made if the wave functions of the three states ψ'', ψ, and ψ_ν are known.

We return now to the anomalous f_n values in the Fulcher bands of H_2. We must take the contributions of all $^3\Sigma_u$ states. Those which do interact strongly with $2p^3\Pi$ and at the same time combine strongly with the lower state (large A_n) are most important. There is no other discrete state known which combines strongly enough with the lower state. If it existed, it would undoubtedly have been discovered.

Of the continuous states, those lying above $3p^3\Pi$ with only one electron excited also can be excluded, as they do not combine with sufficient strength with $2s^3\Sigma$. However, the well-known continuous state $2p\sigma^3\Sigma$, the combination of which with $2s^3\Sigma$ is held responsible for most of the strong continuous spectrum of H_2, satisfies all requirements.

It would be feasible to calculate numerically the value of α with the wave functions of James and Coolidge. However, only those for $2s^3\Sigma$ and $2p^3\Sigma$ are known and the calculations would be quite laborious in any case. We can come to a very rough estimate of the order of magnitude by assuming the action of the continuous spectrum to be replaced by a single lines which has the total intensity of the continuous spectrum and the lower state of which interacts with $3p^3\Pi$ as all the continuous levels together. We assume this line to coincide roughly with the maximum of the continuous spectrum at about 35,000 cm^{-1}. This means $2\delta \sim 5\times 10^4$. $R^2 = 2BK(K+1) \sim 120$ for $K=1$.

$$\alpha^2 = \frac{R^2}{4\delta^2} A = \frac{120}{25}\times 10^{-8} A = 0.5\times 10^{-7} A.$$

In order to obtain the experimentally observed value 0.5 for α^2 we would have to assume that the total intensity of the continuous spectrum would be about ten million times that of the Fulcher bands. No measurements exist of this ratio, but it seems definitely much too high. On the other hand, a more exact calculation of α^2 would probably increase its value, as it would give greater emphasis to the states with smaller δ. With the present state of our information we can therefore conclude that the anomalies in the R/P ratios of the Fulcher bands probably cannot be due to the interaction with the continuous $2p^3\Sigma$ state although that possibility cannot be completely excluded.

There remains the possibility that a continuous state with both electrons excited lies close to the initial state $3p^3\Pi$ of the Fulcher bands and interacts feebly with it. $(2p\sigma)(2s\sigma)^3\Sigma_u$ would be a possibility if it is continuous, as it would be expected to combine strongly with the lower state $(1s\sigma)(2s\sigma)^3\Sigma_g$. There is, however, at present no experimental evidence either for or against such a possibility.

§5. Vibrational (Type B) Perturbations

The perturbation function for vibrational perturbations is given by

$$H^{(1)}\psi = B\left[(M_\xi^2 + M_\eta^2)\Phi - 2r\frac{\partial\Phi}{\partial r} - r^2\frac{\partial^2\Phi}{\partial r^2} - \frac{2r^2}{R}\frac{\partial R}{\partial r}\frac{\partial\Phi}{\partial r}\right] RU,$$

in which r is the internuclear distance and Φ, R, U are the electronic, vibrational and rotational wave functions, respectively. As all the essential quantities are real, the matrix elements are real in this case and the phase in the interference term must be either 0 or π. The formulae for the intensities become then

$$I_a = \frac{R^2}{R^2+\epsilon^2}\left((I_1)^{\frac{1}{2}} \mp \frac{\epsilon}{R}(I_2)^{\frac{1}{2}}\right)^2, \qquad (14a)$$

$$I_b = \frac{R^2}{R^2+\epsilon^2}\left((I_2)^{\frac{1}{2}} \pm \frac{\epsilon}{R}(I_1)^{\frac{1}{2}}\right)^2. \qquad (14b)$$

The upper signs hold if the interaction element is positive, the lower ones if it is negative.

We have now intensity relations completely different from those of the rotational perturbations. We can have now, for instance, a case when $I_1 \sim (\epsilon^2/R^2) I_2$ that one of the perturbed lines is completely absent and the other one has the sum of the intensities of both unperturbed lines, a state of affairs which never can occur in class A

perturbations. In a typical perturbation case we have two sets of rotational levels $W_1(K)$ and $W_2(K)$ such that

$$W_1(K) < W_2(K) \quad \text{if} \quad K < K_0,$$
$$W_1(K) > W_2(K) \quad \text{if} \quad K > K_0.$$

$K = K_0$ is the place of maximum perturbation.

If we regard now the intensities of the set $W_a(K)$ which are the perturbed values of W_1, then we see that below the maximum perturbation the amplitudes are subtracted (if S is positive) and we may get very low intensities, whereas above the maximum perturbation the amplitudes are added and we get abnormally large intensities. This sudden jump in the intensities is characteristic for class B perturbations. We have seen that the intensities behave quite smoothly in class A perturbations. In general we can expect much more irregular intensities for vibrational than for rotational perturbations.

The ratios $R(K-1)/P(K+1)$ are not affected by vibrational perturbations, as only levels with the same Λ interact, and we have therefore $f_a = f_1 = f_2$. (This would be true *independently* for any kind of interaction between levels with the same Λ.)

The only case of a vibrational perturbation in which the intensities have been measured is that of the interaction of the $2s\,^1\Sigma$ and $(2p\sigma)^2\,^1\Sigma$ states and the bands which are produced by the transitions from these levels to $2p\,^1\Sigma$. The intensities which appear at first sight highly erratic are shown in another paper to behave exactly as predicted by the preceding formulae.

OCTOBER 1, 1941 PHYSICAL REVIEW VOLUME 60

An Anomalous Crystal Photo-Effect in *d*-Tartaric Acid Single Crystals*

CHUNG KWAI LUI
Oregon State College, Corvallis, Oregon

(Received August 15, 1941)

Brady and Moore observed that certain crystals which appeared to have flaws and were not very transparent gave a current response which started out in one direction just after the light was turned on, decreased rapidly with time of illumination, and then flowed in the opposite direction. This phenomenon has been investigated in detail. All clear, well-formed, single crystals exhibit this current-reversal phenomenon when light falls on certain points of the crystal surface. These points always lie between two regions which respond with normal current flows in opposite directions. The superposition of the two normal current-response curves gives a resultant which agrees with the observed current-reversal curve within the experimental error. The various current response curves for different illuminated faces of the crystal, including the current-reversal effect, are correlated by assuming a particular direction in the unit cell of the crystal for which the electrical conductivity is a maximum.

IT has been shown by Brady and Moore[1] that tartaric acid crystals exhibit a crystal photo-effect (actinoelectric effect). Just after the light is turned on, the galvanometer used to measure the amplified photo-current exhibits a deflection which rises very suddenly to a maximum, then decreases, and finally reaches a steady value. This behavior will be referred to as the "normal effect." Brady and Moore observed, also, that certain crystals which appeared to have flaws and were not very transparent behaved differently from the normal response curve. When light was turned on such a crystal, the galvanometer deflected first in one direction, then quickly reversed passing through zero to reach a maximum in the opposite direction. It then decreased slowly and finally approached a steady value as shown by curve E, Fig. 2. This phenomenon was investigated in detail in the present experiment. It will be referred to as the "abnormal effect."

* Published with the approval of the Monographs Publication Committee, Oregon State College. Research paper No. 50, School of Science, Department of Physics.

[1] J. J. Brady and W. H. Moore, Phys. Rev. **55**, 308 (1939).

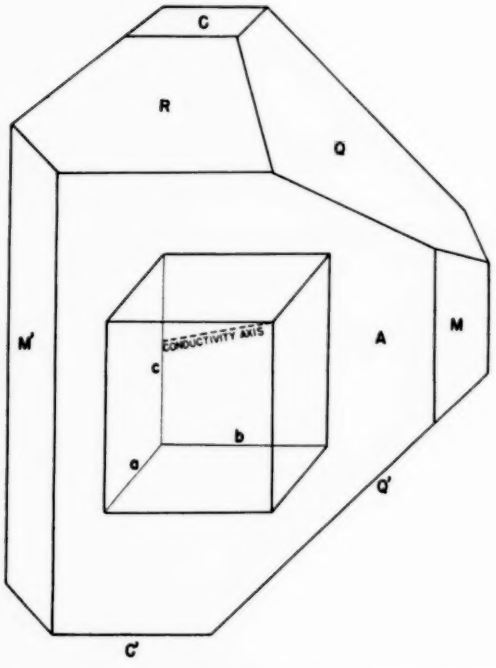

FIG. 1. The unit cell in relation to a single crystal of tartaric acid.

An FP-54 electrometer tube in a DuBridge and Brown amplifying circuit was used for detecting the photo-current. The crystal was held between two parallel brass disks by spring pressure. The light source was a 150-watt tungsten gas filled lamp. The crystals used in this investigation were single crystals artificially grown in this laboratory. All of the observations were made with the electrodes placed against the orthopinacoid faces (Face *A*, Fig. 1).

Measurements of the photo-current were made with and without a coating of "Aquadag" on the crystal surfaces in contact with the electrodes. The only noticeable effect of the Aquadag was an increase in the response, presumably due to a decrease in the contact resistance between the crystal surfaces and the electrodes.

Figure 1 shows the unit cell properly oriented with respect to the single crystal. According to Astbury,[2] the edges of the unit cell have the following lengths: $a=7.7$A, $b=6.0$A, and $c=6.2$A. The axes b and c are perpendicular to each other. a is perpendicular to b, but makes an angle of 100° 17′ with c.

[2] W. T. Astbury, Proc. Roy. Soc. **102**, 506 (1923).

EXPERIMENTAL RESULTS

All clear, well-formed, single crystals exhibit the abnormal effect when light falls on *certain points of the crystal surface*. Figure 2 shows the response for six different faces of a clear single crystal. The curves differ not only in magnitude of the deflection, but even in the direction of the current.

The direction of current flow is the same for illumination of faces *C*, *Q*, *M*, and *Q′* (curves *A*, *B*, *C*, and *D*; Fig. 2). When face *M* (curve *F*) is illuminated, the current flows in the opposite direction to that produced by the illumination of face *C*. The illumination of face *C′* (curve *E*) gives rise to the abnormal effect.

DISCUSSION

A review of the different theories of the crystal photo-effect has been given by Lange.[3] The "diffusion theory" as suggested by Frenkel[4] is one of the most satisfactory. According to the modern theory of solids, the "hole" conductivity

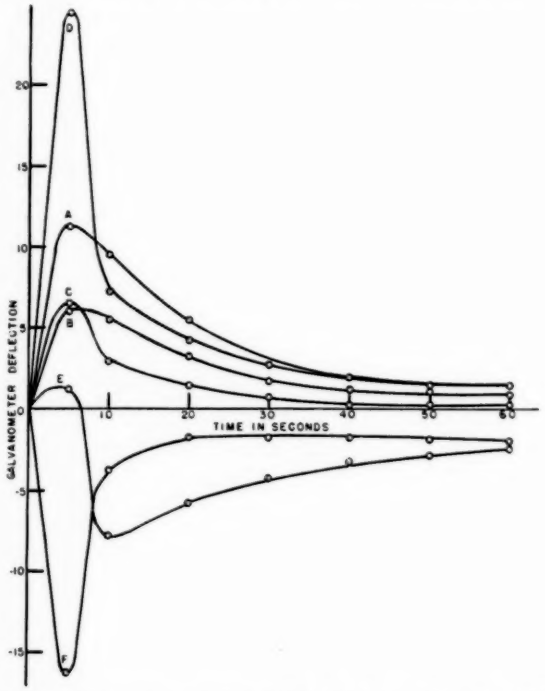

FIG. 2. Response curves obtained from different illuminated crystal faces. *A*—illumination on face *C*. *B*—illumination on face *Q*. *C*—illumination on face *M*. *D*—illumination on face *Q′*. *E*—illumination on face *C′*. *F*—illumination on face *m′*.

[3] B. Lange, *Photoelements* (Reinhold Publishing Corporation, 1938).

[4] J. Frenkel, Nature **132**, 856 (1933).

as well as the electron conductivity must be considered. If one assumes that the diffusion speed for holes is different from that of electrons, an electromotive force can be established by the difference in concentration between holes and electrons at various points in the crystal. According to this view, a cubic crystal would exhibit zero electromotive force if illuminated (transversely) as in Fig. 3. Since tartaric acid crystals belong to the monoclinic system, one might expect that the conductivity would be different along the three crystallographic axes. Therefore, the assumption was made that there is one direction in the unit cell of the crystal along which the conductivity is a maximum. This direction is indicated by a dotted line in Figs. 1 and 3 and was chosen in such a way as to correlate the results of this experiment. It is referred to here as the "conductivity axis." It is interesting to note, however, that the projection of the conductivity axis on the Q face is approximately perpendicular to the equipotential lines reported by Brady and Moore.[1] There is some evidence that the exact direction of the conductivity axis depends on the purity of the crystals. The nature of this dependency requires further investigation.

A difference in the concentration of electric charges (holes and electrons) along the conductivity axis will account for an electromotive force in the crystal. When the top face of the unit cell is illuminated, as in Fig. 3, the number of photoelectrons released near the top will be greater than the number released further down

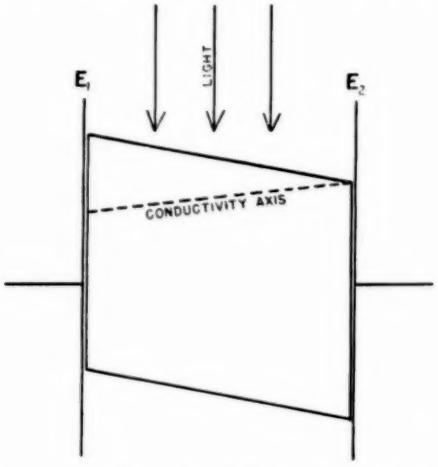

FIG. 3. Two-dimensional diagram of a unit cell.

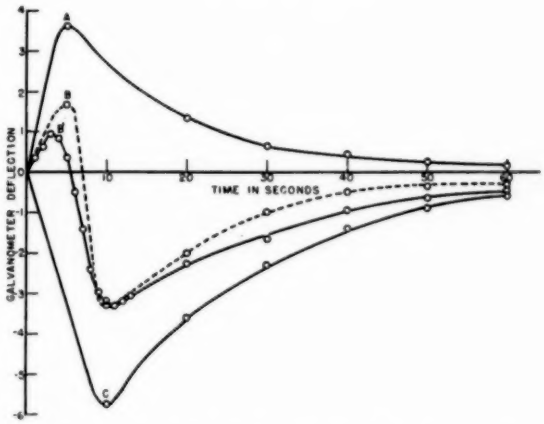

FIG. 4. Curves showing the relationship of normal and abnormal effects. A—illumination on Q' face. B—illumination on C' face. C—illumination on M' face. B'—resultant of curves A and C.

in the crystal due to the diminished light intensity. The concentration of charges along the conductivity axis will then be greater near the edge of the crystal where the conductivity axis comes closer to the upper face. A photo-current will then flow between the electrodes E_1 and E_2. When the bottom face is illuminated, the current will flow in the opposite direction. In both cases the accumulation of charges at the ends of the conductivity axis in contact with the electrodes will result in a decrease of current with time. Because of the asymmetry of the conductivity axis, it is reasonable to expect that the variation of the current with time will depend on the direction of current flow.

Figure 4 illustrates how the abnormal effect may be interpreted as the result of the superposition of two current-time curves. Curve A was obtained by illuminating the Q' face. Curve C was obtained by illuminating the M' face, and curve B was the observed abnormal effect obtained by illuminating a point somewhere between the Q' and M' faces, namely the C' face. The dotted curve, B', is the resultant of curves A and C obtained by adding algebraically their corresponding ordinates. According to this view, the abnormal effect appears as the superposition of two normal effects having opposite current flows.

The author wishes to express her gratitude to Dr. J. J. Brady for suggesting the problem and for his helpful discussions throughout the course of the work.

Letters to the Editor

PROMPT publication of brief reports of important discoveries in physics may be secured by addressing them to this department. Closing dates for this department are, for the first issue of the month, the eighteenth of the preceding month, for the second issue, the third of the month. Because of the late closing dates for the section no proof can be shown to authors. The Board of Editors does not hold itself responsible for the opinions expressed by the correspondents.

Communications should not in general exceed 600 words in length.

A Mesotron Shower

E. O. WOLLAN
University of Chicago, and Chicago Tumor Institute, Chicago, Illinois
September 16, 1941

DURING the month of July about 1500 counter-controlled cloud-chamber photographs were taken at an altitude of about 15,500 feet at a mine of the Cerro de Pasco Corporation at San Cristobal, Peru. The chamber used in this work was 10 inches in diameter, and was illuminated over a depth of about 2 inches. A lead plate of 2-cm thickness was placed horizontally across its center. A 15-cm lead block was placed above the chamber, and

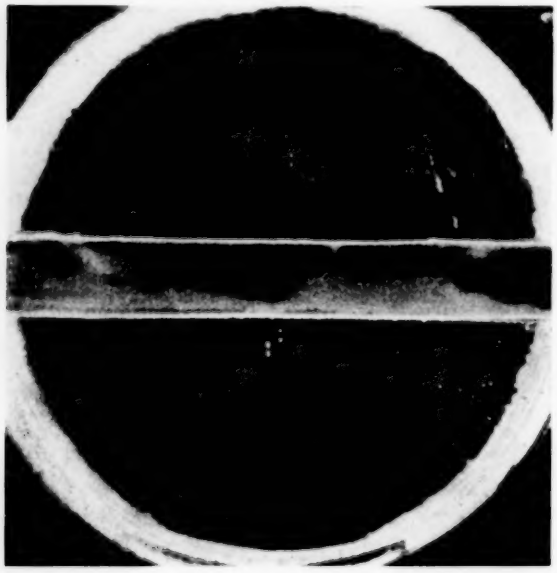

FIG. 1. A mesotron shower.

above the block was located one of the controlling counters, arranged to set off the chamber when the entering radiation was of the ionizing type.

Several photographs were obtained showing two particles diverging from a point above the chamber and traversing the 2-cm lead plate without multiplication. One of the photographs warrants a special note, and is reproduced in Fig. 1. Above the central lead plate there are 10 rays diverging from a point in the lead above the chamber. One of the rays on the right, which ionizes more heavily than the rest, does not appear to pass through the lead plate. This is probably a slow mesotron. Of the three close rays near the center in the upper half of the chamber, two pass straight through the plate. The double track, scattered to the left, is probably that of a single ray whose track has been pulled apart by the field. At least five of the particles which fall on the lead plate pass through, and only one gives rise to a small shower. It thus seems likely that most of the 10 rays seen above the plate are mesotrons which have been produced in the lead above the chamber. When the tracks are projected back, they are all found to originate near the same point. If this case is an example of the multiple production of mesotrons observed in such abundance in the counter experiments at very high altitude[1] it lends weight to the idea that the production[2] is mainly of the explosive type rather than a succession of events in each of which a single mesotron results. In a recent letter by Powell[3] a shower of penetrating particles is shown in which also the secondary mesotrons originate near the same point.

The photograph reproduced here and other examples of the production of mesotrons were reported on at the cosmic-ray symposium in Rio de Janeiro, August 3 to 9. The cordial hospitality shown us there by the members of the Academy of Science of Brazil and the faculty of San Paulo University was greatly appreciated.

To the officials of the Cerro de Pasco Corporation, who cooperated with us in every way, we are most grateful.

[1] M. Schein, W. P. Jesse and E. O. Wollan, Phys. Rev. **59**, 615 (1941).
[2] J. Franklin Carlson and M. Schein, Phys. Rev. **59**, 840 (1941).
[3] Wilson M. Powell, Phys. Rev. **60**, 413 (1941).

On the Protonic Nature of the Primary Cosmic Radiation

GIUSEPPE COCCONI
Physical Institute of the Royal University, Milano, Italy
July 9, 1941

PURSUANT to the experiments of Schein, Jesse and Wollan[1] and the considerations of Johnson[2] and Swann,[3] it seems to be very likely that the primary cosmic radiation consists of protons only. It does not appear that all the electrons present in the high atmosphere and at the sea level can be accounted for by assuming that they are generated only by the decay of mesotrons. From general considerations on mesotron decay apart from all particularity of the process itself, the conclusion can be obtained[4] that the number of decay electrons in equilibrium with the mesotronic component in air is

$$n = KNX/H,$$

where K is a constant, N the total number of mesotrons of any energy, H the atmospheric pressure and X the average thickness of the air (g/cm²) through which the decay electrons pass. (This thickness is actually increasing with the mesotron energy, but in first approximation it might be considered as a constant.)

From the foregoing formula for a constant H, $n/N=(K/H)X=$constant. Since on the other hand it has been shown that the ratio electrons/mesotrons at sea level decreases considerably with the increase of the zenith angle,[4,5] the conclusion must be drawn that at sea level there exists an electronic component of a different nature than that arising from the decay of mesotrons which will be called residue. Also the considerable barometric effect which we recently found for the electronic component at the sea level (16 percent per cm Hg)[6] can be interpreted as a proof of the foregoing. Similar conclusions have also been reached from other considerations.[7]

On the basis of such considerations it can be shown that if the intensity of the cosmic radiation is taken at the sea level as unity, the mesotron component is 0.8, the electronic component arising from decay 0.08, the interaction component 0.04, and the residual component 0.08. At the pressure of about 8 cm Hg (maximum of Pfotzer's curve), the mesotron component increases about ten times[1] and reaches an intensity of about $0.8\times10=8$: the interaction component becomes $0.04\times10=0.4$, and the component arising from the decay (with the above given formula) has a value of $0.08\ (10/0.1)=8$ (the mean energy of the mesotrons in the high atmosphere is actually less than that at sea level, hence X becomes smaller and the estimated value is greater than the real value). Hence these three components are responsible, at 8 cm Hg, for total intensity of about 16: since Pfotzer observed an intensity of about 46, the electronic residue component shall have an intensity of $46-16=30$. It must therefore be considered that the primary protons produce the mesotrons in the atmosphere and furthermore, directly as well as indirectly by means of processes now unknown, the photons and the electrons which are responsible for the large showers[8] and the component called residue by us.

[1] M. Schein, W. P. Jesse, and E. O. Wollan, Phys. Rev. **59**, 615 (1941).
[2] T. H. Johnson, Rev. Mod. Phys. **11**, 208 (1939).
[3] W. F. G. Swann, Phys. Rev. **59**, 770 and 836 (1941).
[4] G. Cocconi and V. Tongiorgi, Ricerca Scient. **12**, 144 (1941).
[5] G. Cocconi and V. Tongiorgi, Phys. Rev. **57**, 1180 (1940).
[6] G. Cocconi and V. Tongiorgi, Ricerca Scient. **12**, 664 (1941).
[7] G. Bernardini, B. N. Cacciapuoti, B. Ferretti, O. Piccioni and G. C. Wick, Phys. Rev. **58**, 1017 (1940).
[8] N. Hilberry, Phys. Rev. **59**, 763 (1941).

On the Presence of Strongly Ionizing Particles in Cosmic-Ray Showers

GIUSEPPE COCCONI
Physical Institute of the Royal University, Milano, Italy
July 11, 1941

IN work with a Wilson cloud chamber on narrow showers a photograph was obtained (Fig. 1) in which, beside the ordinary electron shower generated at sea level in a 60-cm thick aluminum layer over the chamber, another type of shower was observed of two strongly ionizing particles, one of them showing several delta-rays. The tracks in the cloud chamber, which was filled with argon and alcohol vapor and had a diameter of 25 cm, were photographed in two directions (under an angle of 60 degrees between each other). The expansion of the fully automatic cloud chamber[1] was operated by four 20×4.5 cm^2 counter tubes arranged in accordance with the first report published on these experiments,[2] i.e., in such a way as to photograph only the narrow showers (mean angle of divergence 5°) coming from the aluminum above. Each of the two aluminum screens in the chamber is 2 cm thick. This photograph shows that in a narrow shower, made up mostly of electrons, nuclear evaporation processes can occur: in this particular case it does not appear that the primary particle leaves a visible track in the cloud chamber. On the other hand, it can be seen from Bagge's recent paper[3] that nuclear evaporation processes are closely connected with electron showers.

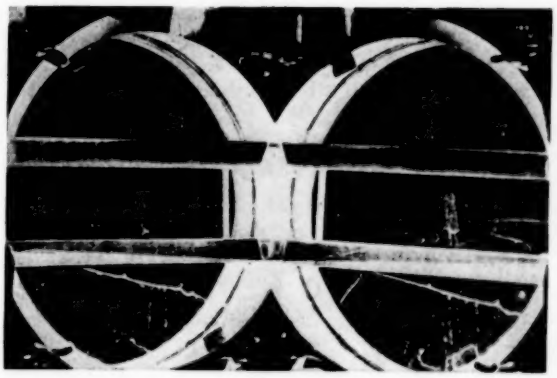

FIG. 1. Narrow shower produced by cosmic rays.

[1] G. Polvani, Ricerca Scient. **12**, 410 (1941).
[2] G. Cocconi, Naturwiss. **29**, 336 (1941).
[3] E. Bagge, Ann. d. Physik **39**, 512 (1941).

A Note on the Radiochemistry of Europium

KASIMIR FAJANS AND ADOLF F. VOIGT
Department of Chemistry, University of Michigan, Ann Arbor, Michigan
September 8, 1941

SEVERAL questions on the radiochemistry of europium have been left unanswered. The 9.4-hour europium isotope first observed by Sugden[1] was studied by several workers.[2–6] It can be obtained by slow and fast neutron and by deuteron bombardment of europium. Slow neutron bombardment also produces a long period which has been reported in several papers. In one[7] it was said to have a half-life of 1–2 years, in another[4] no appreciable decay was observed in six months, and in a third[8] its maximum beta-ray energy was given as 0.8 Mev. Two short periods, 12 min. and 105 min. were reported[4] to be produced in europium by deuteron bombardment along with the 9.4-hour activity.

The purpose of the present experiments was to study the long period and to check the two short periods.

The europium material was kindly furnished by Professor H. N. McCoy and had partly been used in the

previous work in this laboratory.[4] It was purified by the McCoy method of reduction in a Jones reductor and precipitation as europous sulfate.[4,9] The same chemical procedure was used after bombardment. As the reduction is not complete, the europium remaining in solution was precipitated as oxalate which would carry with it any other rare earth which might have been formed in bombardment.

The slow neutron sample, which, as previously reported, gave no decay over the first six months, showed a decay with a half-life of 6–8 years in the following 18 months. That this did not show up during the first six months was due to a flat maximum in the activity curve in the first few months.

The natural radioactivity present in the original europium preparation had been removed chemically before the bombardment. However, the maximum mentioned above showed that the contamination with foreign radioactive material was not completely removed. Further chemical study showed this to be the case and served as an additional purification. The europium sample obtained after this study gave a pure decay with a half-life of the order of 5–8 years as measured for 8 months.

Since this result has shown the original material to be less pure than could be assumed on the basis of the spectroscopic analysis which was made on it (see reference 4), we wished to check the short periods of 12 and 105 minutes obtained before by deuteron bombardment. Purified Eu_2O_3 was bombarded for 20 minutes to one hour and was immediately separated so that the samples could be measured within 20 to 30 minutes after bombardment. Only traces of any period shorter than the 9-hour were found and in several instances there was no indication of any such activity. The initial intensity of these shorter periods was never more than 5 percent of the 9-hour activity. The chemical reactions mentioned above were used and the decay of the sulfate and oxalate precipitates was similar. Thus the short periods were shown not to be produced in pure europium.

This pure material was also used in a prolonged deuteron bombardment which gave a period of the same order (5–8 years) as the neutron induced long period. It is most probably the same isotope. Since europium has two stable isotopes, (151) and (153), and the 9.4-hour isotope has been assigned to (152),[3] the most probable assignment of this long-life activity is to Eu^{154}.

Deuteron bombardment of the purified europium also produced an activity with a half-life of 155 to 170 days. It is not europium, since it is not reduced or precipitated as sulfate, but it precipitates with europium oxalate in acid solution, a typical rare-earth reaction. Its intensity, 500 times the background of the counter used, seems too great for it to be due to an impurity so that it is probably produced from europium. In that case the 160-day activity could be samarium due to a d reaction, or gadolinium due to a $d-n$ or $d-2n$ reaction. It emits negative beta-rays and x- or gamma-rays with an intensity less than 1 percent of the total.

We are indebted to the cyclotron crew of the Physics Department for the preparation of the active material and to the Horace H. Rackham Trust Fund for financial support.

[1] S. Sugden, Nature **135**, 469 (1935).
[2] G. v. Hevesy and H. Levi, Nature **136**, 103 (1935); **137**, 185 (1936).
[3] M. L. Pool and L. L. Quill, Phys. Rev. **53**, 437 (1938).
[4] K. Fajans and D. W. Stewart, Phys. Rev. **56**, 625 (1939).
[5] J. R. Richardson, Phys. Rev. **55**, 609 (1939).
[6] A. W. Tyler, Phys. Rev. **56**, 125 (1939).
[7] H. Scheichenberger, Anz. Akad. Wiss. Wien Math.-naturw. Klasse **75**, 108 (1938).
[8] S. Ruben and M. D. Kamen, private communication, quoted in J. J. Livingood and G. T. Seaborg, Rev. Mod. Phys. **12**, 42 (1940).
[9] H. N. McCoy, J. Am. Chem. Soc. **58**, 1577 (1936).

Radioactive Bromine Isotopes from Uranium Fission

A. Moussa and La. Goldstein
Institut de Physique Atomique, Université de Lyon, France
August 19, 1941

We have been able to identify two radioactive bromine isotopes produced by uranium fission under the influence of thermal and fast (Rn+Be) neutrons. The periods of the two bodies are: Br (1): 35 minutes; Br (2): 2.3 hours. The latter period coincides with a period noted by Langsdorf and Segrè[1] and has to be attributed to the isotope Br^{83}. We have not been able, however, to confirm the existence of a bromine isotope of 3.8 hours period, as has been stated by Hahn and Strassmann[2] though we have used sufficiently long exposures.

The chemical methods we have applied are: (1) Extraction of bromine by organic solvents. This method is analogous to the one applied by Dodson and Fowler[3] in their search for iodine isotopes in the uranium fission. (2) Distillation of bromine from the irradiated uranium solution, after addition of inactive bromide, permanganate and sulfuric acid. In the first procedure the bromine becomes separated from iodine by sodium nitrite, in the second the iodine remains quantitatively in the solution while the bromine becomes completely distillated (as we could prove by direct tests). The separation chlorine-bromine was made by treating the silver halide precipitates with ammonium bicarbonate. Both of these methods furnish the same radioactive bodies. The time dependence of the activities is in both cases exactly the same, and leads to the two periods indicated above. These periods have, therefore, to be necessarily attributed to bromine isotopes.

We have investigated by several experiments the problem, whether Br (1) and Br (2) are directly produced by the fission process or whether they have to be considered as daughter products of bodies resulting from fission. We can conclude from our experiments: (1) that none of the two bodies is a derivate of krypton, neither directly nor indirectly; (2) if selenium should be the mother-substance of Br (1) its period must be smaller than 3 min. (In this case it could have escaped observation.) Br (2) (Br^{83}) could be a derivate of Se^{83} the period of which is 30 min.[1,4] From our experiments it seems that it is not the case. As far as we know, on the other hand, Se has never been found with certainty among the uranium fission products. It seems, therefore, that Br (1) and Br (2) can be considered to be direct fission products.

TABLE I.

NEUTRONS	BR (1)	BR (2)
Fast (Rn+Be)	$\sigma = 0.9 \times 10^{-27}$ cm²	$\sigma = 0.6 \times 10^{-27}$ cm²
Thermal (Cd group)	$\sigma = 1.2 \times 10^{-27}$ cm²	$\sigma = 0.9 \times 10^{-27}$ cm²

We believe that the mass number to be attributed to Br (1) is 84. Indeed, according to our experiments it is unlikely that Br (1) and Br (2) are isomers. On the other hand, Snell[4] has found in the bromine fraction separated from rubidium irradiated by fast neutrons (Li+D) two periods of 35 min. and 34 hr. The second period has to be attributed to Br^{82}, resulting from the reaction Rb^{85} (n, α) Br^{82}. The fact that the first of the Snell periods agrees with the period of Br (1) suggests that we have to do with the same body, probably Br^{84} which could result, in Snell's experiments, from the reaction Rb^{87} (n, α) Br^{84}.

We have determined the cross sections for the production of Br (1) and Br (2) by thermal neutrons (cadmium group) and fast (Rn+Be) neutrons. All of the factors entering into this evaluation (yield of the chemical methods, absorption of the radiation, etc.) have been determined experimentally.

These results show that the radioactive bromine isotopes are produced in a very small proportion (at most 1 percent) during uranium fission due to neutrons.

[1] A. Langsdorf, Jr. and E. Segrè, Phys. Rev. **57**, 105 (1940).
[2] O. Hahn and F. Strassmann, Naturwiss. **27**, 529 (1939).
[3] R. Dodson and R. Fowler, Phys. Rev. **57**, 966 (1940).
[4] A. Snell, Phys. Rev. **52**, 1007 (1937).

Temperature Dependence of the Periodic Deviations from the Schottky Line

EUGENE GUTH AND CHARLES J. MULLIN
Department of Physics, University of Notre Dame, Notre Dame, Indiana
July 12, 1941

IN recent communications[1,2] it was stated that a disagreement exists between the data of Seifert and Phipps[3] and of Turnbull and Phipps[4] on the one hand and those of Nottingham[1] on the other hand regarding the temperature dependence of the amplitudes of the periodic deviations from the Schottky line. The amplitudes were defined as the sum of the ordinate of a maximum and a neighboring minimum with the Schottky line as a reference.

In view of the great importance of the temperature dependence for the theory of the periodic deviations a re-examination of the original data of Nottingham has been made in the light of the theory,[2] which was missing when Nottingham wrote his letter. This re-examination shows that Nottingham's data are not inconsistent with the theory, according to which the amplitudes should be inversely proportional to the absolute temperature; however, these data alone are not sufficient to establish quantitatively the theoretical dependence, because of the superposition of "patch-effects." As pointed out already[2] the data of Phipps and collaborators agree with the theoretical temperature dependence of the amplitudes.

Finally, it seems worth while to point out that the magnitudes of the amplitudes of the deviations obtained by Phipps and collaborators agree closely with those obtained by Nottingham in spite of the considerable difference in the nature of the surfaces of the filaments used. Nottingham's amplitudes are about 10–15 percent higher than those of Phipps and collaborators, thus yielding an even better agreement with theory, which, when the current penetrating the potential barrier at the metal surface is considered,[5] yields amplitudes somewhat larger than those observed by Phipps *et al.* The remarkably close agreement between the locations of the maxima and minima found by Phipps *et al.* and those found by Nottingham already has been pointed out by Nottingham.[1]

In order to calculate the positions of the maxima and minima from theory, an assumption about n, the number of free electrons per atom of the emitting metal, must be made. With $n=1$ for tungsten, the calculated positions were found[2] to differ somewhat from the observed positions. If it is assumed that this difference is due principally to the fact that n is really less than one for tungsten, then the observed positions may be used to estimate the value of n. A calculation based on this assumption indicates an upper limit of $n=0.35$ for tungsten. From the magnitude of the double layer necessary to yield the observed dependence of the work function of tungsten upon its different crystal faces, Smoluchowski[6] obtained[7] $n=0.33$ in agreement with the above value.

We are indebted to Dr. Nottingham for putting his original unpublished data at our disposal and for friendly discussions.

[1] W. B. Nottingam, Phys. Rev. **57**, 935 (1940).
[2] E. Guth and C. J. Mullin, Phys. Rev. **59**, 575 (1941).
[3] R. L. E. Seifert and T. E. Phipps, Phys. Rev. **56**, 652 (1939).
[4] D. Turnbull and T. E. Phipps, Phys. Rev. **56**, 663 (1939).
[5] E. Guth and C. J. Mullin, to be submitted for publication in Phys. Rev.
[6] R. Smoluchowski, Phys. Rev. **59**, 944A (1941).
[7] R. Smoluchowski, personal communication.

Positive Excess in Mesotron Spectrum

G. BERNARDINI, *University of Bologna*
and
G. C. WICK, M. CONVERSI, AND E. PANCINI, *University of Rome, Rome, Italy*
July 19, 1941

SEVERAL years ago Rossi[1] and Mott-Smith[2] tried to observe the deflection of cosmic particles in a magnetic field by a system of two coincident counters with magnetized iron plates interposed. The effects observed, if at all real, were small and pointed to the existence of positive particles.

Later this method was superseded by the more powerful technique of the Wilson chamber, and it became clear that

TABLE I. *Counting rates for various magnetic fields.* (Coinc./hr.)

INDUCTION IN GAUSS	AT ROME (50 m.s.l.) ARRANG. I	AT ROME (50 m.s.l.) ARRANG. II	AT CERVINIA (3460 m.s.l.) ARRANG. I	AT CERVINIA (3460 m.s.l.) ARRANG. II
2400	81.1 ±1.2	77.7 ±1.2	162 ±2.1	160 ±2.1
5000	83.1 ±1.2	77.2 ±1.1	165 ±2.5	157 ±2.5
10,400	88.5 ±0.9	80.5 ±0.8	175 ±2.1	159.5 ±2.0
15,500	97.5 ±1.0	84.7 ±0.9	206 ±1.8	176 ±2.0
17,000	103.3 ±1.5	91.2 ±1.3	217 ±2.7	184.8 ±2.9

the smallness of the effects previously observed was due to the fact that positive and negative particles are present in approximately equal numbers. More recently, however, Jones,[3] Leprince-Ringuet,[4] and Hughes[5] found a positive excess of about 20 percent.

It seemed to us worth while, therefore, to repeat the experiment of Rossi with a somewhat improved triple coincidence arrangement (Fig. 1). The iron plates A, B, C, D, are magnetized by means of coils, A and B parallel to each other and antiparallel to B and D. The field can be so directed as to concentrate the positive particles (arrangement I, as in the figure) or alternatively so as to concentrate the negative particles (arrangement II). We found the results given in Table I.

The experiment affords conclusive evidence in favor of the existence of a positive excess, in accordance with the finding of Jones, Leprince-Ringuet, and Hughes.

An elaborated evaluation has been made of the "allowed cone" of incident directions for many points in the horizontal symmetry plane of the first counter and it has thus become possible to interpret the above results quantitatively to a certain extent. Assuming that the positive excess is evenly distributed over the whole spectrum, we find that the difference I−II must increase almost linearly with the magnetic field, which is seen to be the case (Fig. 2).

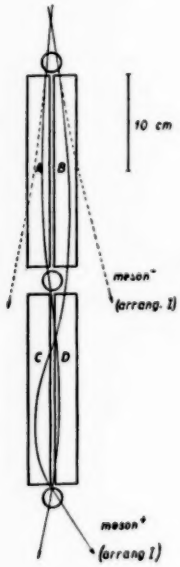

FIG. 1. Arrangement of counters and magnetized iron plates.

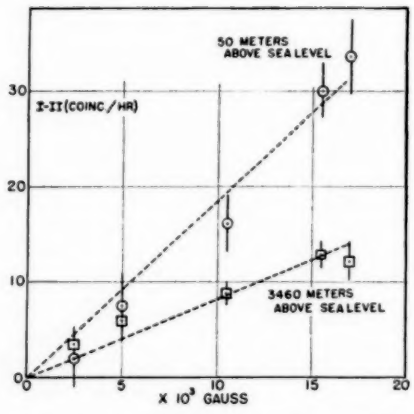

FIG. 2. Coincident counting rates for various field strengths.

If the ratio of positives to negatives is $(1+\epsilon)/(1-\epsilon)$ the "experimental excess" expected is

$$\frac{\text{I}-\text{II}}{\text{I}+\text{II}}=\epsilon\frac{B}{25{,}000}.$$

From this we find $\epsilon=0.11$ at Rome and $\epsilon=0.12$ at Cervinia.

The method, owing to its simplicity, seems well-suited for an investigation of the positive excess under conditions when the elaborate Wilson chamber technique is impossible. For stratosphere work permanent magnets could be used. Experiments at great elevation are now in preparation.

[1] B. Rossi, Nature **128**, 300 (1931).
[2] L. M. Mott-Smith, Phys. Rev. **39**, 403 (1932).
[3] H. Jones, Rev. Mod. Phys. **11**, 235 (1939).
[4] L. Leprince-Ringuet and J. Cussard, J. de phys. **8**, 207 (1937).
[5] D. J. Hughes, Phys. Rev. **57**, 592 (1940).